The New Role of TGF-β Superfamily Signaling in Melanoma

Dissertation

zur

Erlangung der naturwissenschaftlichen Doktorwürde (Dr. sc. nat.)

vorgelegt der

Mathematisch-naturwissenschaftlichen Fakultät

der

Universität Zürich

von

Eylül Tuncer

Aus der Türkei

Promotionskommission

Prof. Dr. Lukas Sommer (Leitung und Vorsitz der Dissertation)

Prof. Dr. med. Onur Boyman

Prof. Dr. med. Markus Manz

Prof. Dr. Burkhard Becher

Zürich, 2017

Table of Contents

1. Summary

Cutaneous melanoma is the most deadly skin cancer with a yearly rising incidence. The aggressiveness of this cancer is based on the stark metastatic potential of melanoma cells. Thus, melanoma patients usually die from metastatic disease rather than from primary tumor growth, which underscores the importance of studying mechanisms involved in melanoma cell dissemination and metastasis formation. Previously, the "phenotype switching" concept has been considered to be key for metastatic melanoma progression. In this model, melanoma cells have the capacity to dynamically switch between a proliferative and an invasive state. These are characterized by $MITF^{high}/AXL^{low}$ and $MITF^{low}/AXL^{high}$ expression, respectively. Among the signaling pathways that can drive reversible phenotype switching is SMAD-dependent TGF-β superfamily signaling. Importantly, the data describing the roles of phenotype switching and TGF-β signaling in melanoma have mostly been gathered by means of *in vitro* experiments and are somewhat controversial. Thus, it remains largely unknown to which extent phenotype switching and TGF-β superfamily signaling contribute to *in vivo* melanoma growth and metastasis.

In my PhD thesis, I investigate the relevance of phenotype switching for melanomagenesis. In particular, I decipher the differential roles of TGF-β signaling during melanoma formation and metastatic progression. Using genetically engineered mouse models, I show for the first time that phenotype switching is not obligatory for melanoma cell invasion and metastasis. In melanoma, TGF-β signaling has so far been associated with anti-proliferative and pro-invasive activities. Intriguingly, my results reveal that overall canonical TGF-β signaling, which depends on the co-SMAD protein Smad4, is required for tumor initiation and promotes, rather than antagonizes, melanoma cell proliferation *in vivo.* Consistent with these data, I identify BMP7 as a factor that stimulates melanoma cell proliferation and is able to override the anti-proliferative/pro-invasive activity of TGF-β. However, invasiveness can be promoted in proliferative cells by decreasing the levels of the inhibitory SMAD

protein SMAD7. Using genome-wide expression analyses of patient data and SMAD7-depleted melanoma cells, I further reveal that SMAD7 loss regulates both cell cycle progression as well as cell migration and adhesion. Thus, integrated TGF-β superfamily signaling during *SMAD7* silencing propagates $MITF^{high}/AXL^{high}$ cells that simultaneously proliferate while displaying an invasive gene expression signature. Likewise, conditional *Smad7*-inactivation in melanoma *in vivo* provokes emergence of such double positive cells, which ultimately leads to massive metastasis formation.
In summary, my findings demonstrate that proliferation is compatible with increased invasiveness and reveal a novel mechanism underpinning melanoma aggressiveness.

2. Zusammenfassung

Schwarzer Hautkrebs (auch Melanom genannt) ist die tödlichste Form aller Hautkrebsarten, derweil die Häufigkeit von Melanomerkrankungen stetig zunimmt. Die Aggressivität dieser Krebsart rührt daher, dass Melanomzellen mühelos metastasieren. Aus diesem Grund sterben Melanompatienten meist nicht am Primärtumor sondern an den Metastasen. Deshalb ist es von zentraler Bedeutung, die Mechanismen zu studieren, welche zur Metastasenbildung beitragen. Es wird angenommen, dass während der Melanommetastasierung ein Prozess namens „Phänotyp-Umschaltung“ eine zentrale Rolle spielt. In diesem Modell können Melanomzellen dynamisch zwischen einem proliferierendem und einem invasivem Stadium hin und her wechseln. Diese zwei Zustände werden durch die Expression von $MITF^{high}/AXL^{low}$, respektive $MITF^{low}/AXL^{high}$, definiert. Eine zentrale, zelluläre Signaltransduktionskaskade, welche Phänotyp-Umschaltung induzieren kann, ist die SMAD abhängige TGF-β-Superfamilie-Signalkaskade. Viele der Daten, welche das Phänotyp-Umschaltungsmodell und die Rolle der TGF-β-Signalkaskade während der Melanomentwicklung untermauern sollten, basieren aber nur auf *in vitro* Experimenten und wiedersprechen sich teilweise. Ob die Phänotyp-Umschaltung und die TGF-β-Signalkaskade tatsächlich für die *in vivo* Entstehung und Metastasierung des Melanoms relevant sind, ist jedoch weitgehend unbekannt.

Während meines Doktorates habe ich die Relevanz des Phänotyp-Umschaltungsphänomen während der Metastasenbildung eruiert. Zudem habe ich die unterschiedlichen Rollen der TGF-β-Signalkaskade während dem Wachstum und der Metastasierung des Melanoms studiert. Mit der Verwendung von genetisch manipulierten Mäusen konnte ich zum ersten mal aufzeigen, dass Melanomtumoren metastasieren können, ohne auf die Phänotyp-Umschaltung zurückzugreifen. Die TGF-β-Signalkaskade wurde traditionellerweise mit anti-proliferativen und pro-invasiven Kapazitäten von Melanomzellen in Verbindung gebracht. Meine Resultate zeigen jedoch auf, dass der gesamte Effekt der TGF-β-Signalkaskade, welche von dem co-SMAD Protein Smad4 abhängt, für die Proliferation von Melanomzellen relevant ist und dadurch die Melanomentstehung fördert. Im Rahmen dieser Resultate habe ich auch BMP7 als Faktor identifiziert, welcher die Proliferation von Melanomzellen stimuliert und den anti-proliferativen Effekt von TGF-β aushebelt. Durch die Unterdrückung des inhibitorischen SMAD Proteins SMAD7 kann jedoch wiederum die Invasivität von proliferierenden Melanomzellen angeheizt werden. Analysen von Patientendaten und Genexpressionsmustern haben aufgezeigt, dass sich in diesen Zellen die Expression von Proliferations- und von Invasionsgenen verändert. Dies führt dazu, dass sich durch die Auslöschung von SMAD7 Melanomzellen ansammeln, welche $MITF^{high}/AXL^{high}$ sind und gleichzeitig proliferieren und invasive Verhaltensmuster zeigen. Durch die Deletion des *Smad7* Genes in Mäusen habe ich auch die Ansammlung solcher Zellen in Mausmelanomen beobachtet. Dies steht im Zusammenhang mit einer stark erhöhten Metastasenbildung im Melanom-Mausmodell.

Zusammenfassend zeigen meine Resultate auf, dass die Proliferation und die Invasion von Melanomzellen gleichzeitig auftreten kann, was zu einem aggressiven Melanomtypus führt.

3. Introduction

3.1 Definition and Epidemiology of Cutaneous Melanoma

Cutaneous melanoma is the least common but the most deadly skin cancer type originating from neural-crest derivative melanocytes during development, colonize mainly the skin and eye, a broad range of other tissues throughout the body (Mort et al. 2015). In total, an estimated 76, 380 new cases of melanoma were diagnosed in 2016 (Rebecca L. Siegel et al. 2016). Over the past 3 decades, the number of people diagnosed with melanoma has increased sharply. Incidence rates differ among different populations, with the highest rates worldwide being reported in Australia and New Zealand, where the incidence rate reaches ~60 cases per 100,000 inhabitants per year (Figure 1A). In Europe, the rate is ~20 events per 100,000 per year, whereas, in the United States, a rate of ~30 events per 100,000 per year has been reported. (Schadendorf et al. 2015). The rise in incidence rates yearly about is 2.5% in males and 3.9% females (Raaijmakers et al. 2015). Incidence rates are higher in women than men before age 40, with a peak difference at age 20–24 (Liu et al. 2013). After the age 65, surprisingly, rates in men double those in women. (Rebecca L Siegel et al. 2016) (Figure 1B). Other than age and gender, a various number of risk factors are associated with melanoma susceptibility. For instance, cutaneous melanoma affects individuals with blue eyes, red hair and fair skin. In addition to the skin category, the high incidence rate of melanoma in white populations living closer to the equator obviously highlights the importance of sun exposure as a risk factor. Ultraviolet (UV) radiation has been predominantly linked to C>T nucleotide transition signature however, many melanomas lack this signature and have fewer point mutations. (Hayward et al. 2017) . Therefore, we still have to investigate the mechanisms involves in disease progression in order to further progress in melanoma epidemiology, prevention and targeted treatment globally.

A.

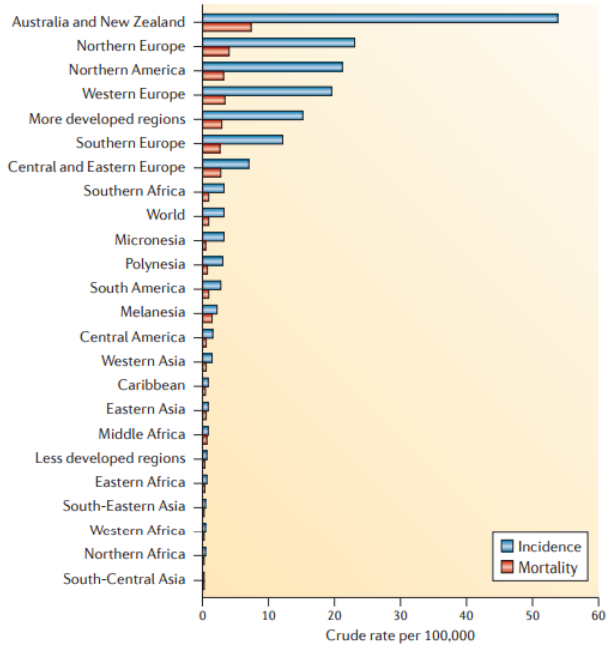

B.

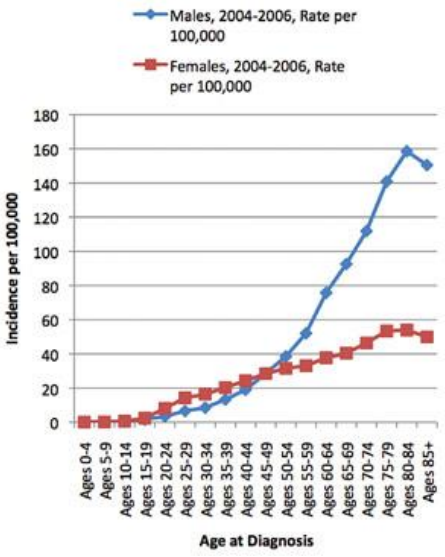

Figure 1A. Incidence and mortality of cutaneous melanoma. The rates of incidence and mortality from melanoma per 100,000 inhabitants per year show differences between countries. **Figure 1B. Melanoma incidence of male and female at different age.** Incidence is greater among women than men between age 20 and age 40, but greater among men than women at ages greater than 50.

3.2 Clinical features

The clinicopathological classification system for melanoma was based on gross clinical and pathological features and includes four major subtypes – superficial spreading melanoma (SSM), nodular melanoma (NM), lentigo malignant melanoma (LMM) and acral lentiginous melanoma. The first three were first described by Wallace Clark in 1967 (Hermanek et al. 1976). Superficial spreading melanoma (SSM) is the most common subtype, accounting for approximately 70% of cases, occurs most often on the trunk, appears as an asymmetrical flat skin lesion with irregular pigmentation and border (Dummer et al. 2005) (Figure 2A).

Nodular melanoma (NM) accounts for about 15% of melanomas and often appears on the trunk, head, neck and tends to grow more rapidly in thickness (vertical growth phase) than in diameter. (Figure 2B) Instead of arising from an existing mole, it may appear in a spot where a lesion did not previously exist, therefore, the prognosis is often worse because it takes longer for the patients to be aware of the changes in the skin. NM is often pigmented; however, some NM lesions can be less pigmented or even non-pigmented. (Figure 2B). (Maverakis et al. 2015; Rustin 1990). Lentigo malignant melanoma (LMM) accounts for 13% of melanomas and correlates with chronic sun exposure in fair-skinned older individuals. The lesion is usually large (3-6 cm or greater), with a variable nodular area from 1mm to 2cm in width (Wang et al. 2016) (Figure 2C). Acral lentiginous melanoma (ALM) occurs mainly on the nail beds, palms, and soles and is a relatively rare subtype (Bradford et al. 2009). Clinically, the lesion is characterized by a tan, brown-to-black, flat macule with color variations and irregular borders. (Figure 2D).

There are also unusual variants such as amelanotic, desmoplastic, verrucous, polypoid melanoma, minimal-deviation melanoma or blue nevus, and account for %5 of the cases. Among these, the more treacherous examples include the desmoplastic melanoma with prominent pigment synthesis and the malignant blue nevus. The inability to recognize unusual melanoma variants is because of the antigenic profiles of these tumors not commonly associated with a melanocytic histogenesis (Barnhill & Gupta 2009).

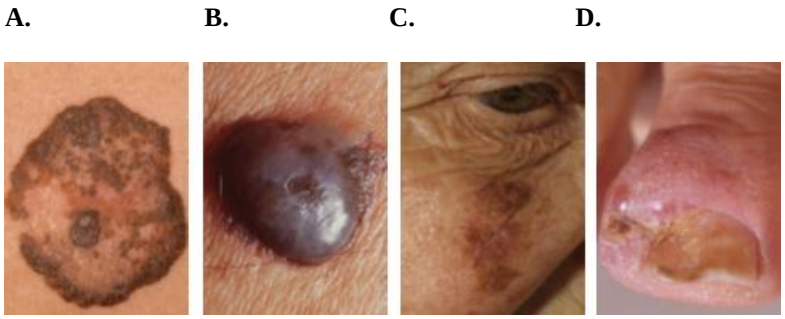

Figure 2. Different primary melanoma types. Four major subtypes of primary melanoma presentation are shown. (Hoek website "Heterogenety in melanoma") **2A,** Superficial spreading melanoma. **2B**, Nodular melanoma. **2C**, Lentigo maligna melanoma. **2D**, Acral lentiginous melanoma.

3.2.1 The Clinical Presentation and Morphology

The ABCDE criteria can be useful in early melanoma detection. The criteria include: **A** fo**r a**symmetry of lesions, **B** for **b**order irregularity, **C** for **c**olour variegation, **D** for **d**iameter (greater than 5mm) and **E** for evolving (particularly focusing on changes to shape, size, symptoms (itching), surface (bleeding, papular or nodular formation) and pigmentation over time) (Abbasi et al. 2004). The criteria are not helpful to diagnose lesions with vertical growth involvement or amelanotic melanomas; thus, other methods such as histopathological examination are often used together for accurate diagnosis.

3.3 Pathological features and staging

3.3.1 Clark's level of invasion and Breslow's thickness

Previously, very thin tumors were classified according to Clark's level of invasion; however, the key features for the new staging system includes the thickness of the tumor, known as Breslow's thickness. Clark's level of invasion classification method measures the depth of invasion of a melanoma into the skin according to anatomic layer. In addition to the anatomic level, the cell proliferation rate (mitotic index) is also used for the prognosis (Hermanek et al. 1976).The Clark levels characterized by five levels. Level I is represented by the melanomas limited to the outermost layer of the epidermis, also called "melanoma in-situ." Level II is defined by the infiltration of the melanoma cells in to the dermis of the skin. This stage is progression from radial growth phase to vertical growth phase. Level III, IV considered by the invasion into the reticular dermis. Level V is marked by infiltration of melanoma cells into the fat layer of the skin beneath the dermis and infiltration into the third layer of the skin, the subcutaneous. (Hermanek et al. 1976). Contrary to Clark levels , Breslow's measures the tumor thickness in millimeters from the upper granular cell layer to the deepest point of the invasive tumor cell (Breslow 1970).

3.3.3 TNM staging system

The TNM classification of malignant tumors (TNM) staging system was defined by the American Joint Committee on Cancer (AJCC) and revised in 2011 based on the analysis of 17,600 patients in the AJCC Melanoma Staging Database. TNM classification describes the stage of a certain cancer which originates from a primary tumor with alphanumeric codes. T stands for primary tumor, N for regional lymph nodes, and M for metastases. Stage 0 melanomas are non-invasive and still have the integrity of the epidermal basement membrane. Stage I (≤ 2 mm according to Breslow's method) and stage II melanomas are only localized primary tumor and there is no sign tumor cell spread to lymph nodes or other parts of the body. Stage III is characterized by regional spread through lymphatic vessels and stage IV by distant metastasis. (Balch et al. 2009). The latest summary of TNM classification of cutaneous melanoma mentioned above in *Table 1*.

Table 1. TNM Staging for melanoma revised in 2011.

Stage	**Primary Tumour**
T_{is}	In situ
T1	≤ 1,0 mm - a) without ulceration / b) with ulceration
T2	1.01 – 2.0 mm a) without ulceration / b) with ulceration
T3	2.01 – 4.0 mm a) without ulceration / b) with ulceration
T4	> 4.0 mm a) without ulceration / b) with ulceration
N	**Regional Lymph nodes**
N1	One lymph node a) micrometastasis b) macrometastasis
N2	2-3 lymph nodes a) micrometastasis b) macrometastasis c) in-transit metastases / satellite metastases *without* metastatic lymph nodes
N3	≥ 4 metastatic lymph nodes, matted lymph nodes or combinations of in-transit metastases / satellite(s) or ulcerated melanoma *and* metastatic lymph nodes
M	**Distant Metastases**
M1a	Distant skin, subcutaneous, or lymph node metastases (normal LDH)
M1b	Lung metastases (normal LDH)
M1c	All other visceral (normal LDH) or any distant metastases (elevated LDH)
LDH = Lactate dehydrogenase	

3.4 Pathogenesis of cutaneous melanoma

The whole genome sequencing data available from the data portal of The Cancer Genome Atlas (TCGA) and the data portal of the International Cancer Genome Consortium (ICGC) for various cancers has proved that cancer types differ in their overall mutation rates, predominant mutation types and distribution of mutations along their genome (Lawrence et al. 2013). These mutations in cancer genomes are most likely due to the consequence of the intrinsic changes in infidelity of the DNA replication machinery, mutagen exposures, enzymatic modification of DNA, or defective DNA repair (Pfeifer 2010). In case of melanoma, UV induced mutagenic effect seems to have major contributor to the mutation rate. Large-scale melanoma exome data samples demonstrate a high base mutation rate in compared to many form of solid cancer (Hodis, Ian R. Watson, et al. 2012) (Figure 3A).

A.

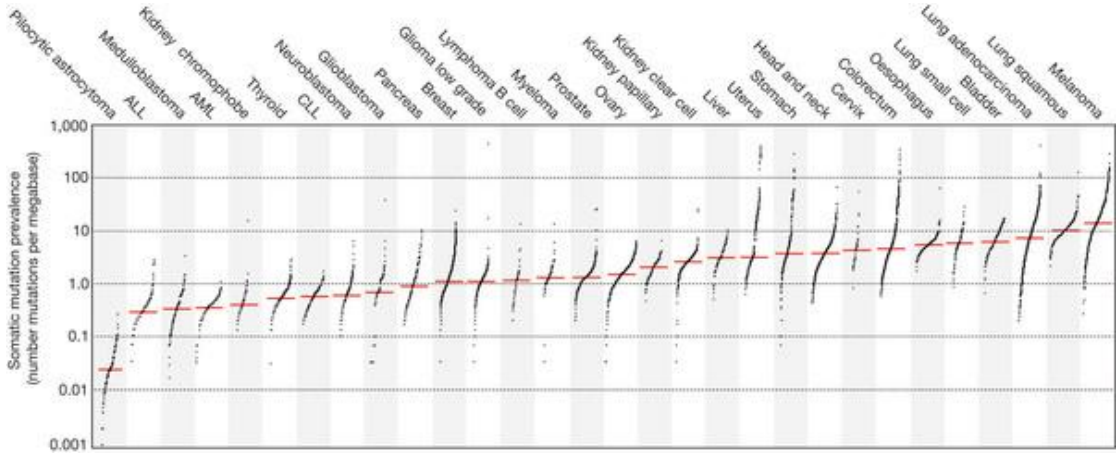

Figure 3A. The prevalence of somatic mutations across human cancer types. The prevalence of somatic mutations was highly variable, ranging from about 0.001 per megabase (Mb) to more than 400 per Mb. Every dot represents each sample whereas the red horizontal lines are the median numbers of mutations in the respective cancer types. ALL, acute lymphoblastic leukaemia ; AML, acute myeloid leukaemia; CLL, chronic lymphocytic leukaemia.

3.4.1 Chronically sun damaged melanoma vs. non-sun damaged melanoma

The most common types of melanoma are found on sun-exposed skin and be subtyped based on their cumulative levels of exposure to ultraviolet (UV) radiation. To a large extend, it can be also categorized by their anatomical origins and levels of sun exposure (chronically sun damaged CSD versus non-chronically sun damaged non-CSD melanomas) (Shain & Bastian 2016). CSD melanomas often originate from the head, the neck and the dorsal surfaces of the distal extremities and shows macroscopic and microscopic signs of continuing exposure to UV radiation (Broekaert et al. 2010). Instead, non-CSD melanomas typically affect the more irregularly sun-exposed areas such as the trunk and proximal extremities. Furthermore, CSD melanomas have high mutation load mainly neurofibromin1 (NF1), NRAS, BRAF non^{V600E} or KIT mutations while non-CSD melanomas are associated with a moderate mutation burden and a predominance of BRAF^{V600E} mutations (Bastian 2014; Viros et al. 2008).

The high mutation rate of CSD melanomas are associated with UV induced DNA damage (Ikehata & Ono 2011). UV radiation frequently leads to DNA mutations such as the formation of pyrimidine dimers or deamination of cytosine into thymidine. These DNA mutations mostly induces G->T transversions and G->A transitions (Besaratinia & Pfeifer 2006). UV exposure generates highly mutagenic DNA photoproducts in which two adjacent pyrimidines are covalently linked to form cyclobutene pyrimidine dimers (CPD) or pyrimidine (6–4) primidone photoproducts (6–4PP). Furthermore, these unrepaired photoproducts can interfere with DNA replication and transcription throughout the genome can eventually give rise to mutations in coding regions of genes including oncogenes and tumor suppressor genes. These alterations in the genome could promote benign lesion formation by allowing the clonal expansion of melanocytes carrying specific mutated genes.

3.4.2 Melanoma Progression

Melanoma progression is a complex process. Primary tumor formation has classically been thought to use a linear model in which normal melanocytes progress through different precursor lesions and, ultimately, to melanoma. However, there are different melanoma types that can be linked to different precursor lesions. Each subtype of melanoma can evolve through different evolutionary routes, passing through (or sometimes skipping) various stages of transformation (Shain & Bastian 2016). For instance, almost 12% of melanomas can arise with no an identifiable cutaneous precursor lesion, suggesting that not all steps necessarily occur during progression of individual malignant melanomas (Damsky et al. 2011) (Figure 4B). In contrast, the linear model for melanoma formation often suggests a linear path of progression from nevus to dysplastic nevi, to melanoma in situ, to invasive melanoma (Bandarchi et al. 2010) (Figure 4A). After formation of identifiable primary tumor, melanoma cells are assumed to enter lymphatic vessels, reach to the proximal lymph node, and subsequently infiltrate systemic circulation. Once reaching the systemic circulation, cells must adhere to the microvasculature of a target organ, extravasate, and subsequently proliferate to form a clinically relevant metastasis (Figure 4B). For each step, the molecular and environmental mechanisms vary between different melanomas and different target organs to achieve the metastasis formation. In the linear model, progression of individual lesions is thought to be driven by the acquisition of several genetic/epigenetic changes. Therefore, fully developed melanoma metastasis harbor numerous changes in their genome.

The classification of specific mutations can be based on the melanoma type still, the most recurrent somatic mutations in both CSD and non-CSD melanomas affect genes in key signaling pathways that govern proliferation, growth and metabolism, resistance to apoptosis, cell cycle control and replicative lifespan (Hodis, Ian R. Watson, et al. 2012; Huang et al. 2013; Horn et al. 2013; Krauthammer et al. 2012; Hayward et al. 2017). The presence of certain mutations in certain precursor lesions and the

association of these precursor lesions with specific types of melanoma help us to understand the order of sequential information for these pathways become disrupted, yet, it is partly understood.

A. **B.**

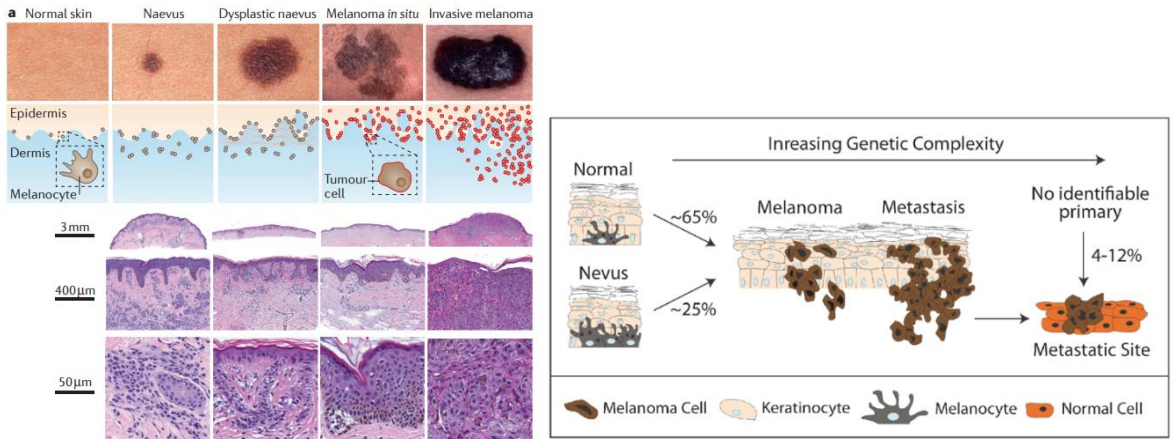

Figure 3A. The morphological spectrum of melanocytic neoplasms. Top row: clinical images showing a free-standing nevus, a dysplastic nevus, melanoma in situ and invasive melanoma. Second row: schematics illustrating the architectural features for each type of lesion Rows 3,4,5: photomicrographs illustrating the representative histopathological features of each type of lesion **B. Schematic steps in melanoma metastasis. according to Damsky et al 2011.**

3.4.3. Significantly mutated genes in melanoma

The latest complete melanoma genomes / exomes sequencing data from cutaneous, acral and mucosal subtypes of melanoma resolved novel signatures of mutagenesis inferable to UV (identified 228,987 mutations, including both SNVs and indels across different types) (Tsao, Chin, L. a Garraway, et al. 2012). UV signature mutations in melanoma found in many genes and mainly associated with a C>T nucleotide transition (Health et al. 2013; Brash 2015). However, many melanomas lack the UV signature and have very low number of point mutations. (Berger et al. 2012; Krauthammer et al. 2012).

Moreover, the number of affected genes in non-coding sequences were found in a similar extend to recurrent mutations in coding sequences. Nonetheless, researchers could have still categorized the subtype of cutaneous melanomas based on the significantly mutated genes such as BRAF, NRAS, NF1 and TP53 subtypes. In case of acral melanoma BRAF, NRAS and NF1 were the predominant mutations found whereas in mucosal melanoma SF3B1 was additionally identified (Hayward et al. 2017; Shain & Bastian 2016). Remarkably, mutations affecting the TERT promoter were the most frequent of all; however, these mutations were functionally linked with telomere protection and lengthening but in turn they do not result in significant telomere lengthening. (Hayward et al. 2017). The previously described melanoma oncogenes and tumor suppressors *BRAF*, *NRAS*, *CDKN2A*, *TP53*, and *PTEN*, along with recently discovered mutated genes *RAC1*, *MAP2K1*, *PPP6C*, and *ARID2* had potential roles in components of signaling pathways. (Hodis, Ian R. Watson, et al. 2012; Krauthammer et al. 2012; Tsao, Chin, L. a Garraway, et al. 2012; Haass et al. 2014). Aside from these recently identified different mutations, cutaneous melanoma was classified into four molecular subtypes based on their main genetic driver: *BRAF*-mutant, *NRAS*-mutant, *NF1*-mutant, and triple wild-type tumors (Figure. 4A).

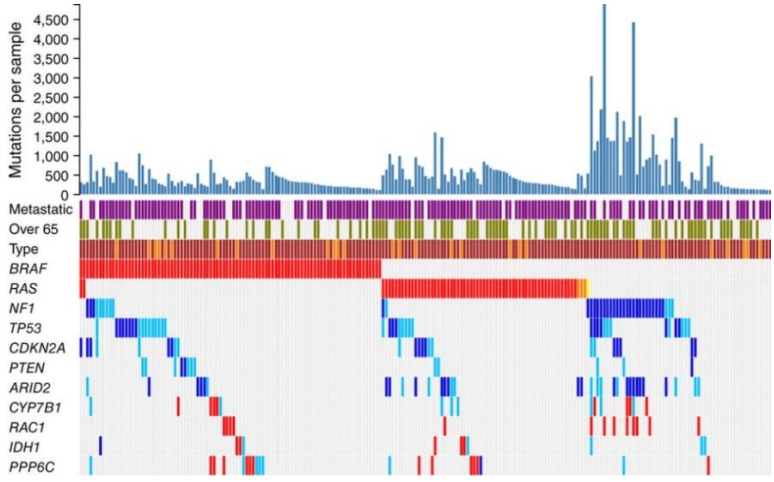

Figure 4A. Main melanoma-driver genes that reach genome-wide significance according to background mutation-frequency estimation. Purple, metastatic melanoma; green, patients over 65 years old; red, mutations at recurrent positions; dark blue, inactivating mutations (nonsense, splice, indel); light blue, predicted harmful mutations. Brown and darker orange represent sun-exposed tumors and tumors of unknown origin, respectively.

3.4.3.1 BRAF Subtype

The mitogen-activated protein kinase (MAPK) pathway is implicated in various cancers because of its role in the regulation of cell growth, survival, invasion. The MAPK signaling begins with the activation of the protein RAS by receptor tyrosine kinases. Activated RAS induces the membrane recruitment of various RAF proteins. Following recruitment, RAF proteins phosphorylates MEK, another key protein kinase, and phosphorylates ERK, which can directly and indirectly activate many transcription factors that are crucial for cell proliferation and survival. (Gaggioli et al. 2007; Santarpia et al. 2012; Knight & Irving 2014; Rauen 2013). In melanoma, activation of this pathway mostly occurs by the presence of *BRAF* hot-spot mutations (Davies et al. 2002a). *BRAF* somatic missense mutations have been detected in 66% of malignant melanomas. These mutations were mainly found in the kinase domain, with a single substitution; V600E (Valine -> Glutamine) accounting for 80% of all such cases (Davies et al., 2002). Interestingly, 82% of benign nevi also present with *BRAF* mutations, yet it is not sufficient for malignant transformation (Dong et al. 2003; Omholt et al. 2003). The appearance of BRAF mutations in early nevi indicates that the acquirement of activation of BRAF is a clonal, key driving event (Dong et al. 2003; Omholt et al. 2003). Also, there are other well-documented V600 amino acid residue substitutions: V600K (Valine->Lysine), and V600R (Valine->Arginine). The second most frequent *BRAF* mutation targeted the K601 residue. (Davies et al. 2002b)The patient samples harboring BRAF V600E hot spot mutation are not having a common UV induced signature. In these samples, the transversion of T → A resulting of the substitution at distinct nucleotide that is different from UV-induced pyrimidine dimer formation (Davies et al., 2002). It has been also shown that BRAF mutations arising on non-CSD melanomas are more common than CSD melanomas, acral melanomas and mucosal melanomas that the tissues are relatively unexposed to sunlight (Curtin et al. 2005; Chin 2003). Also, patients in the *BRAF* subtype were younger than patients in the other subtypes (Cancer Genome Atlas Network 2015).

3.4.3.2 RAS Subtype

The second main subtype is defined by the presence of RAS hot-spot mutations mostly including NRAS Q61K/L/R or NRAS G121D. 13–25% of all malignant melanomas have been shown the presence of somatic mutations in *NRAS* locus (Ball et al. 1994; Curtin et al. 2005; van 't Veer et al. 1989). Surprisingly, RAS mutations recurrent in congenital nevi and absent in acquired nevi (Roh et al. 2015). These mutations are missense mutations which lead to an amino acid substitution at positions 12, 13, or 61. The outcome of these mutations is constitutive activation of NRAS and subsequently activation of MAPK signaling pathways. NRAS mutations are more common in melanomas derived from CSD skin (Hayward et al. 2017).

3.4.3.3 NF1 Subtype

The third most frequent mutation seen in MAPK signaling was NF1 protein, neurofibromin 1 that negatively regulates RAS proteins. NF1 is a GTPase-activating protein known to downregulate RAS activity through its intrinsic GTPase activity and loss of function of *NF1* is an alternative way to activate the canonical MAPK signaling pathway (Sharma et al. 2013). *NF1* mutations in melanoma typically occur on CSD skin or in older individuals, show a high mutation burden, and interestingly are wild-type for *BRAF* and *NRAS*. (Cancer Genome Atlas Network 2015). As well, *NF1* mutations characterize certain melanoma subtypes mainly desmoplastic melanoma (Maertens et al. 2013).

3.4.3.4 Triple Wild-Type Subtype

The triple wild type subtype defined by a lack of hot-spot *BRAF*, *NRAS*, or *NF1* mutations and in these subtype, several known driver mutations for uveal melanoma such as *GNAQ*, *KIT*, *CTNNB1* and

EZH2 were found. Strategies to target melanomas that are *BRAF/NRAS/NF1*-wild type have recognized even more indefinable to cure. The analysis of somatic copy-number alteration (CNA) among subtypes have demonstrated that the Triple-WT had significantly more copy-number alterations and was enriched for crucial amplifications targeting known oncogenes (Hayward et al. 2017). For instance, the oncogene *KIT, PDGFRA* and *KDR* (*VEGFR2*), were frequently co-amplified in these samples. Some of the *BRAF*/*NRAS*/*NF1* wild type melanomas from patient data showed also amplification in crucial oncogenes such as cyclin D1 and *CDK4* as well as *MDM2* and *TERT* (Hodis, Ian R. Watson, et al. 2012).

3.4.3.5 Genes involved in familial melanoma

The family history of the melanoma is one of the most significant risk. It has been reported that those born in families with history of melanoma have a 30-70% increase in the chance to develop melanoma. Approximately 10% of melanoma cases report a first- or second-degree relative with melanoma (Aoude et al. 2015). Even though familial melanoma accounts for only few percentage of all melanoma cases, it is very crucial to understand the genetic basis of the germline mutations for melanoma susceptibility in order to develop new methods for early detection.

3.4.3.5.1 High penetrance genes

Principally, there main melanoma predisposing genes have been discovered. So far, *CDKN2A* is the main high-risk gene involved in melanoma susceptibility. Germline mutations in the coding region are observed in around 20%. (Aoude et al. 2015). The locus encodes two following important cell cycle regulator proteins: inhibitor of cyclin-dependent kinase 4A ($p16^{INK4A}$) and alternate reading frame (*ARF* $p14^{ARF}$($p19^{ARF}$ in mice) (Serrano et al. 1996). A second high-penetrance gene is cyclin-dependent kinase 4 (*CDK4*), even though only three families have been reported to harbour the mutation. (Zuo et al. 1996). These two proteins roles in the same cell-cycle regulatory pathway, namely that G1 to S phase

transition. The constitutive activation of CDK4 protein is oncogenic, since this kinase negatively regulates Retinoblastoma (Rb) by phosphorylation. Once phosphorylated, pRB disassociates from the transcription factor E2F1 and rescuing E2F1 from cytoplasm bound state letting it to shuffle into the nucleus and regulating genes that are essential for G1 to S phase transition (Duronio & Xiong 2013). In contrast, p16 is a tumor suppressor, is a CDK inhibitor, inhibits the kinase activity of CDK4 and subsequently, decelerates the cell cycle by prohibiting transition from G1 phase to S phase (Stone et al. 1995; Nobori et al. 1994). Mutated $p16^{Ink4a}$ is no longer able to inhibit CDK4 mediated phosphorylation of the Rb and, resulting in the same effect, mutated CDK4 is unable to bind functional $p16^{Ink4a}$. Similar to p16, $p14^{ARF}$ is a tumor suppressor protein but acts through a different pathway. ARF protein induces cell cycle arrest by stabilizing of p53 via HDM2 mediated ubiquitination (Pomerantz et al. 1998; Stott et al. 1998).

3.4.3.5.1 Low penetrance genes

A third susceptibility-gene, the melanocortin 1 receptor (MC1R), shows low penetrance so it confers lower risk (Kennedy et al. 2001). MC1R gene determines individual's skin phenotype by influencing the ratio of eumelanin to pheomelanin (Lin & Fisher 2007). Eumelanin does responsible for the brown to black color for the skin, eye and hair while pheomelanin accounts for yellow to red color that is less photoprotective. Thereby, pheomelanin variants are more prone to produce reactive oxygen species (ROS) and subsequent DNA damage (Lin & Fisher 2007; Wong & Rees 2005). Due to the shift from eumelanin to pheomelanin, carriers for *MC1R* variants have red hair, freckles, fair skin with reduced tanning ability. Pheomelanin increased type has diminished UV-light protection, and consequently, melanocytes with such *MC1R* variants are very sensitive to the DNA damaging effects of UV radiation (Scott et al. 2002).

Recently, new genes involved in melanoma susceptibility have been identified; breast cancer 1 *(BRCA1)*, BRCA1-associated protein 1 *(BAP1*), and telomerase reverse transcriptase *(TERT)*. (Potrony

et al. 2015). Analysis of these genes allow us to identify a larger number of high-risk individuals with a potential of developing familial. It is important that these individuals receive adequate management along with frequent dermatological examinations, genetic counselling and instrumental examinations aimed at the early identification of other tumors associated with cutaneous melanoma.

The number, size and color of melanocytic nevi is related to frequency and amount of intermittent sun exposure and associated with an elevated risk of melanoma (Slominski et al. 2001; Gandini et al. 2005). Thus, clinicians use the ABCD (A) asymmetry, (B) vague border, (C) variegated pigmentation, (D) diameter exceeding 5 mm, (E) elevation score as a prediction rule to determine the risk for nevi to progress to developing melanoma.

3.4.4 Molecular alterations in signal pathways of melanoma

3.4.4.1 PTEN signaling

Since its discovery, phosphatase and *ten*sin homolog deleted in from chromosome *ten* (PTEN) known as an elusive tumor suppressor gene (Salmena et al. 2008). A broad variety of human cancers including melanoma harbour PTEN alterations such as loss of heterozygosity (LOH) and rearrangements of chromosome 10 (Aguissa-Touré & Li 2012). PTEN has both lipid and protein phosphatase functions that are essential for regulating the cruical pro-survival PI3K/AKT signaling pathway (Worby & Dixon 2014). PTEN negatively regulates the phosphatidylinositol-3-kinase (PI3K) pathway by dephosphorylating PIP_3, subsequently decreases the intracellular PtdIns $(3,4,5)P_3$ levels and downstream AKT activity (Cantley 2002) (Figure 5). AKT activation promotes the downregulation of antiapoptotic proteins and the upregulation of proapoptotic signals resulting in controlled cellular survival, growth and proliferation. Another consequence of AKT activation is cell-cycle arrest at G1/S that is mediated by the upregulation of the cyclin-dependent kinase inhibitor p27. (Shanmugasundaram et al. 2013). Thus, loss of PTEN regulation often results in reduced proliferative and apoptotic control (Aguissa-Touré & Li 2012).

PTEN has also phosphatase function which targets proteins and protein phosphatase activity of PTEN is apparently less essential for tumorigenesis. For instance, dephosphorylation of focal adhesion kinase (FAK) has been shown to inhibit adhesion and migration properties of human cancer cells (Tamura et al. 1999). Additionally, PTEN is thought to intersect and inhibit growth factor-stimulated mitogen activated-protein kinase (MAPK) signaling by dephosphorylating certain adapter proteins, resulting in reduced MEK activity (Carracedo & Pandolfi 2008). For instance, previously it has been shown that activation of MAPK via growth signals such as epidermal growth factor (EGF) and platelet-derived growth factor (PDGF) can be blocked by exogenous PTEN expression in human glioblastoma cells (Furnari et al. 1997; Furnari et al. 1998).

As a summary, the loss of PTEN lipid and protein phosphatase activity one of the crucial event for tumor biology and may result in aberrant cell growth and surveillance from apoptosis, as well as cell migration. In melanoma, PTEN loss has been mostly observed as a later event, even though a level-dependent loss of PTEN protein has been implicated in early stages of tumorigenesis (Wu et al. 2003). In addition, PTEN alterations strongly correlate with $BRAF^{V600E}$ hot spot mutation, even though analysis of human cell lines shows that inactivation of PTEN and RAS activation are not coincident in melanoma (Goel et al. 2006). In melanoma, loss of PTEN on chromosome 10 has been observed in 30-60% of sporadic cases and PTEN mutations or deletions have been found in 30-40% of established cell lines (Shain & Bastian 2016; Goel et al. 2006).

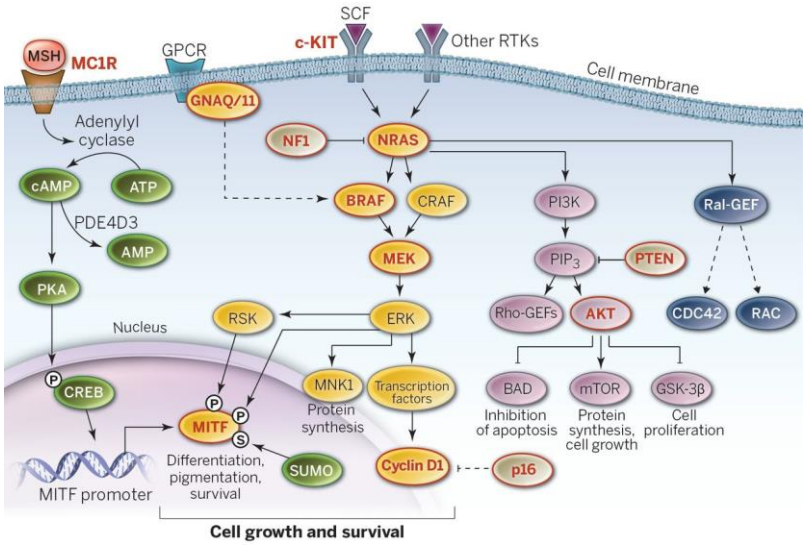

Figure 5. Signaling pathways in melanoma. MAPK signaling promotes cell growth and survival. RAS family members are activated by RTKs and signal through effector proteins, including RAF kinases, PI3K, and Ral-GEFs.

3.4.5.2 The RAS/RAF/MEK/ERK pathway

The mitogen-activated protein kinase (MAPK) pathway is implicated in many type of cancers and activated in 80% of all cutaneous melanomas. Activation of this pathway occurs via growth factor stimulation, activating mutations in signaling components or other type of growth-factor receptors (Gray-Schopfer et al. 2007). The signal is transduced by specific receptor tyrosine kinases, cytokines, and G-protein-coupled receptors (Lu et al. 2006). There are 3 different RAS proteins in human including HRAS, KRAS, NRAS. Upon RAS activation, the kinase activity of target RAF proteins (ARAF, BRAF and CRAF in humans) is induced via complex formation. (Roberts & Der 2007; Leevers et al. 1994). This activated complex leads to the phosphorylation of mitogen-activated protein kinases (MAPK also known as ERK) via activation of MEK proteins (MEK1 and MEK2) (Arthur & Ley 2013). Subsequently, the signal is transduced in to the nucleus in order to regulate the expression of several genes involved in cell proliferation, differentiation and survival by phosphorylating nuclear transcription factors such as *ETS*, *ELK-1*, *MYC* or indirectly by targeting intracellular signaling molecules. It also effects the post-translational phosphorylation of apoptotic regulatory molecules like

BAD, *BIM*, *MCL-1*, caspase 9 and BCL-2. The pathway is constitutively activated by growth factors such as epidermal growth factor (EGF), platelet-derived growth factor (PDGF), vascular endothelial growth factor (VEGF), stem cell factor (SCF), fibroblast growth factor (FGF), hepatocyte growth factor (HGF), and glial-cell-derived neurotrophic factor (GDNF) (Santarpia et al. 2012).

In melanoma, constitutive activation of MAPK pathway leads to induce proliferation, survival, invasion, and angiogenesis. The abovementioned somatic *BRAF* mutations occur 80% of cases in early melanomagenesis. (Davies et al. 2002a) Yet, most nevi do not progress into malignant melanoma suggesting that *BRAF* mutation may be required but not sufficient to induce malignant transformation. Activated BRAF has been shown to result in a senescence-like state and further melanoma progression requires the presence or absence of additional genetic events such as loss of tumor suppressor. Furthermore, mutations in *NRAS* oncogene that is approximately 15%–30% of cases, cause senescence phenotype when expressed in normal melanocytes (Tsao, Chin, L. a Garraway, et al. 2012; Dong et al. 2003). In addition to NRAS and BRAF some other MAPK pathway components frequently also are mutated in human melanoma cell lines and melanoma samples such as in *MAP3K5* and *MAP3K9*. (Stark et al. 2011). MAPK signaling pathway is currently good target for anticancer therapy respecting to its high frequency of mutations. Nevertheless, identification of perfect pathway component to therapeutically target for maximal clinical benefit to melanoma patients remains a challenge.

3.4.5.3 WNT Signaling

WNT pathway signals via three distinct pathways; the canonical B-catenin pathway, the Ca^{2+}/PKC pathway and the planar cell polarity pathway and mediates cell proliferation, differentiation, polarity and cell fate determination. (Webster et al. 2015). WNT signaling is very crucial in development however, aberrant signaling has been implicated in many human cancers. The various Wnt family of proteins, with the main receptors and co-receptors, emphasise the complexity and diversity of WNT signaling. WNT signaling is initiated by frizzled family of receptors, which are G-protein-coupled

receptors. Besides to Frizzleds, WNT signaling also requires multiple co-receptors, such as ROR1 and ROR2, LRP5/6 and Ryk (Wu & Nusse 2002; Webster et al. 2015). The well-known WNT canonical signaling pathway involves the intermediate signaling β-catenin protein and is termed the canonical pathway (Nelson 2004). Non-canonical WNT signaling includes both the Ca^{2+}/PKC pathway and the planar cell polarity pathway mediated via JNK signaling. (Komiya & Habas 2008; Habas & Dawid 2005).

Canonical WNT signaling promotes pigment-cell formation by medial crest cells, thereby crucial for the development of melanocytes from their neural crest precursors (Dorsky et al., 1998). The regulation of melanocyte development is via the activation of microphthalmia-associated transcription factor (MITF) that is appeared to be the master regulator of melanocyte identity. Given the role in development, it is likely that the elevated level of WNT signaling makes a considerable contribution to the transformed phenotype of melanoma cells. For instance, there are lots of evidences for the activation of the canonical β-catenin pathway through the immune-histochemical detection of nuclear β-catenin in a subset of primary melanomas suggests a role for this pathway in melanoma development (Rimm et al., 1999, (Rubinfeld 1997; Huber & Weis 2001; Arozarena et al. 2011) Mutations of B-catenin have been described in melanoma cell lines and various primary melanoma showed 4% of oncogenic mutations. Furthermore, active WNT/b-catenin signaling was observed in 30% of melanoma tumors.(Chien et al. 2009). Constitutive expression of β-catenin is enough to promote tumor progression in transgenic mouse models, although it is well known that β-catenin is critical in the early stages of melanocyte transformation and melanoma genesis, its significance in metastases and prognosis is still a matter of debate. (Delmas et al. 2007).

3.4.5.4 TGF-β Signaling and deciphering the molecular components

The members of the transforming growth factor-β (TGF-β) super-family are multifunctional cytokines controlling various cellular processes, including cell proliferation, differentiation, apoptosis, fate

determination as well as embryo patterning during development (Shi & Massagué 2003; Siegel & Massagué 2003). The TGF-β super-family have more than 40 human cytokine members including the TGF-βs, activins, NODAL, bone morphogenetic proteins (BMPs), growth and differentiation factors (GDFs) and anti-Müllerian hormone (AMH) (Siegel & Massagué 2003). TGF-β superfamily ligands signal through two transmembrane serine/threonine kinase receptors, a type II ligand binding receptor and a type I signal transducing receptor. The functional receptor at the cell surface desires both type I and type 2 heterodimer formation (Wrana et al. 1992).

A. **B.**

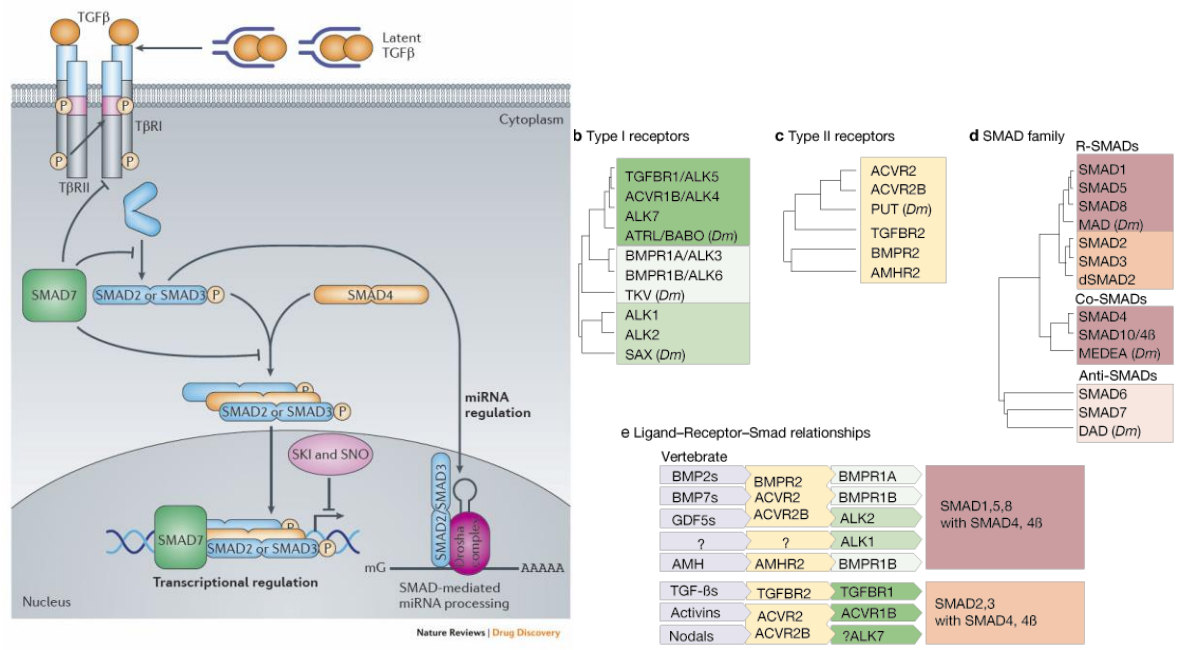

Figure 6A, Canonical TGF-β signaling. The active form of the TGF-β ligand is a dimer of two molecules held together by hydrophobic interactions and a disulfide bond. This dimer induces the formation at the cell surface the active receptor hetero-tetramers. The type II receptors phosphorylate the type I receptors; the type I receptors are then enabled to phosphorylate cytoplasmic R-Smads (in case of TGF-β type I receptors phosphorylates Smad2/3) which then complex with the co-Smad, Smad4 and translocate to the nucleus to bind DNA at specific Smad binding elements (SBE). This pathway is inhibited by Smad7. **7B, Table showing the specificity of TGF-β superfamily ligand-receptor interactions in human.**

Upon ligand binding to a type II receptor at the cell surface, a type I receptor is recruited and phosphorylated by the type II receptor. Phosphorylation leads to the activation of its receptor kinase domain. The activated type I receptor recruits and phosphorylates receptor-regulated Smads (R-SMADs). Phosphorylated R-SMADs bind to the co-mediator SMAD (Co-SMAD) and translocate to the nucleus where the heteromeric complex interacts with other transcriptional factors (TF) including co-activators and co-repressors (Silvestri et al. 2010) (Figure 6A).

3.4.5.4.1 SMAD Proteins

Specific TGF-β superfamily ligands recruits different combinations of type I and type II receptors, as indicated Figure 6B (Massagué 1998). In human, there are seven type I receptors, namely activin receptor like kinases (ALK1-7) and five various type II receptors (TGFβR-II, ActR-IIA, ActR-IIB, BMPR-II, and AMHR-II) are responsible for the signal transmission. (Schmierer & Hill 2007) Receptors have cysteine-rich extracellular domain, a single-pass transmembrane domain and an intracellular kinase domain. SMAD2 and SMAD3 are type of R-SMADs that are effectors of TGF-β, activin or NODAL signaling and are phosphorylated by ALK4, ALK5 and ALK7. (Schmierer & Hill 2007)On the contrary, SMAD1, SMAD5 and SMAD8 are involved in BMP signaling and they are phosphorylated by ALK1, ALK2, ALK3 and ALK6.(Massagué & Gomis 2006). The receptor-mediated phosphorylation of the R-SMADs occurs at their carboxyl terminus on two serine residues in an S-M-S or S-V-S motif. The recognition of different R-Smads by the various type I receptor kinases is highly specific and the phosphorylation promotes binding to SMAD4, subsequently accumulation in the nucleus (Hata & Chen 2016).

SMAD proteins are defined by two conserved MAD-homology (MH) domains, namely MH1 and MH2. Among R-SMADs, these domains share more than 90% homology at the amino acid level, however an additional 30 amino acid were discovered in MH1 domain of Smad2 (Figure 7). This insertions inhibits its ability to bind DNA (Dennler et al. 1999). The MH1 domain is responsible for binding to specific

CAGA sequence, known as Smad-binding DNA element (SBE) (Jonk et al. 1998). The ability to bind the accurate promoter is also dependent on the co-activators and co-repressors at the transcriptional level (Massague & Gomis 2006). In contrast, the MH2 domain does not bind DNA and instead is having interactions to provide specificity and selectivity. (Imoto et al. 2003; Wang et al. 2009). The TGF-β signals is mediated by the direct association of extreme carboxyl terminus of the MH2 domain with the TGFβ receptor complex. The R-SMADs are then directly phosphorylated by the type I TGFβ receptor kinase on the last two serines of a conserved SSXS motif located at the extreme carboxyl terminus of the MH2 domain.

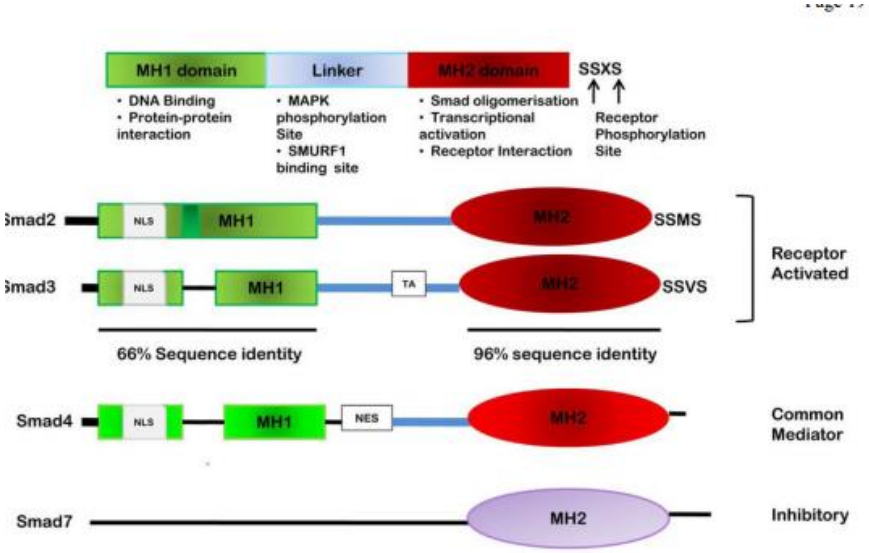

Figure 7. Domain structure of Smads. MH1 domain of Smad2 contains an additional 30 amino acids denoted by dark green box. Smad3 contains a trans-activation (TA) in its linker region. Smad4 contains Nucleus Export Signal (NES) in its linker region. Smad2,3 and Smad4 contains a Nucleus Localization Signal (NLS) in their MH1 domain. Smad7 lacks MH1 domain.

Another type of SMAD proteins is composed of the inhibitory SMADs (I-SMADs), SMAD6 and SMAD7. Remarkably, SMAD7 inhibits signaling by both TGF-β and BMPs mediated signals whereas SMAD6 preferentially inhibits BMP signaling (Hayashi et al. 1997; Kretzschmar et al. 1997). The MH1 domain of I-SMADs have amino-N domains and they are quite dissimilar to R-SMADs with respect to amino acid sequence. (Dennler et al. 1999)However, they conserve the extreme carboxyl-terminal MH2

domains (Silvestri et al. 2010) The N domains are essential for specific inhibition of TGF-β signaling by Smad7, whereas the MH2 domains are involved in the inhibition of TGF-β signals through interaction with type I receptors. SMAD7 negatively regulates the TGF-β signaling at the different levels; including competing with R-SMADs for receptor binding, recruiting E3-ubiquitin ligases (SMAD ubiquitination regulatory factor 1 and 2 (Smurf1 and Smurf2) leading to type I receptor degradation or recruiting factors for type I receptor dephosphorylation (Yan et al. 2009a).

3.5 TGF-β Superfamily ligands and cancer

3.5.1 TGF-β isoforms

TGF- β family consists of three members (TGF- β1-3) that show high similarity and homology even though they are encoded by three distinct genes, they share ~80% amino acid sequence homology. (Fimmel et al. 1999). The TGF-β cytokine is synthesized as a pre-TGF-β protein containing the C-terminal and N-terminal domains. After the cleavage by furin-like endoproteinase, the pro-polypeptide called the latent-associated peptide (LAP), at which , the LAP dimer remains associated with the mature TGF-β dimer (Shi et al. 2011). This complex, known as the small latent complex, is secreted. However, this complex often associates through the LAP to one of four latent TGF-β binding proteins (LTBP) to be secreted as a large latent complex. Release of the mature TGF-β molecule is induced by cleavage of the LAP by various proteases. (Schiller et al. 2004; Javelaud & Mauviel 2004). TGF-β then mediates its effect through the heteromeric receptor complex consisting of TβR-II and ALK5.

In cancer, TGF-B isoforms have many crucial functions; as a tumor suppressor, TGF-β has control on proliferation, apoptosis, and instead, as a tumor promoter, it plays a crucial role in angiogenesis, migration and invasion, immune surveillance (Massagué 2008). Additionally, many clinical studies have been demonstrated that the levels of TGF-B ligands are increased in patients from different type of cancers such as colon cancer, breast cancer, melanoma (Friedman et al. 1995; Chod et al. 2008; Krasagakis et al. 1993). In early-stage tumors, levels of TGF-β are positively associated with a favorable prognosis, while in late-stage tumors, they are positively associated with poor prognosis (Padua &

Massagué 2009). Thereby, it is well accepted that TGF-β pathway has dual role in cancer (Inman, 2011; Principe et al., 2014).

The recent paradigm for the role of TGF-β in tumorigenesis is that accumulation of genetic alterations in the signaling switches it is role from tumor-suppressive to tumor-promoting actions (Jakowlew 2006; Neuzillet et al. 2015). Indeed, tumor progression requires shutting down the tumor-suppressive arm of the signaling, which can be achieved by two mechanisms. The first one is inactivating the signaling by either through mutation or through allelic loss of heterozygosity (LOH), of the core components: the receptors or the SMAD transcription factors (Padua & Massagué 2009). Inactivating mutations in the gene for TβR-II are found in colon and gastric cancers, as well as in glioma (Chung et al., 1996; Izumoto et al., 1997; Ku et al., 2007; Markowitz et al., 1995). Inactivating mutations in the gene encoding ALK5 are less frequent but are found in breast, colorectal, ovarian, head and neck, and pancreatic cancers, and T-cell lymphoma (Chen et al., 1998; Chen et al., 2001a; Chen et al., 2001b; Goggins et al., 1998; Ku et al., 2007; Schiemann et al., 1999). Mutations in *Smad2* are relatively rare and are limited to a few cases in colon, lung, gastric, and head and neck cancers (Han et al., 2004; Qiu et al., 2007; Riggins et al., 1996; Tsang et al., 2002; Uchida et al., 1996). *Smad4* mutations occur in approximately half of cases of pancreatic cancer and are also detected at a lesser frequency in other carcinomas including colon carcinomas (Hahn et al., 1996; Schutte et al., 1996). Loss of Smad4 also correlates with cancer progression and metastasis (Losi et al., 2007; Luttges et al., 2001; Xu et al., 2000). These genetic inactivation's of core components of the TGF-β pathway result in removal of tumor-suppressive activities. Nevertheless, this is not the case of many cancers such as breast, prostate cancers, melanomas, and gliomas that often retain functional TGF-β signaling. These tumors can benefit from the remaining TGF-β activities promoting tumor progression and metastasis.

3.5.2 TGF-β's tumor suppressor role

TGF-β is a ubiquitous cytokine that is well described for its ability to inhibit epithelial cell proliferation via regulating several crucial genes involved in controlling cell cycle progression. In early-stage tumors, the TGF-β pathway promotes cell cycle arrest and apoptosis (Dooley & ten Dijke 2012; Yin et al. 2012; Jakowlew 2006). In case of cell cycle progression, activated target genes are the CDK inhibitors including $p21^{Cip1}$, $p27^{Kip1}$ and $p15^{Ink4b}$ (Hannon & Beach 1994; Kamesaki et al. 1998; Datto et al. 1995; Scandura et al. 2004). $p15^{Ink4b}$ interacts and inactivates CDK4 and CDK6, and thus prevents progression through the G1/S cell cycle controlling point (Hannon & Beach 1994). Activation of $p15^{Ink4b}$ is further enhanced by the downregulation of c-Myc. TGF-β signaling represses the expression of c-Myc and therefore inhibits its recruitment to the $p15^{Ink4b}$ promoter, relieving c-Myc induced repression of $p15^{Ink4b}$ (Seoane et al., 2001; Staller et al., 2001). In addition to inhibiting proliferation, TGF-β may also induce apoptosis. (Schuster & Krieglstein 2002). For example, TGF-β has been shown to regulate the expression of pro- and anti-apoptotic molecules, including p53, Bad, Bax, Bik, Bcl-2 and Bcl-XL (Heldin et al. 2009; Jakowlew 2006)

3.5.3 TGF-β's tumor promoter role

Malfunction of TGF-β signaling can result in many pathological changes, among which epithelial-mesenchymal transition (EMT) is a well-studied process that endows cancer cells with increased aggressiveness. EMT refers to the reprogramming of epithelial cells to a mesenchymal cell. The TGF-β pathway regulates, acting alone or in cooperation with other signaling pathways, these transcription factors, which confers TGFβ a potent inducer of EMT (Yang et al. 2004; Heldin et al. 2012) The pro-oncogenic role for TGF-β signaling was well defined in breast cancer. It has been demonstrated that presence of a dominant negative TβR-II together with an initiating oncogenic lesion leads to increase the frequency of malignant transformation of breast epithelial cells and increase the aggressiveness of a low-grade breast carcinoma (Tang et al., 2003). Conversely, the loss of TGF-β signaling did not affect primary tumorigenesis, but suppressed metastasis in a high-grade breast carcinoma (Tang et al., 2003).

The SMAD proteins are also implicated in breast cancer metastasis. The expression of dominant negative SMAD3 or expression of a mutant form of the TGF-β type I receptor, in human mammary epithelial cells, significantly diminished their ability to colonize the lungs. (Theohari et al. 2012). Moreover, overexpression of the inhibitory Smad7 impaired mammary carcinoma cell invasion. (Yu et al. 2016). The major role in promoting breast cancer metastasis comprises other ways of acting such as at the tumor stroma level. Remodeling the surrounding extracellular matrix (ECM), through stimulation of matrix metalloproteinase (MMP) expression and modulation of the plasminogen activation system, resulting in TGFβ-mediated matrix degradation and, consequently, an increasing release of stored TGFβ from the ECM that acts as a TGFβ reservoir Indeed, in many types of cancer, increased production of TGF-β correlates with higher tumor grade and stimulates angiogenesis, contributes to myofibroblast differentiation and causes local and systemic immunosuppression, further contributing to tumor progression and metastasis.

1.5.3 TGF-β's in melanoma

In normal melanocytes, TGF-β1 act as an inhibitor of proliferation. Normal melanocytes and melanoma cells express and secrete high quantities of the three TGF-β isoforms, TGF-β1, TGF-β2 and TGF-β3 and these ligands are able to induce their own expression via positive amplification loop. While melanomas express TGF-β constitutively, melanocytes require exogenous growth factor stimulation for TGF-β production (Rodeck et al., 1994). Normal melanocytes are growth-inhibited by TGF-β; however melanoma cells show resistance to its antiproliferative activity. As previously mentioned, alterations in the components of the pathway in melanoma are very rare, therefore various mechanisms have been suggested to understand the escape from a cytostatic response to TGF-β. For instance, phosphorylation of the SMAD2 and SMAD3 linker regions was detected to be high in both melanoma cell lines and melanoma samples. Such event has previously been associated with the weaker SMAD2/3 activity, leading to downregulation of TGF-β- responsive genes such as p21, p15 and c-MYC.

Activation of TGF-β pathway in melanoma cell lines has been well demonstrated. The basal phosphorylation level of SMAD3 is detectable in vitro in melanoma cells, demonstrating a constitutive activation of the TGF-β receptors. It has also been shown that phosphorylation of SMAD2 in melanoma cells is associated with SMAD2 phosphorylation in neighboring keratinocytes, indicating that TGF-β pathway could affect the tumor microenvironment. Furthermore, TGF-β blockade by means of either a neutralizing pan-TGF-β antibody or SMAD7 overexpression inhibited basal SMAD -dependent transcriptional activity in melanoma cells.

In human melanocytic lesions, higher levels of nuclear phosphorylated SMAD2 are found in benign melanocytic nevi, melanomas in situ, and primary invasive melanomas, suggesting that hyperactivated TGF-β/SMAD pathway can be related to melanoma progression in the skin, and may be a critical switch from radial to vertical growth during melanoma progression

The tumor promoter of TGF-β has been demonstrated via strongly induce plasminogen activator inhibitor-1 (PAI-1) synthesis, leading to a significant decrease in tissue-type plasminogen activator (tPA) and urokinase-type plasminogen activator (uPA) secretion, which in turn led to tumor growth inhibition in a mouse melanoma model (Ramont et al., 2003). On the other hand, metastasis has also been shown to be facilitated by TGF-β's induction of matrix metalloproteinase-9 (MMP9) and β1 and β3 integrins, downregulation of E-cadherin expression (Janji et al., 1999), as well as by enhancement of melanoma cell adhesion to the endothelium (Teti et al., 1997). Also, TGF-β stimulation of neighboring stromal fibroblasts which translated into an increased production and deposition of extracellular matrix proteins was shown to increase survival and metastasis of melanoma in mice (Berking et al., 2001).

3.5.2 Activin

Activin is a TGF-β-family cytokine, was initially found with its ability to stimulate follicle-stimulating hormone release by the anterior pituitary (Ling et al., 1986). Activin has known to regulate a variety of events, including cell proliferation, differentiation, apoptosis, homeostasis, immune response, wound healing and different endocrine functions (reviewed in Chen et al., 2006. In human, the two most common subunits are βa and βb expressed and, once subunits are linked, they either form the two homodimers activin A and activin B or the heterodimer activin AB. These ligands signal through the type II activin receptors (ActRII and ActRIIB) and the type I receptors ALK2, ALK4, and ALK7, with ALK4 being the most important signal transducing receptor which in turn phosphorylates R-SMADs; SMAD2/SMAD3 (Shi et al. 2011).

3.5.3 Activins in melanoma

The role of activin in cancer is not very clear however, mutations in several genes involved in the activin signaling pathway have been characterized. For instance, somatic ACVR1B gene mutations have been found in pancreatic carcinoma and Smad2 as well as Smad4 are mutated in colorectal and pancreatic carcinomas. Also, Activin A ligand is overexpressed in human skin cancer, as well as other tumors, and transgenic expression of activin A in mouse skin enhanced tumorigenesis through effects specifically on the local immune response, by increasing the number of TReg cells. Regarding tumor cell autonomous response, studies have been linked to activins effects on tumor cell growth. Increased activity of the pathway either by Cripto silencing or FLRG silencing inhibits human breast cancer cell growth. It has been shown that activin enhances the expression of $p15^{Ink4b}$, reduces the expression of cyclin A and phosphorylate pRb in breast cancer (Burdette et al., 2005). The inhibition of proliferation by activin has been supported by other studies with human tumors including cells from prostate and pituitary gland (reviewed in Chen et al., 2006). Nevertheless, activin has been shown to increase proliferation of ovarian cancer cell lines highlighting, the actions of activin in tumor growth are highly

context-dependent. (Steller et al., 2005), Alternatively, the pro-angiogenic role of activin is thought to be more crucial in cancer. Activin function as an inhibitor of angiogenesis. Overexpression of the activin gene in neuroblastoma cells has been shown to reduce the proliferation rate of primary tumors with reduced vascularity in a xenograft mouse model (Panopoulou et al., 2005). Recent work from Daniel B. Constam and co-workers provided an evidence with respect to the angiogenic role. They have shown that activin-A secretion stimulates melanoma cell dedifferentiation and tumor vascularization by functional blood vessels, and it increases primary and metastatic tumor burden. The differential expression of the β_B subunit in high- and low-metastatic melanoma cell lines suggested that activin may have a role in metastasis in melanoma (Hashimoto et al., 1996). The group of Stove et al. have been shown that melanocytes but not melanoma cell lines were growth inhibited by activin. These melanoma cell lines further show high expression levels of activin inhibitory molecule follistatin suggesting a model for an effective way to escape its growth inhibitory action Stove et al., 2004).

3.5.4. NODAL

NODAL is a developmental morphogen rarely detected in normal adult tissues and known to play a role in stem cell maintenance, regulation of organ development and positioning (Pereira et al. 2012;)The signaling typically initiates after binding to a receptor complex consisting of the EGF-like protein Cripto-1 and type I (ALK4/7) and type II (ActRIIB) Activin-like kinase receptor.(Kenney et al. 2004) A prominent role of NODAL signaling in the developing mouse embryo and in HESCs is to drive pluripotency and self-renewal (Galvin et al. 2010; Park 2011). NODAL signaling pathway has been considered as a very attractive target for tumor therapy since it is not expressed in adult tissues, and the CRIPTO 1 capable of potentiating this signaling pathway by acting as a coreceptor, is only expressed at low levels, but both are often reactivated in tumors (Lawrence et al. 2011; Friedman et al. 1995)

.

3.5.5 NODAL signaling in melanoma

The role in cancer for NODAL has recently been demonstrated in pancreatic cancer, where NODAL is essential to drive cancer stem cell renewal (Donahue & Dawson 2011). In a mouse model of pancreatic cancer, pharmacological inhibition of NODAL signaling in the cancer stem cells abolished their self-renewal capacity. In melanoma, the expression pattern of the NODAL protein and transcript in a panel of human normal, neoplastic and stem cell types have been screened (Donahue & Dawson 2011). This study revealed that, similar to human ES cells, melanoma cells express NODAL while in normal melanocytes its expression is not detected (Strizzi et al. 2012). In addition to being expressed in melanoma cells, same group identified that NODAL expression positively correlates with melanoma tumor progression toward a metastatic phenotype. NODAL is highly expressed by aggressive metastatic melanoma cell lines such as C8161, WM278 and 1205Lu, while expression is weakly detected or absent in non- metastatic melanoma cells. (Topczewska et al. 2006; Fang et al. 2013). Also, IHC analysis has demonstrated that NODAL protein is rarely observed in poorly invasive RGP melanomas however, expression is increased in up to 60% of cases with invasive VGP melanomas and melanoma metastases

Besides the role as a useful biomarker for melanoma progression, Nodal has also been demonstrated to be important for maintaining melanoma cell plasticity, invasiveness and tumorigenicity. The lab of Hendrix with functional studies have been proved that inhibition of NODAL abrogated melanoma growth, decreased expression of VE-cadherin, and prevented the formation of vasculogenic networks or channels-like structures, phenomenon named as vasculogenic mimicry (VM). Based upon these observations, other groups reasoned that expression of NODAL might be spatially associated with the VM in human melanoma. (Postovit et al. 2008; Topczewska et al. 2006). Humanized murine model for the study of VM in melanomas, Nodal mRNA expression was associated with tumor cells that in adjacent sections formed CD144-positive, CD31- negative channels. (McAllister et al. 2010). Additionally, increased staining intensity was focally associated with CD144-positive anastomosing channels. These data suggest that melanoma cells selectively express Nodal mRNA in a channeled

pattern typical of VM, and further support the key role of this ligand in melanoma progression. The role of Nodal in melanoma has been correlated with stem cell-like patterns of protein expression Hendrix and co-workers have been shown that expression of the Nodal coreceptor, Cripto-1, in a subset of slow-growing, sphere-forming malignant melanoma cells (Strizzi et al. 2012; Topczewska et al. 2006). These cells also expressed increased levels of stem cell markers Oct4 and Nanog. In this regard, Hendrix has speculated that Nodal expression in melanoma cells may correlate with a more potentially stem-like subpopulation of malignant cells within the tumor.

3.5.6. BMPs

BMPs are so called because they were originally discovered by inducing bone and cartilage formation. These proteins are the largest ligand subfamily in the TGF-ß superfamily of ligands dedicated to different functions. The BMP ligand family is composed of, following ligands: Bmp2, Bmp3, Bmp4, Bmp5, Bmp6, Bmp7, Bmp8a, Bmp8b, Gdf2 (also named Bmp9), Bmp10, Gdf11 (also named Bmp11), Gdf7 (also named Bmp12), Gdf5 (also named Bmp14), Gdf6 (also named Bmp13) and Bmp15. The role of BMP signaling in carcinogenesis is quite context dependent, i.e., both pro-tumor and anti-tumor effects have been described (Liu et al. 1996; Kretzschmar et al. 1997). The most prominent indication that BMP signaling pathways contribute to tumorigenesis comes from genetic studies of familial cancer syndromes. Mutation of BMPR-IA (Alk3) is genetically responsible for familial juvenile polyposis. (Nishanian & Waldman 2004). Other germ line mutations in BMPRIA (Alk3) have also been identified in a subset of families with Cowden syndrome, an inherited breast cancer syndrome (Zhou et al. 2001). In addition, it has been shown that various sporadic human cancers also exhibit aberrations in BMP ligand expressions. Overexpression of BMP2, 4, and 5 is observed in premalignant and malignant lesions of oral epithelium (Jin et al. 2001). In prostate cancer, BMP6 is found in metastatic lesions and its expression correlates with increased recurrence and decreased survival. Also, high levels of BMP7 were also detected in bone metastasis of prostate cancer. (Li & Koeneman 2009). Previous observations demonstrated that prostate carcinoma cells produce increasing amounts of BMPs as the disease progress

and the upregulation of BMP7 expression in metastatic cells is a critical component of the mechanism of developing osteoblastic lesions.(Li & Koeneman 2009) BMP7 is also upregulated in breast carcinoma and paradoxically its expression correlates with differentiation markers.

In colorectal carcinoma, BMP2 acts as a tumor suppressor and its expression is lost during the disease progression. Similarly, BMP2 is downregulated in breast cancer and BMP2 treatment inhibits growth of breast carcinoma cells in vitro. (Chapellier et al. 2015; Rosen 2009). BMP2 also exhibits antiproliferative and proapoptotic effects on myeloma, gastric, prostate, and ovarian. Indeed, BMP signaling has also been functionally associated to stimulate cell migration, tumor invasiveness, angiogenesis, and matrix remodeling. Specifically, BMP2, while growth-inhibitory in A549 lung carcinoma cells, enhances migration and invasion in an autocrine manner. In prostate cancer cells, BMP7 activates the VEGF promoter through an autocrine loop and upregulation of VEGF in turn, promotes angiogenesis and osteoblastic activity at bone metastatic sites. Despite the progress achieved revealing the functional significance of BMP pathways in carcinogenesis little is known about BMP signaling in melanoma.

3.5.7 BMPs in melanoma

Multiple BMPs are upregulated during melanoma progression. Upregulation of BMP 2, 6, 7 and 8 was found in melanoma cell lines compared to normal melanocytes (Rothhammer et al. 2005). At the transcript level screening of BMPs expression among isogenic cell lines isolated from the same patient at different disease stages has been shown that in particular, BMP7 correlates with tumor aggressiveness (Hsu et al. 2005). Forced expression of BMP7 resulted in growth inhibition of different melanocytic cells, however invasive melanoma cell lines show %50 less growth inhibition response compared control cell lines (Wang & Hirschberg 2003). It has been suggested that advanced melanoma cells escape from growth inhibition by BMP7 through upregulation of BMP antagonist, noggin.

3.5.8 Negative growth regulators and tumorigenesis

The paradigm that melanoma cells produce negative growth regulators, such as TGF-β, has been discussed by many scientists over the years. It is only until recently that advances in understanding molecular aspects of the TGF-β receptors, their signal transduction pathways, and their effects on gene modulation enabled the formulation of a widely accepted model, in which TGF-β plays a dual role in tumorigenesis. In early stages of tumor progression, TGF-β functions as a tumor suppressor critical for maintaining homeostatic control of growth. As the melanoma cells progress toward a more aggressive phenotype, they develop resistance to the growth-inhibitory and pro-apoptotic effects of TGF-β, while secreting ever-increasing quantities of TGF-β. In response to elevated TGF-β levels, the tumor cells become more migratory and invasive. Taken together, it is conceivable that like TGF-β, BMP7 may exert both anti-tumor and pro-tumor effects in melanoma progression that are dose- and context dependent. Despite the increased production of endogenous BMP7, advanced melanoma cells are resistant to growth inhibition through disruption of BMP7 signaling by noggin upregulation and high levels of BMP7 in turn promote metastasis through angiogenesis and matrix remodeling.

3.6 Phenotype Switching model

The classic Clark model depicts linear transformation of melanocytes to malignant melanoma and subsequent development of invasion and metastasis (Takata et al. 2010). To form metastases, tumor cells first have to acquire an invasive potential, which allows the cells to emigrate from the primary tumor, to reach the blood stream, and eventually to colonize distant organs. This process of invasiveness involves tightly regulated switch process of different cellular phenotypes. In melanoma, a very similar phenomenon, i.e. the dynamic and reversible transition from a proliferative to an invasive state, has also been described and is known as “phenotype switching”. The expression analysis of various human melanoma cell lines identified these phenotypes with very diverse gene expression profiles correlated with distinct behaviors *in vitro*. The highly proliferative, poorly invasive phenotype is characterized by

melanocytic differentiation markers whereas the highly invasive phenotype group is characterized by the expression of many genes whose expression is very similar to the EMT program during development (Vandamme & Berx 2014a).

The EMT program functions during the process of melanocytes to emerge from the neural crest cells and has shown to have a crucial role in acquisition of metastatic properties during the vertical growth phase of melanoma (Bennett 2008). Recently, EMT markers has been shown to have a fluctuating expression profile in various type of cancers as well as melanoma during the disease progression. The traditional transcription factors (EMT-TFs) during induction of EMT in many cancers act a repressor of E- Cadherin and include SNAIL1/2, ZEB1/2, and TWISTs. (Caramel et al. 2013; Thiery et al. 2009). However, among others, ZEB1, TWIST1 and ZEB2 found to have different levels of expression in normal melanocytes and different phenotypic states of melanoma cells. Analysis of normal epidermal melanocytes from a melanoma patient revealed low ZEB1 and high ZEB2 expression, whereas the melanoma cells at deep sites of the primary tumor from the same patient showed high expression of ZEB1 and low expression of ZEB2 (Caramel et al. 2013). The loss of ZEB2 in melanocytes resulted in dedifferentiation, and in melanoma cells resulted in increased ZEB1 expression and contributed to invasive behavior and metastasis (Denecker et al. 2014). Furthermore, immunohistochemistry analysis of a cohort of patient samples revealed high expression of ZEB1 and TWIST1, with low expression of ZEB2 corresponded with significantly reduced metastasis-free survival (Caramel et al. 2013). In the same study, SNAIL2 and ZEB2 transcription factors are found to be expressed in normal melanocytes and behave as tumor-suppressor proteins by activating an MITF driven melanocyte differentiation program whereas ZEB1 and TWIST1 repress this differentiation process and possess oncogenic properties. Consistent with the literature on the role of MITF in phenotype switching, these studies also proved that MITF was regulated by the switch in ZEB expression and downregulation of MITF lead to an invasive phenotype (Keith S Hoek & Goding 2010; Vandamme & Berx 2014b). In addition to switch in ZEB expression, several groups have proposed loss of E-cadherin/gain of N-cadherin (cadherin switch) was a major determinant of phenotype switching in melanoma and believed to responsible for melanoma cell detachment from the epidermis(Alonso et al. 2007). Only few studies correlated the

expression levels of cadherins with clinical outcome in patients with melanoma. These studies suggest that the interchange between epithelial-like and mesenchymal-like phenotypes is context dependent in different types of melanoma such as uveal melanoma, but the ability to switch phenotype in various types of melanoma has been implicated in conferring a higher risk of death due to metastasis. (Keith S Hoek & Goding 2010; Onken et al. 2006)

3.6.1 MITF and AXL

MITF (microphthalmia-associated transcription factor) characterizes a melanocytic lineage-specific transcription by regulating the expression of melanocyte differentiation genes such as tyrosinase, silver homologue (GP100) and melanoma-associated antigen recognized by T cells-1 (MART-1 or MELANA) (Levy et al. 2006). Also, it is known as the master regulator of melanocyte development as well as the crucial regulator for melanoma formation. MITF expression is heterogeneous and present in the majority of melanomas (Tsao, Chin, L. A. Garraway, et al. 2012). Alterations in MITF expression have been found in a relatively small subset of melanomas. However, *MITF* is still considered an oncogene after Garraway and co-workers detected *MITF* amplification in 10% of primary cutaneous and 15-20% of metastatic melanomas (Garraway et al. 2005). Furthermore, it has been shown that elevated MITF levels in synergy with activated MAPK signaling promote melanoma growth. On the other hand, distant metastasis showed low levels or absence of MITF expression. (Nazarian et al. 2010; Hodis, Ian R. Watson, et al. 2012; De Snoo & Hayward 2005). Thus, expression of MITF has been suggested to be used as a marker to distinguish melanoma cells in the proliferative or invasive state.

In addition to these observations, MITF was initially found to be essential in both the survival of melanoblasts migrating from the neural crest and in the differentiation process of the retinal pigment epithelium. (Opdecamp et al. 1997). Next, its role was implicated in the expression of differentiation genes important for the melanosome function as well as in the differentiation-associated cell cycle arrest via upregulation of the p16 and p21 cyclin-dependent kinase inhibitors (Garraway et al. 2005). However, other observations have proved its requirement for the inhibition of invasion and promotion

of proliferation via suppression of p27 protein together with upregulation of DIA1 protein (Carreira et al. 2006).

These studies allow Garraway and co-workers to draw a rheostat model for MITF function in melanoma. According to this model, low MITF is a hallmark of stem-like cells, whereas high MITF is characteristic for proliferative or differentiated cells depending on the expression levels. Alternatively, it also has been shown that transient MITF depletion generates a G1 arrested, high p27, invasive type cell that is predicted to have stem-like properties while longer-term MITF depletion in melanoma leads to senescence (Strub et al. 2011) (Figure 8). Thus, understanding the properties of MITF-low cells and MITF-high cells is still a key issue that could have important implications for melanoma therapy.

Other groups working on the role of MITF in melanoma have extended the rheostat model in association with resistance to MAPK inhibitors. For instance, increased MITF expression causes resistance to ERK inhibition and is consistent with other reports showing that MITF is sufficient to render melanoma cells resistant to MEK or ERK inhibitor-induced cell death (Smith et al. 2013; Huang et al. 2013). In contrast, sensitive melanomas also exhibited high activity of MITF and high expression levels of downstream differentiation markers like *TYRP1*, *MLANA*, and *PMEL*. However, knock down of MITF expression in these sensitive cell lines induced a phenotypic transition towards resistance (Wellbrock & Marais 2005).

Another main finding in mechanism for melanoma resistance is that the expression of MITF is commonly deregulated. Both MITF-high and MITF-low resistant tumors were found *in vivo*. During treatment with a MAPK pathway inhibitor, up to 75% of melanomas expressed increased MITF expression. However, only around 25% of high MITF melanomas progressed further. (Smith et al. 2016). Recent works have clarify that the high expression of MITF could also contribute to resistance (Konieczkowski et al. 2014; Tirosh et al. 2016; Smith et al. 2013) . It is not very clear why MITF expression can be upregulated in resistant melanoma cells but some studies have demonstrated that the

upregulated expression levels of the MITF target genes such as BCL2A1 and PGC1α are important for resistance to MAPK pathway inhibition. (R. Haq et al. 2013; Rizwan Haq et al. 2013)

Analysis of MITF-low subset of melanoma cells lacking melanocyte differentiation antigens have shown to express high levels of receptor tyrosine-kinases such as AXL (Sensi et al. 2011). Smith and co-workers demonstrated that almost 50% of melanoma tumors that have progressed after MAPK pathway inhibition have decreased MITF expression. Moreover, these cells show more invasive phenotype than the MITF-high subset of resistant cells. (Smith et al. 2016). Previously, microarray analysis of several BRAF and NRAS mutated melanoma cell lines revealed that MITF and AXL belong to two gene expression patterns association with two distinct phenotype (Hoek, Schlegel, et al. 2008). Melanoma cells with the AXL signature were also found to be less responsive to a wide range of inhibitors and identified as a novel mechanism for acquired resistance (Müller et al. 2014; Aplin 2011; Konieczkowski et al. 2014). Additionally, both in primary and acquired resistance, MITF levels inversely correlated most frequently with the expression of AXL. (Müller et al. 2014). Same group has proved that low MITF/AXL ratio predicts early resistance to targeted therapy and MITF-low/AXL-high/drug-resistance phenotype is common among mutant BRAF and NRAS melanoma cell lines. These observations revealed that MITF low and AXL high gene expression program correlates with MAPK inhibitor resistance in melanoma patients However, the cause of upregulation of AXL expression in melanoma cell lines is not fully understood. Not only for melanoma but also for other type of cancers AXL is a marker for resistance to various targeted therapies (Garraway et al. 2005; Chen et al. 2008; Wu et al. 2014). It is not implicated as an oncogenic driver itself, but AXL is often overexpressed in acute myeloid leukaemia (Estey & Döhner 2006). Not only for melanoma but also for other type of cancers AXL is a marker for resistance to various targeted therapies (Garraway et al. 2005; Chen et al. 2008; Wu et al. 2014). It is not implicated as an oncogenic driver itself, but AXL is often overexpressed in acute myeloid leukaemia (Estey & Döhner 2006). It is a member of the TYRO3, AXL, and MERTK family of receptor tyrosine kinases (Graham et al. 2014).

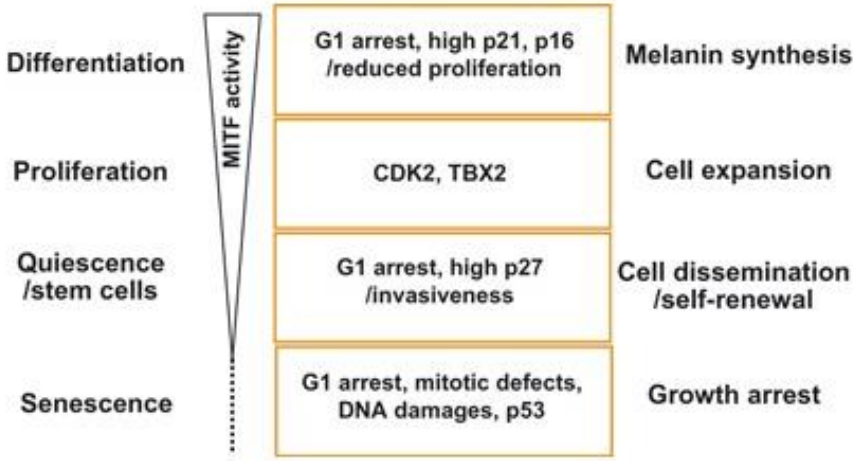

Figure 8. High MITF level is associated with differentiation and intermediate level with proliferation. MITF regulates distinct functions in melanocytic cells at different levels of expression Melanoma cells may switch from a quiescent dedifferentiated ('stem-like') phenotype MITF-low to a proliferative phenotype MITF intermediate and finally to a differentiated, again cell cycle arrested phenotype MITF-high (adapted from Carreira et al., 2006)

It is a member of the TYRO3, AXL, and MERTK family of receptor tyrosine kinases (Graham et al. 2014). The majority of AXL signaling occurs in a ligand dependent manner mediated by GAS6 and activating mutations within the AXL kinase domain are rarely found in cancer (The Cancer Genome Atlas, TCGA). AXL signaling can be activated by GAS6 in an autocrine or paracrine manner and clinically, GAS6 expression in tumor specimens has been shown to be an prognostic factor in urothelial, ovarian, lung adenocarcinoma, gastric cancer, and glioblastoma (Wu et al. 2014). Aside from these observations, single-cell RNA sequencing by Tirosch and co-workers have allowed for the identification of gene expression programs that are associated with rare drug-resistant populations within human melanoma tumors (Tirosh et al. 2016). Although the distinction between $AXL^{high}/MITF^{low}$ *vs.* $AXL^{low}/MITF^{high}$ phenotypes was used to classify melanomas at the bulk tumor level (Müller et al. 2014), single cell RNA sequencing of human melanoma samples has recently led to the identification of a fraction of double-positive $AXL^{high}/MITF^{high}$ cells the function of which remains to be elucidated (Tirosh et al. 2016).

4. Approaches to investigating the roles of TGF-β signaling in melanoma

During melanoma progression, malignant cells become resistant to the anti-proliferative effect of TGF-β and the growth factor even promotes tumor aggressiveness at the later stages. Up to now, this knowledge has been gained with *in vitro* experiments. To address the role of TGF-β signaling in melanoma development in an *in vivo* model, we took the advantage of the murine Tyr::NRas^{Q61K} INK4a$^{-/-}$ melanoma model mice which develops congenital nevi and subsequently primary tumors in 6 months. We clarified the significance of TGF-β signaling for the initiation and progression of melanoma by manipulating the canonical TGF-β pathway in the melanocytic lineage of Tyr::N-Ras^{Q61K}INK4a$^{-/-}$ mice. We conditionally ablated key players the TGF-β pathway – either TGF-βRII or SMAD4 to fell TGF-β signaling or the main negative regulator SMAD7 to preserve an active signaling cascade. To supplement our *in vivo* findings, we will conduct *in vitro* assays on cell cultures also established from patient derived human melanoma cells.

According to our results, we have evidence that in this mouse model, melanoma arises from the bulge region of the hair follicle. Thus, it is likely that upon N-Ras activation MSCs escape the inhibitory effect of TGF-β and become malignant. We aimed to conditionally ablate TGFβ-RII and SMAD4 in the melanocytic lineage of tumor developing mice at early and late time points. At the time point of tumor initiation lack of TGF-β signaling might support tumor formation, but at later stages, when melanoma cells become TGF-β dependent, TGFβ-RII ablation might prevent further tumor development and metastasis. To complement the studies, we will also conditionally ablate Smad7, an inhibitory key player in the TGF-β pathway (Moustakas and Heldin, 2009). This allows us investigating, whether constantly active TGF-β signaling is sufficient to prevent melanoma initiation. With these studies, we intend to gain knowledge about the *in viv*o function of TGF-β signaling in melanoma initiation and progression.

5. My Contribution to the projects

In the course of my doctorate, I contributed to several projects in Prof. Lukas Sommer Lab; First year, I helped my supervisor Dr. Daniel Zingg with respect to experiments. These results have been accepted for publication and gave a new insight about the novel role of epigenetic modifier EZH2 in melanoma initiation and progression in the cancer field.

- **The epigenetic modifier EZH2 controls melanoma growth and metastasis through silencing of distinct tumour suppressors,** Daniel Zingg,[1] Julien Debbache,[1] Simon Schaefer **Eylul Tuncer**,[1] Phil F. Cheng, Yudong Zhang,[1] Raquel Calçada,[1] Jessica Haeusel,[1] Mitchell P. Levesque,[2] Kwok-Kin Wong,[3] Reinhard Dummer,[2] and Lukas Sommer[1.] ***Nat Communication 2015***
- **EZH2-mediated primary cilium deconstruction drives metastatic melanoma formation** Daniel Zingg,[1] Ana T. Antunes,[1] Simon. M. Schaefer,[1] Julien Debbache,[1] Phil F. Cheng,[2] **Eylul Tuncer,**[1] Yudong Zhang,[1] Raquel Calçada,[1] Jessica Haeusel,[1] Mitchell P. Levesque,[2] Kwok-Kin Wong,[3] Reinhard Dummer,[2] and Lukas Sommer[1] ***Under Revision Cancer Cell 2017***

The project deciphering the role of TGF-β Signaling in melanoma formation and progression was started by Dr. Daniel Zingg. He established Smad7lox/lox and TgFBrII lox/lox melanoma prone mice. have analyzed the phenotypes and gained more experience with transgenic murine melanoma models. (The data for TGFBRII mice is not shown due to the absence of phenotype). In the following years, I have established the Smad4 lox/lox colony in melanoma prone background. I conducted the majority of *in vivo* and *in vitro* experiments and analyzed most of the data. The results are illustrated in my Phd. thesis and recently accepted for revision in Journal Clinical investigations.

- **SMAD signaling promotes melanoma metastasis independently of phenotype switching** **Eylül Tuncer[1]**, Daniel Zingg[1], Sandra Varum[1], Phil Cheng[2], Sandra N. Freiberger[2], Chu-Xia Deng[3], Ingo Kleiter[4], Mitchell P. Levesque[2], Reinhard Dummer[2], and Lukas Sommer[1] ***Under Revision 2017 JCI***

6. Results

6.1 Journal of Clinical Investigations Under Revision 2017

SMAD signaling promotes melanoma metastasis independently of phenotype switching

Eylül Tuncer[1], Daniel Zingg[1], Sandra Varum[1], Phil Cheng[2], Sandra N. Freiberger[2], Chu-Xia Deng[3], Ingo Kleiter[4], Mitchell P. Levesque[2], Reinhard Dummer[2], and Lukas Sommer[1*]

[1]Stem Cell Biology, Institute of Anatomy, University of Zurich, Winterthurerstrasse 190, CH-8057 Zurich, Switzerland

[2]Department of Dermatology, University Hospital Zurich, Gloriastrasse 31, CH-8091 Zurich, Switzerland

[3]Faculty of Health Sciences, University of Macau, Macau SAR, China

[4]Department of Neurology, University Medical Centre Regensburg, Universitätsstraße 84, D- 93053 Germany

***Correspondence:** Lukas Sommer, Institute of Anatomy, University of Zurich Winterhurerstrasse 190 CH-8057, Zurich Switzerland

Phone: Tel.: +41 44 63 55443;

Fax: +41 44 63 56895;

*E-mail: lukas.sommer@anatom.uzh.ch (L.S)

Conflicts of Interest

The authors declare no competing financial interests.

6.1 Abstract

Malignant progression of melanoma is thought to require the dynamic shifting of neoplastic cells between proliferative and invasive phenotypes. Contrary to this conventional "phenotype switching" model, we now show that augmented SMAD-dependent signaling in melanoma leads to emergence of malignant cells simultaneously displaying proliferative and invasive properties. Specifically, conditional deletion of *Smad4*, which abrogates canonical SMAD signaling, prevented tumor initiation, proliferation and metastasis formation *in vivo*, pointing to the requirement of both pro-proliferative and pro-invasive TGF-β superfamily factors for metastatic melanoma formation. Ligand screening identified BMP7 to promote melanoma cell proliferation even in the presence of pro-invasive TGF-β factors. However, an invasive phenotype was induced in melanoma cells upon inactivation of the inhibitory SMAD factor SMAD7, surprisingly without counteracting melanoma cell proliferation. Consequently, conditional *Smad7* deletion *in vivo* sustained melanoma growth and at the same time promoted massive metastasis formation. Together with clinical data analysis, our findings indicate that modulation of SMAD7 levels triggers malignant transformation of melanoma by overcoming phenotype switching.

6.1 Introduction

Despite recent progress in therapy, melanoma is still by far the deadliest skin cancer, *with a f*ive-year survival rate of only 15% to 20% (Rebecca L Siegel et al. 2016). It is thought that the aggressiveness of the disease is largely due to an intrinsic plasticity of melanoma cells, allowing the dynamic and reversible switching from a high proliferative/low invasive to a low proliferative/high invasive state (Goding 2011; Cheli et al. 2011).This so-called "phenotype switching" has been functionally associated with metastasis formation and therapy resistance (Schlegel et al. 2015; Hoek, Eichhoff, et al. 2008; Hölzel & Tüting 2016). At the transcriptional level, the phenotype switching model has been linked to a shift between a transcriptional program governed by high expression of the microphthalmia associated

transcription factor (MITF), a melanoma lineage-survival oncogene, and a transcriptional program associated with high expression of the receptor tyrosine kinase AXL, a marker for resistance to various targeted therapies (Garraway et al. 2005; Chen et al. 2008; Wu et al. 2014). In contrast to proliferative melanoma cells characterized by high MITF expression, $MITF^{low}$ cells with high invasive properties were shown to be linked to G1 cell cycle arrest (Carreira et al. 2006). However, while the distinction between $AXL^{high}/MITF^{low}$ *vs.* $AXL^{low}/MITF^{high}$ phenotypes was used to classify melanomas at the bulk tumor level (Müller et al. 2014), single cell RNA sequencing of human melanoma samples has recently led to the identification of a fraction of double-positive $AXL^{high}/MITF^{high}$ cells the function of which remains to be elucidated (Tirosh et al. 2016).

Phenotype switching has also been linked to tumor progression in several epithelial tumors (Yao et al. 2010; Thomson et al. 2008). In those cases, a reversible epithelial-to-mesenchymal transition (EMT) promotes invasiveness and stem cell-like features in cancer cells (Valastyan & Weinberg 2011), which is driven by a network of embryonic EMT-inducing transcription factors (EMT-TFs) of the SNAIL, TWIST, ZEB, and bHLH/E47 protein families (Lamouille et al. 2014). Although melanoma is not an epithelial tumor, an EMT-like process can be observed in cell culture and has been associated with metastatic spread of the disease (Vandamme & Berx 2014b). In particular, activation of the MAPK pathway by oncogenic BRAF or NRAS promotes a switch from SNAIL2/ZEB2 expression to expression of TWIST1 and ZEB1, which enhance invasiveness of melanoma cells (Caramel et al. 2013).

One of the major candidate pathways for driving reversible phenotype switching is SMAD-dependent TGF-β superfamily signaling, which controls EMT in many cancers (Javelaud et al. 2008; Massagué 2012). Sustained expression of EMT-TFs in breast cancer cells is directly regulated by autocrine TGF-β signaling (Gregory et al. 2011). In melanoma, different TGF-β isoforms, NODAL as well as different BMP ligands were shown to be expressed by tumor cells and to promote invasiveness in cell culture or in organotypic human skin cultures (Fang et al. 2013; Hoek, Eichhoff, et al. 2008; Rothhammer et al. 2007; Schlegel et al. 2015; Topczewska et al. 2006). In support of this, attenuation of TGF-β signaling

by overexpression of SMAD7, an inhibitory SMAD protein (Yan et al. 2009b), or by treatment with a small molecule inhibitor, reduced bone metastasis formation by cells injected into the cardiovascular system in immunocompromised mice (Javelaud et al. 2007; Mohammad et al. 2011).

However, other studies reported that melanoma cells exhibit partial resistance to the anti-proliferative activity of TGF-β family factors (Rodeck et al. 1999). Moreover, TGF-β dependent SMAD signaling and transcription was not restricted to invasive cells, but also observed in proliferative human melanoma cells (Rodeck et al. 1999). Likewise, in human tissue samples, nuclear pSMAD2/3 which mediates canonical TGF-β signaling was detected at all stages of the disease, including in benign hyperplastic lesions, cutaneous primary melanoma, as well as invasive melanoma (Lo & Witte 2008). Finally, inhibition of SMAD2/3 signaling by SMAD7 overexpression not only affected the invasiveness of melanoma cells, but also reduced their capacity to grow *in vitro* and upon transplantation into immunocompromized mice (Javelaud et al. 2007).

The combined data suggest that SMAD-mediated signaling may exert various functions in melanoma, which are likely influenced by the cellular context and the TGF-β superfamily ligands the tumor cells are exposed to (Massagué 2012). Therefore, in an attempt to mimic the tumor microenvironment with respect to TGF-β-dependent SMAD signaling, we treated melanoma cells with various combinations of TGF-β family factors and addressed the relevance of overall TGF-β/SMAD signaling in melanoma *in vivo* by means of a genetic mouse model, in which tumors emerge spontaneously within an undisturbed 3D environment. Accordingly, we searched for factors modulating the proliferative and invasive capacities of melanoma cells and revealed SMAD7 to control transcriptional programs associated with concomitant $MITF^{high}/AXL^{high}$ expression and increased macrometastasis formation. These experiments identify integrated SMAD signaling as a key driver of melanoma initiation, growth, and metastatic progression, pointing to a new therapeutic vulnerability in melanoma.

6.1.1 Conditional *Smad4* deletion in a genetic mouse model of melanoma prevents tumorigenesis by reducing tumor cell proliferation

To investigate the function of integrated TGF-β superfamily signaling in melanoma we used a genetically engineered mouse model in which spontaneous melanoma formation is induced by expression of *Tyr::Nras*^{Q61K} on an *Ink4a*-deficient background (Ackermann et al. 2005). Downstream of TGF-β superfamily signaling, the receptor-associated SMAD (R-SMAD) proteins SMAD2/3 and SMAD1/5/8 are activated by TGF-β/ACTIVIN/NODAL or BMP signals, respectively (Goumans et al. 2003; Liu et al. 1996). Activated R-SMADs interact with the common partner SMAD4, which is essential for all canonical transcriptional responses (Schmierer & Hill 2007). To generate conditional *Smad4*-deleted melanocytes in our murine melanoma model, we crossed *Tyr::Cre*^{ERT2} *Smad4*$^{lox/lox}$ *R26R::LacZ Tyr::Nras*^{Q61K} *Ink4a*$^{-/-}$ with *Smad4*$^{lox/lox}$ *R26R::LacZ Ink4a*$^{-/-}$ mice (Figure 1A). To achieve inducible Cre-dependent recombination and thus loss of Smad4 expression, mice were injected intraperitoneally with tamoxifen (TM) at 1 month of age for 5 consecutive days, followed by their analysis at given time points after tumor formation in control mice (Figure 1B). Recombination efficiency was 66 ± 6%, as assessed by counting the percentage of cells with *R26R::LacZ*-mediated β-galactosidase expression among Pax3-positive melanocytic cells in hyperplastic lesions 2 months after TM injection. Depletion of *Smad4* at a stage before appearance of cutaneous melanoma in control mice resulted in a marked decrease of hyperplastic dermal lesions (Figure 1C). While hair follicles were mostly associated with ectopic pigmentation in *Tyr::Nras*^{Q61K} *Ink4a*$^{-/-}$ mice (76 ± 5% hair follicles with ectopic pigmentation), *Smad4* ablation inverted this phenotype towards a pigmentation pattern typical for wild-type mice (13 ± 3% hair follicles with ectopic pigmentation) (Figure 1D). Cells positive for the melanocytic marker Pax3 in hyperplasia of *Smad4*-ablated animals were also positive for β-Galactosidase, suggesting that Smad4 is not essential for the survival of the melanocytic lineage (Figure 1, E and F). Importantly, loss of *Smad4* was also associated with a significant decrease in the number

of recombined skin melanomas (Ø ≥ 2mm), which readily emerged in control mice after approximately 5 months of age (Figure 1, G and H). Consistent with the decreased skin tumor load, *Smad4* conditional knock out (cKO) mice displayed strongly reduced numbers of metastatic lung nodules as compared to control animals (Figure 1I). Consequently, melanoma-specific survival was highly increased in *Smad4* cKO mice (Figure 1J).

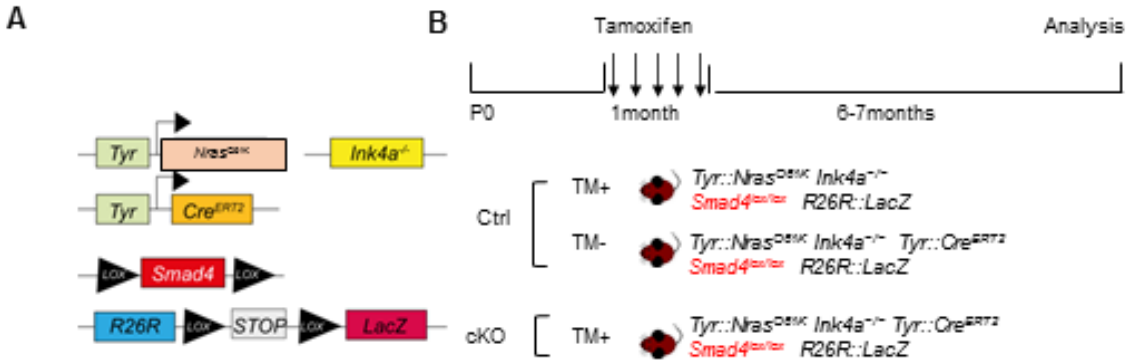

Figure 1 Conditional *Smad4* deletion in a genetic mouse model of melanoma prevents tumorigenesis (**A**) Schematic of the melanoma mouse model used in this study, which harbors *NrasQ61K*, *Ink4a−/−*, *Tyr::CreERT2* and *R26R* Cre-reporter alleles. (**B**) Experimental strategy used to analyze early loss of *Smad4* in *Tyr::NrasQ61 Ink4a−/− Tyr::CreERT2 R26R::LacZ* mice.

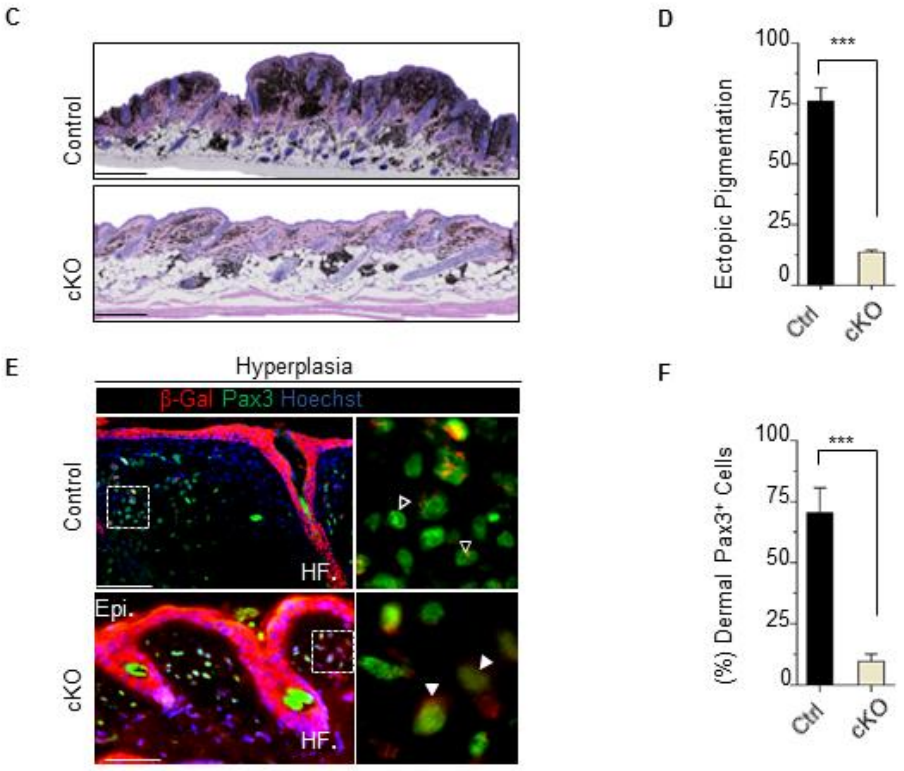

Figure 1. Continues Conditional *Smad4* deletion in a genetic mouse model of melanoma prevents tumorigenesis (**C**) Representative hematoxylin and eosin staining of trunk skin sections of control and cKO mice at day of sacrifice showing dermal hyperpigmentation. (**D**) Quantification of the percentage of hair follicles exhibiting ectopic pigmentation in control and cKO mice (n = 350 hair follicles quantified from six different mice for each genotype). (**E**) Immunofluorescent staining for Pax3 (control) and Pax3/β-Gal (cKO) on back skin sections at 6 months to quantify extent of dermal hyperplasia. Open arrowheads indicate Pax3-positive, white arrowheads Pax3/β-Gal double-positive cells. (**F**) Quantification of the percentage of dermal Pax3 cells between hair follicles. (n= 300 hair follicles from six different mice for each genotype.

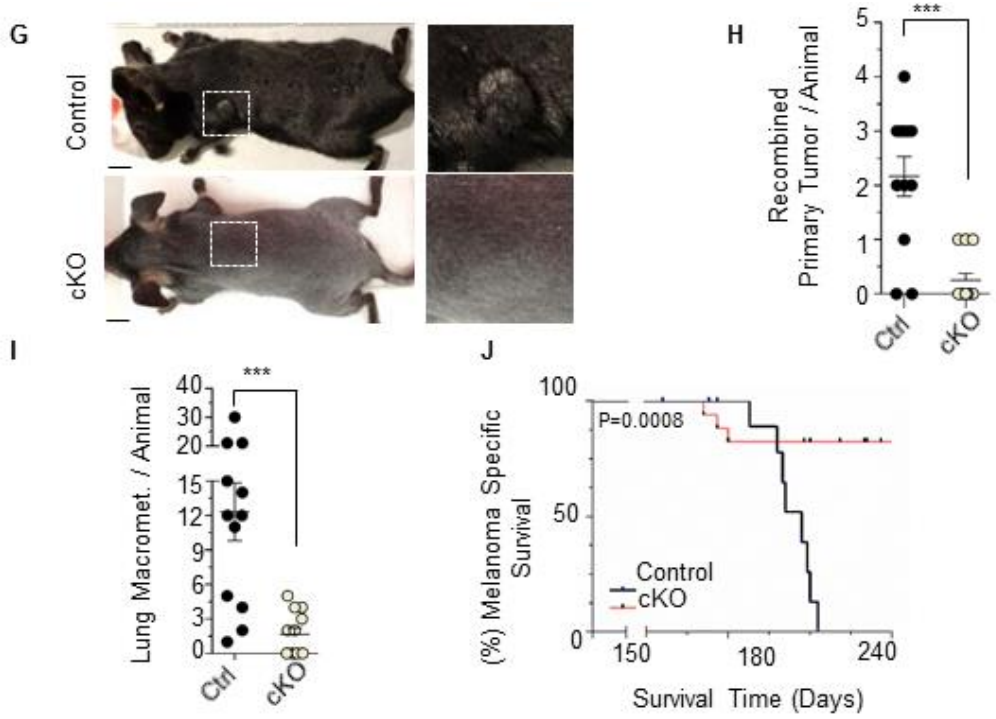

Figure 1. Continues Conditional *Smad4* deletion in a genetic mouse model of melanoma prevents tumorigenesis (**G**) Macroscopic pictures of a control and a *Smad4* cKO littermate at 6 months post *Smad4* ablation. (**H**) Quantification of recombined primary tumor numbers per control and cKO mice at the day of sacrifice (n=10). (**I**) Quantification of lung macro-metastases counts at day of sacrifice using macroscopic pictures and staining on sections (n=12). (**J**) Kaplan–Meier curves comparing melanoma-specific survival of control and *Smad4* cKO animals (n=12 (cKO), n=12 (control)). Data represented as a mean of three independent experiments ± SEM. p<0.001***. P values calculated with unpaired Student's t-test (**D, F, H**) and (**I**), log-rank Mantel–Cox test (**J**). HF, hair follicle; Epi, Epidermis; TM, tamoxifen. Scale Bars, 50µm (**E**), 500µm (**C**), 500µm (**G**)

6.1.2 Loss of Smad4 leads to decreased proliferation in established skin tumors

Our findings reveal a requirement for *Smad4* in melanoma initiation. To address the cellular mechanism mediated by Smad4-dependent signaling, we conditionally deleted *Smad4* by TM treatment at a stage when skin melanoma had already appeared in *Tyr::Nras*^{Q61K} *Ink4a*$^{-/-}$ *Tyr::Cre*^{ERT2} *Smad4*$^{lox/lox}$ *R26R::LacZ* mice (Figure 2A). No obvious phenotypic and cellular differences were observed between heterozygous *Smad4*$^{lox/wt}$ and *Smad4*$^{wt/wt}$ mice on a melanoma-driving genetic background. Hence, *Tyr::Nras*^{Q61K} *Ink4*$^{-/-}$ *Tyr::Cre*^{ERT2} *Smad4*$^{lox/wt}$ *R26R::LacZ* animals were used as control animals for further analysis. High recombination efficiency was apparent at the day of sacrifice (Figure 2B). While apoptosis in recombined melanoma cells was generally low in *Smad4* cKO mice and comparable to levels seen in control melanoma tissue, labeling of β-galactosidase-positive recombined cells with the proliferation marker Ki67 demonstrated significantly reduced proliferation in *Smad4* cKO melanoma cells *in vivo* as compared to control melanoma cells (Figure 2, C-E). Indeed, whereas recombined control tumors harbored 44 ± 5% Ki67 / β-galactosidase double-positive cells, this number was reduced to 13 ± 2% in *Smad4* cKO mice upon TM-induced Cre-mediated recombination (Figure 2D). We next ascertained if the altered proliferation rate observed *in vivo* was due to changes in melanoma cell cycle progression. For this purpose, we performed RNA interference-mediated silencing (siRNA) of *SMAD4* in human melanoma cells (Figure 2, F and G). Of note, the percentage of cells in G1/G0 phase in siSmad4-transfected cultures was increased relative to the siControl-transfected cells, indicating that downregulation of *Smad4* expression suppressed cell cycle progression by promoting a G1/G0 cell cycle arrest. Thus, Smad4-mediated signaling is required not only for the formation, but also for the proliferation of melanoma lesions, indicating that it promotes rather than counteracts tumor growth *in vivo.* Strikingly, even when *Smad4* was depleted in our mouse model only once skin tumors were established, tumor-bearing mice exhibited significantly increased survival (Figure 2, H and I), revealing a crucial requirement for canonical TGF-β superfamily signaling for melanoma progression.

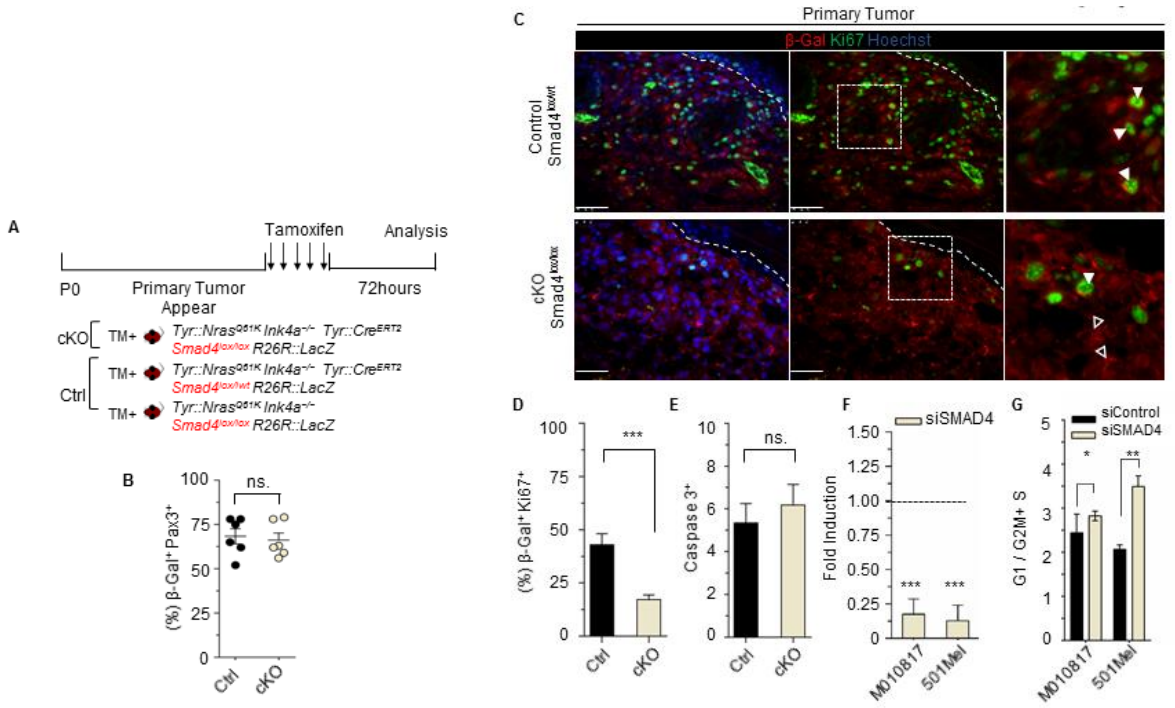

Figure 2. Loss of Smad4 leads to decreased proliferation in established skin tumors (**A**) Experimental strategy used to analyze the deletion of *Smad4* in already established skin melanomas. *Tyr::NrasQ61K Ink4-/- Tyr::CreERT2 Smad4lox/wt R26R::LacZ* and *Tyr::NrasQ61KInk4-/- Smad4lox/lox R26R::LacZ* used as control animals. (**B**) Recombination efficiency was calculated by counting percentage of β-gal/Pax3-double positive cells on primary tumor sections (n=6, cKO and control). (**C**) Representative immunofluorescent co-staining of Ki67 with β-Galactosidase on skin melanoma sections 72 hours after conditional deletion of *Smad4*. White arrowheads indicate Ki67/β-Gal double-positive cells, open arrowheads Ki67-negative/β-Gal-positive cells. (**D**) Quantification of Ki67 and β-Gal double-positive cells in control and cKO mice (n=4). (**E**) Quantification of apoptotic cells by IHC for activated caspase-3 on skin sections of control and cKO mice (n=4). (**F**) Reverse transcription qPCR (RT–qPCR) for expression of *SMAD4* in M010817 and 501Mel after siRNA treatment. (**G**) Quantification of the ratio of cells in G1 phase to cells in S, G2 and M phases upon SMAD4 knockdown in M010817 and 501Mel cell lines.

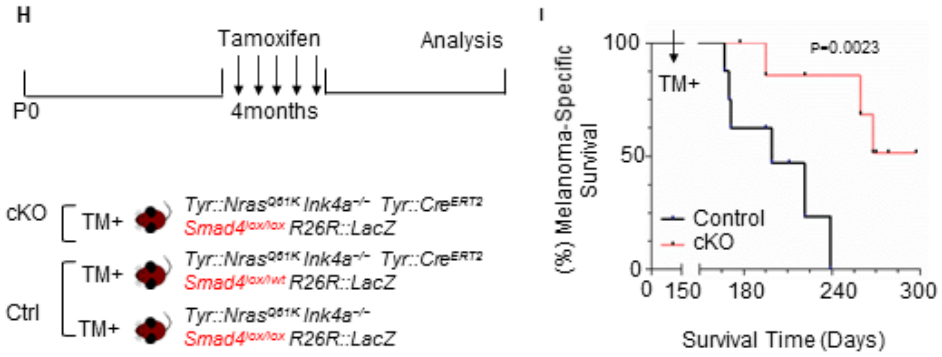

Figure 2 ***Continues*****. Loss of Smad4 leads to decreased proliferation in established skin tumors.** (**H**) Experimental strategy used to analyze effects on survival upon late deletion of *Smad4* in *Tyr::NrasQ61K Ink4-/-* melanoma murine model. (**I**) Kaplan–Meier curves comparing melanoma-specific survival of control and *Smad4* cKO animals (n=11 (cKO), n=8 (control)). Data represented as the mean ± SEM. ns. non-significant, p< 0.01**, p< 0.001***. P values calculated with unpaired Student's t-test (**D-G**) or with log-rank Mantel–Cox test (**I**). TM, tamoxifen. Scale Bars, 50µm.

6.1.3 BMP7 signaling promotes melanoma cell growth

Until now, members of the TGF-β superfamily have been associated with cytostatic and/or pro-invasive functions in melanoma cells (Siegel & Massagué 2003). However, our *in vivo* data indicate that one or more factors that signal through Smad4 must have the opposite effect, supporting tumor cell proliferation rather than cell cycle arrest. Most of the TGF-β family ligands known to elicit responses in human melanoma cells are expressed by the tumor cells themselves, where they induce their own expression through a positive amplification loop (Fimmel et al. 1999; Rothhammer et al. 2005; Stove et al. 2004; Topczewska et al. 2006). Likewise, several TGF-β superfamily factors, including notably TGF-β2 and BMP7, were concomitantly expressed by tumors derived from *Tyr::Nras^{Q61K} Ink4a$^{-/-}$* mice (Supplemental Figure 1A). Thus, we functionally investigated these factors in order to explore ligands potentially responsible for melanoma cell proliferation. Cell cycle analysis revealed that, among the factors analyzed, BMP7 could stimulate cell cycle progression in the two cell lines tested, with a

significant increase from 18 ± 1% and 18 ± 2% of cells in S phase in control cultures to 22 ± 3% and 24 ± 3% after BMP7 treatment, respectively (Supplemental Figure 1, B and A). In contrast, the other TGF-β superfamily factors tested suppressed proliferation in human melanoma cells, as previously reported (Topczewska et al. 2006; Schlegel et al. 2009) (Supplemental Figure 1B and C). TGF-β2 and NODAL have been shown to induce invasiveness in melanoma cells (Topczewska et al. 2006; Schlegel et al. 2015). In agreement with these earlier reports, human melanoma cells exposed to TGF-β2 or NODAL, as much as BMP4, changed their morphology and exhibited a decreased cell-substrate adherence capacity (Supplemental Figure 1D). In contrast, BMP7 did not affect adhesiveness of human melanoma cells (Supplemental Figure 1D).

To corroborate our data, we correlated expression levels of BMP7 and TGF-β2 with RNA-seq data obtained from *various* proliferative and invasive human *melanoma cell* lines in *culture.* Among others, TGF-β2 mRNA was robustly expressed in patient-derived cell cultures representing an invasive melanoma phenotype ($WNT5A^{high}$, $SOX9^{high}$, $ZEB1^{high}$, AXL^{high}) (Supplementary Fig. S1e). In contrast, markers for proliferative melanoma cells ($SOX10^{high}$, $MITF^{high}$) correlated with BMP7 expression levels (Supplemental Figure 1E).

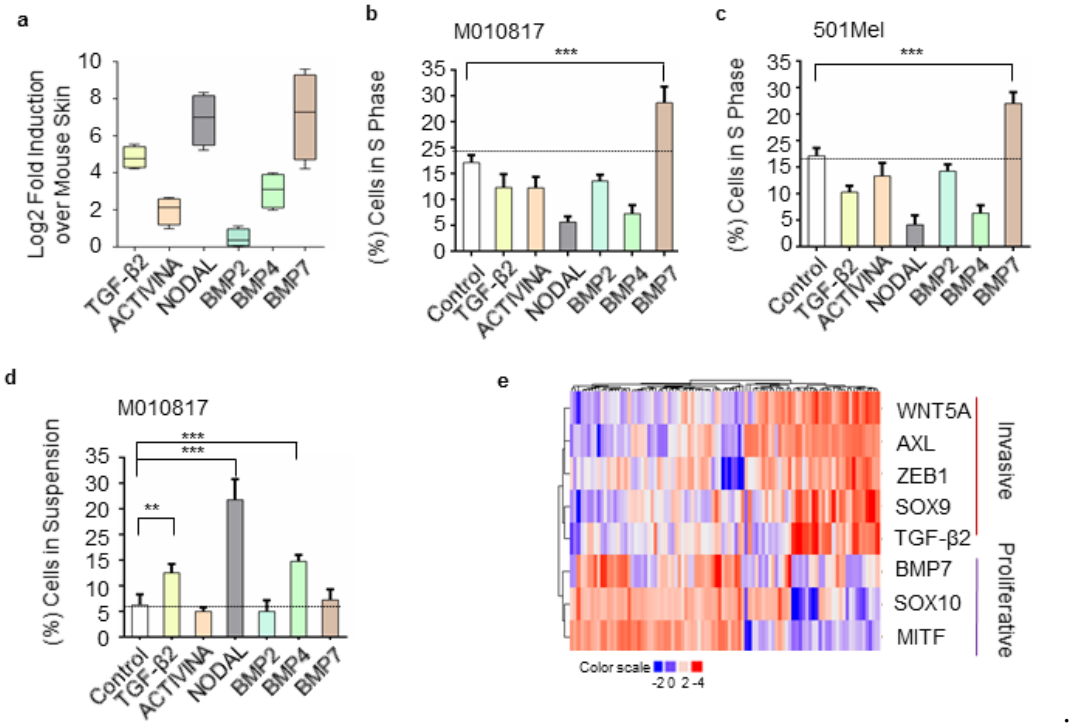

Supplementary Figure S1 BMP7 signaling promotes melanoma cell growth (a) *log2* Fold change of ligand mRNAs in primary tumors derived from *Tyr::NrasQ61K Ink4-/-* murine melanoma model (n=7). qRT–PCR data represent the mean of transcript levels (Log2) in three biological samples for each condition. Boxplot whiskers indicate minimum and maximum expression. (**b-c**) M010817 and 501Mel cells were starved prior to 48 hours ligand treatment, using the ligand concentrations mentioned in Supplementary Table S7. Cells were stained with propidium iodide (PI) together with EdU and fluorescence intensity was measured by FACS analysis. Bars represent the percentage of cells distributed in S cell cycle phase. (**d**) Quantification of cell-substrate adherence capacity of melanoma cells. Cells in suspension that had detached upon ligand treatment were re-seeded on fibronectin-coated plates and adherent cell colonies were stained with crystal violet. The area covered by re-attached cells was calculated by Cell Profiler. (**e**) Clustering of RNA-seq-based expression data revealing invasive and proliferative cell states *in vitro.* Samples in the invasive cluster have high expression of the following genes: WNT5A, AXL, ZEB1, SOX9, and TGF-β2. Genes with high expression in the proliferative sample cluster include BMP7 and known markers of the melanocyte lineage and melanoma, such as SOX10 and MITF**.** Correlations of RNA-seq expression data was as follows: BMP7 and MITF r= 0.43 ***p<0.001, BMP7 and SOX10 r=0.39 ***p<0.001, TGF-β2 and ZEB1 r=0.33 **p<0.01, TGF-β2 and AXL r=0.55 ***p<0.001, TGF-β2 and WNT5A r=0.63, TGF-β2 and SOX9 r=0.29, **p<0.01.

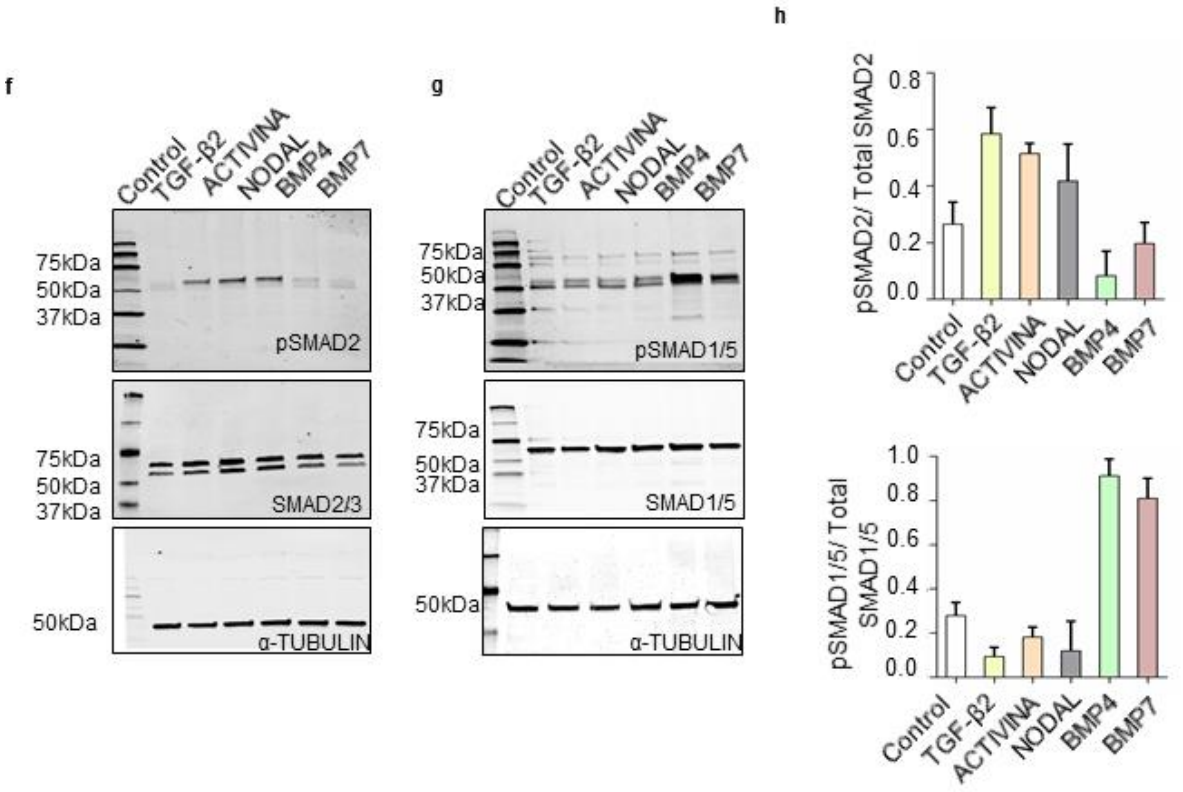

Supplementary Figure S1 ***Continues*****. BMP7 signaling promotes melanoma cell growth** pSMAD2/3 and pSMAD1/5/8 were detected in melanoma cells upon ligand treatment by using western blot analysis. (**h**) Quantification of western blot analysis, phosphorylation levels of SMAD2/3 and SMAD1/5/8 were determined by using phospho-SMAD specific antibodies and normalized to total SMAD2 and SMAD1/5 levels, respectively. Data are represented as a mean of three independent experiments ± SEM. P<0.05*, P<0.01**, P<0.001***. P values calculated with one-way ANOVA followed by comparisons to the control group with Bonferroni correction, adjusted $\alpha = 0.05/5 = 0.01$, unpaired Student's t-test (**a-d**) or Pearson correlation test (**e**). Data represented as a mean of three independent experiments ± SEM. P<0.001***. For (**h**), P values were calculated with unpaired Student's t-test.

Since activation of R-SMADs is required for canonical TGF-β signaling, we investigated whether proliferative vs. invasive ligands preferentially signal through specific SMADs. Western blot analysis for pSMAD1/5/8 and pSMAD2/3 (indicators of BMP and TGF-β signaling activity, respectively)

verified signaling specificity between different TGF-β superfamily members in human melanoma cells (Supplemental Figure. 1F, G and H). Remarkably, both BMP4 and BMP7 signaled through SMAD1/5/8 phosphorylation, although BMP4 counteracted proliferation and induced an invasive program when added to melanoma cells, whereas BMP7 increased the percentage of cells in S phase (Supplemental Figure 1B and C). Thus, the distinct biological activities of TGF-β superfamily members cannot simply be explained by differential usage of the known canonical SMAD signaling pathway.

6.1.4 Loss of SMAD7 is clinically relevant and associated with a MITF^{high}/AXL^{high} transcriptional state

Our data show that certain TGF-β superfamily factors expressed in melanoma display opposite effects on cell growth and invasiveness. This suggests that growth and metastatic spread of melanoma are influenced through fine-tuning the activities of these factors. To identify modulators and effectors of TGF-β/SMAD signaling possibly relevant for melanoma progression, we first examined RNA sequencing (RNA-seq) and clinical data from The Cancer Genome Atlas (TCGA). Survival analysis of the TCGA melanoma dataset (TCGA-SKCM) showed that among 36 SMAD signaling components, the inhibitory SMAD protein SMAD7 stood out as the clinically most relevant factor (Figure 3A). In fact, patients with low SMAD7 transcript levels had significantly shorter overall survival as compared to those having high SMAD7 transcripts ($p= 0.036$) (Figure 3B). The SMAD7^{high} and SMAD7^{low} patient cohorts did not exhibit obvious differences with respect to clinically relevant *BRAF* and *NRAS* mutations (data not shown). The difference in survival was even more evident when comparing those SMAD7^{low} and SMAD7^{high} groups of patients that displayed advanced stage disease at the time of analysis (stage II – IV) ($p= 0.0125$) (Figure 3B). Finally, gene ontology (GO) analysis using differential gene signatures of SMAD7^{low} and SMAD7^{high} patients revealed that categories crucial for melanoma biology, such as regulation of EMT, cell adhesion and migration, cytoskeletal remodeling, as well as upregulation of MITF were significantly enriched (Figure 3C).

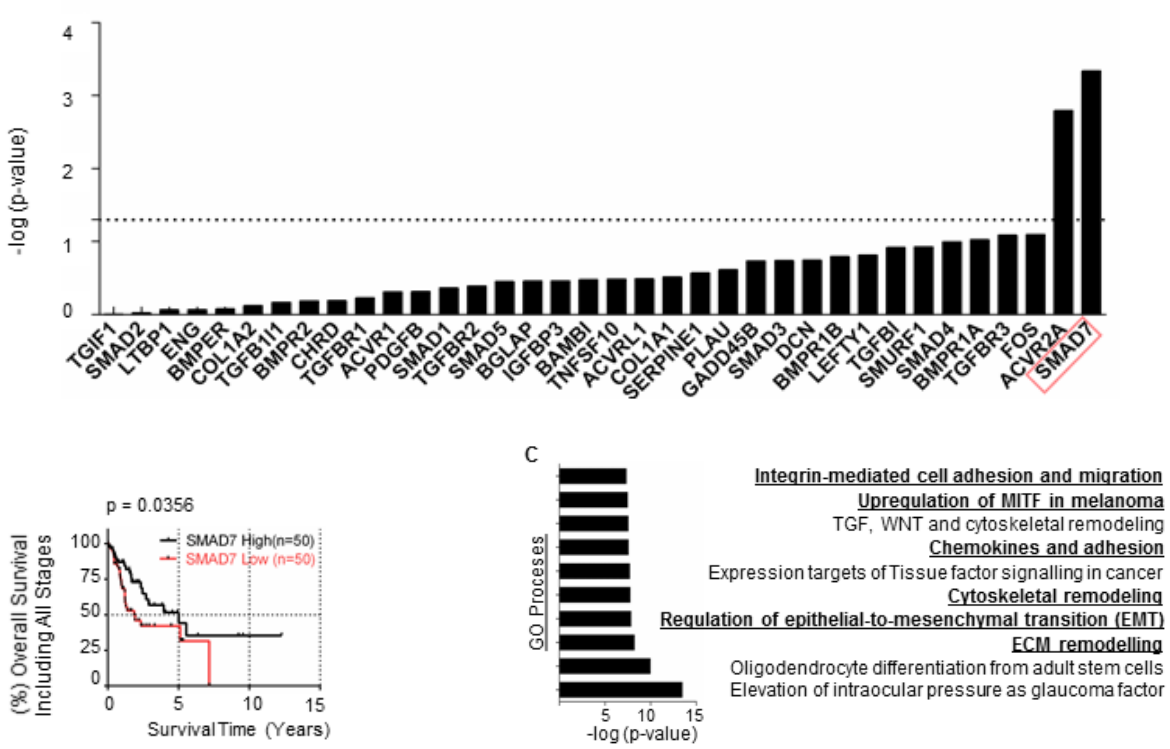

Figure 3. Low SMAD7 levels are associated with altered cell adhesion and cell cycle programs in human melanoma patients and patient-derived human melanoma cell lines. (**A**) P values are given for Kaplan Meier analysis comparing percent overall survival of melanoma patient cohorts based on TCGA data for 36 identified transcripts of TGF-β/BMP pathway components. For each gene, low/high expression levels of each gene were based on transcript levels found in bottom and top 50 patients, respectively. (**B**) Kaplan–Meier curves comparing overall percent survival with respect to SMAD7 transcript levels based on 350 patients. (**C**) Significantly changed top ten-ranking GeneGo process networks associated with low/high SMAD7 expression based on MetaCore Database.

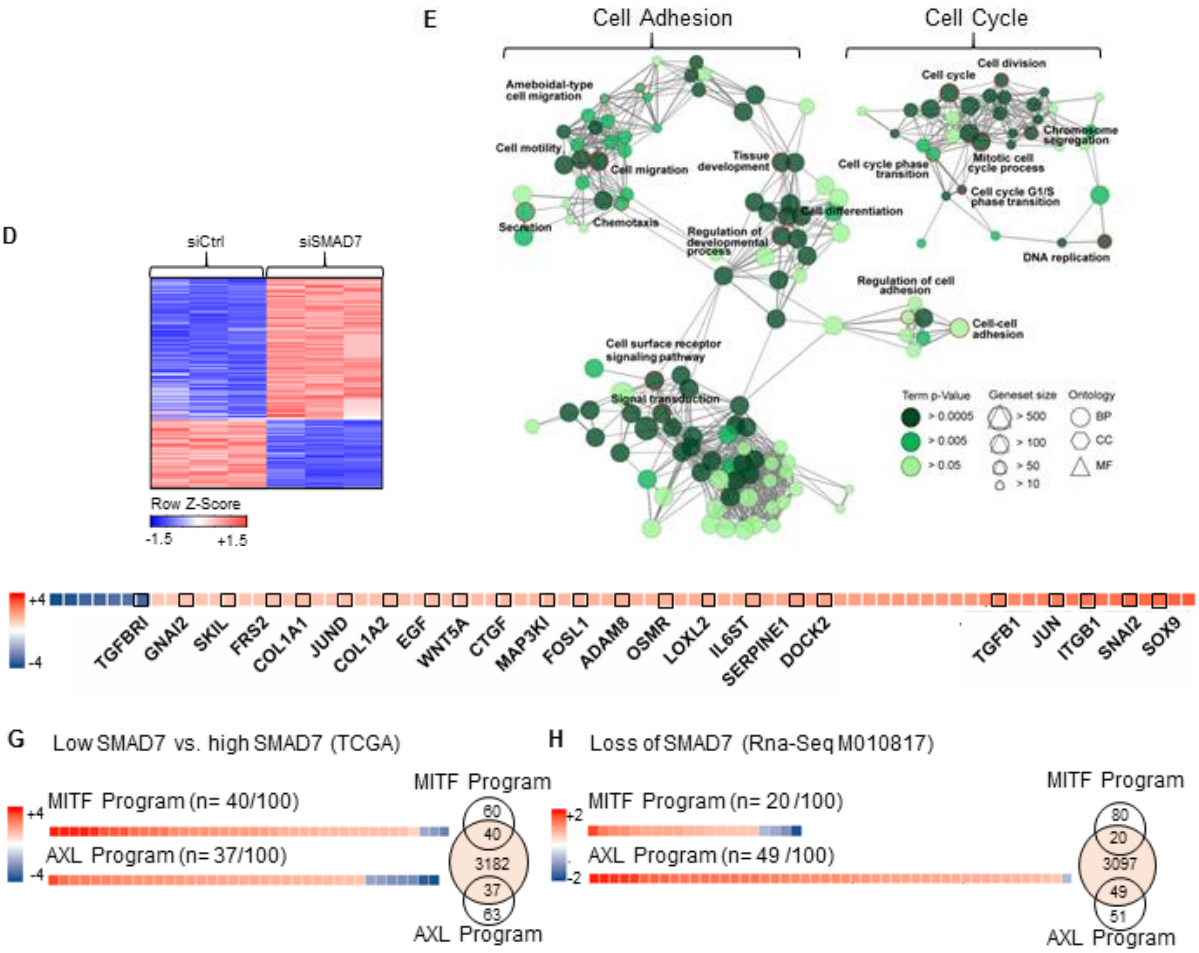

Figure 3. ***Continues*** **Low SMAD7 levels are associated with altered cell adhesion and cell cycle programs in human melanoma patients and patient-derived human melanoma cell lines**. (**D**) Heat map showing genes differentially expressed in SMAD7 knockdown and control M010817 cells (3557 genes, row z-score from three replicate RNA sequencing experiments). The gene list was generated using a 1.5-fold-change cut-off, and p-value of 0.05. Of these, 1586 were up-regulated and 1971 commonly down-regulated. (**E**) Gene ontology analysis based on differentially regulated genes upon SMAD7 knockdown. Each individual node shows an enriched GO term p value < 0.05) (Corrected with Bonferroni step down procedure). BP, biological process; MF, molecular function; CC, cellular component. A fully labeled version is given in Supplementary Figure S3. (**F**)Heat map of differentially expressed EMT genes (n= 84/225). Red; increased, blue; decreased expression. Highlighted cells indicate invasive genes according to *Verfaillie and colleagues*. 39 (**G, H**) Venn diagram showing the overlap between MITFhigh and AXLhigh gene expression programs derived from patient melanoma samples obtained by single cell sequencing2 with genes changed between low/high expressing SMAD7 patients or upon siRNA-mediated knock down of SMAD7 in M010817. Heat maps indicate differentially expressed MITF and AXL program genes, respectively.12 Gene list, see Supplemental Table S3 (**H**).

To address the physiological role of SMAD7 and its potential association with TGF-β signaling in melanoma cells, we first reduced SMAD7 levels by RNA interference-mediated silencing. This led to significant upregulation of both pSMAD2/3 and pSMAD1/5/8 expression, demonstrating the capacity of SMAD7 to inhibit canonical TGF-β signaling in melanoma cells (Supplemental Figure 2, A-F). To characterize the molecular pathways regulated by SMAD7-mediated signaling in melanoma, siSMAD7 and siControl treated M010817 cells were subjected to RNA-seq. Similar to the TCGA patient analysis (Figure 3D), the GO analysis based on cytoscape demonstrated highly significant enrichment in pathways associated with cell cycle core components and cell-cell adhesion (Figure 3E, Supplementary Figure 2G and Supplemental Table 1). Specifically, a comprehensive EMT program, including cell-cell adhesion molecules and transcriptional regulators previously associated with an invasive gene signature in melanoma (Verfaillie et al. 2015), was upregulated upon knock down of SMAD7 (Figure 3F and Supplemental Table 2). Importantly, we also observed changes in a variety of crucial cell cycle regulators, such as cyclins, cyclin dependent kinases (*CYCLINB1, CYCLINB2, CYCLIND1, CYCLIND2, CYCLINA, CYCLINE, CDK2, CDK4)* and S phase genes (*TOP2A, KI*67) (Supplemental Figure 2G and Supplemental Table 1).

6.1.5 Loss of SMAD7 boosts pro-invasive TGF-β/NODAL signaling in the presence of pro-proliferative BMP7

According to our bioinformatics analysis, SMAD7 appears to be implicated in both cell cycle and cell adhesion/EMT control in melanoma. To functionally test this hypothesis, we performed SMAD7 loss-of-function studies in the context of combinatorial TGF-β superfamily signaling. As expected, TGF-β2 or NODAL treatment counteracted proliferation in human melanoma cells and reduced cell-substrate adhesiveness, which was accompanied by upregulation of an EMT gene expression signature characteristic for invasive melanoma (Figure 4, A and B; Supplementary Figure 3, A and B).

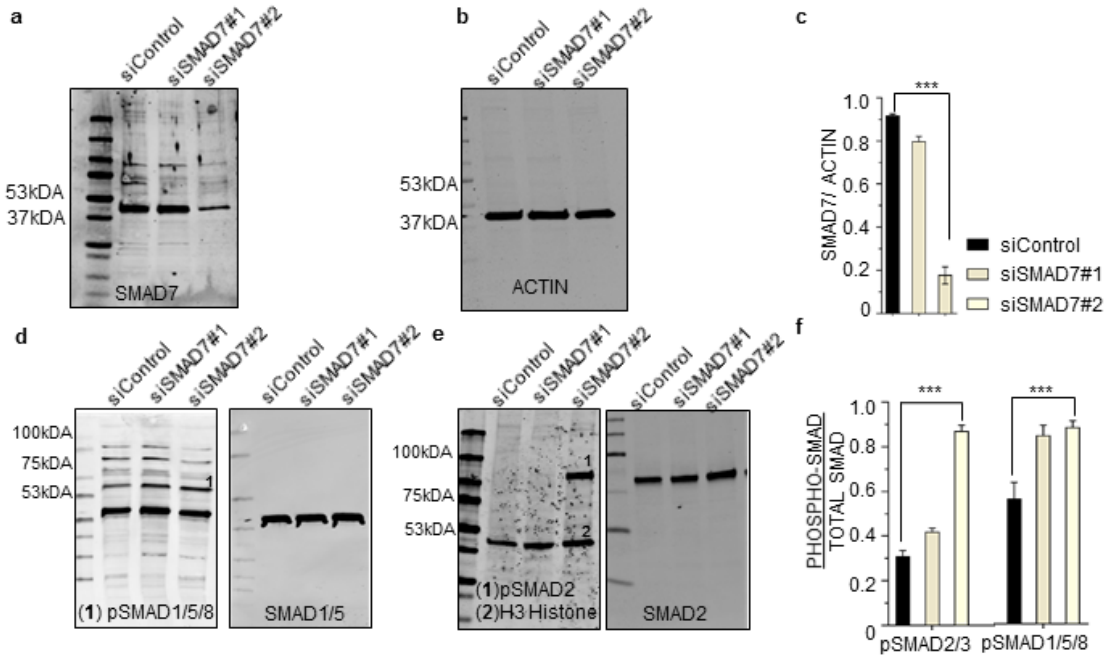

Supplementary Figure S2 Knock down of SMAD7 in human melanoma cell lines. (a-c) Western blot of M010817 whole cell extracts treated with SMAD7 siRNAs**. (d-f),** SMAD7 siRNA effects on phosphorylation of SMAD1/5/8 and SMAD2/3. Phosphorylation levels of SMAD2/3 and SMAD1/5/8 were determined by using phospho-SMAD specific antibodies and normalized to total SMAD2 and SMAD1/5 levels, respectively.

An increase in the expression of EMT regulators has been reported before to anti-correlate with a $MITF^{high}$ gene expression program(Müller et al. 2014)·(Richard et al. 2016). Moreover, the ratio of MITF/AXL expression has been used to define proliferative *vs.* invasive behaviors of melanoma cells(Cheli et al. 2011; Müller et al. 2014). Therefore, we next assessed which of the genes that constitute the published $MITF^{high}$ and AXL^{high} programs(Tirosh et al. 2016) were differentially expressed in the TCGA-based $SMAD7^{low}$ patient group and in SMAD7-silenced human melanoma cells, respectively. Surprisingly, genes of both the MITF as well as the AXL program were mostly upregulated in $SMAD7^{low}$ patients or upon loss of SMAD7 (Figure 3, G and H; Supplemental Table 3) These data indicate that contrary to the reported $MITF^{high}/AXL^{low}$ and $MITF^{low}/AXL^{high}$ binary "phenotype switching" states, melanoma cells with decreased SMAD7 levels exhibit a $MITF^{high}/AXL^{high}$ transcriptional state.

Silencing of SMAD7 reinforced these biological activities of TGF-β2/NODAL. Of note, BMP7 stimulated proliferation of human melanoma cells even when added together with TGF-β2 and NODAL, respectively, at concentrations at which the latter factors alone decreased proliferation (Figure 4, A and B; Supplemental Figure 3, A and B). Moreover, when melanoma cells were treated with TGF-β2 or NODAL in combination with BMP7, the EMT signature of malignant melanoma was suppressed, and the cells failed to detach from the substrate (Figure 4, C-E; Supplemental Figure 3, C-E). Thus, in the presence of TGF-β2 or NODAL, pro-proliferative BMP7 is dominant and able to override the cytostatic, pro-invasive effects of TGF-β2/NODAL in human melanoma cells.

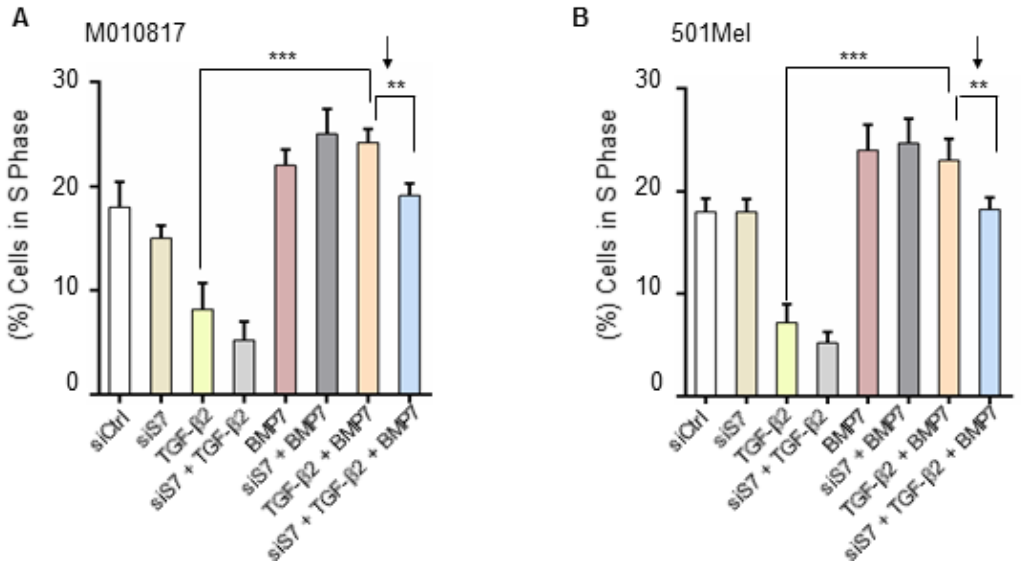

Figure 4. Loss of Smad7 boosts pro-invasive TGF-β/NODAL signaling in the presence of pro-proliferative BMP7. A, **B** Quantification of cell cycle S phase measured 3 days post ligand treatment through PI and EdU staining. M010817 and 501Mel cells were treated either with TGF-β2 (10ng/µl), BMP7 (100ng/µl), or both, with or without siRNA-mediated SMAD7 knockdown. Treatment with BMP7 resulted in escape of cells from the TGF-β2-mediated cell cycle arrest and increased proliferation. SMAD7 knock down of BMP7/TGF-β2-treated cells led to decreased numbers of cells in S cell cycle phase as compared to BMP7/TGF-β2-treated cells (n=3).

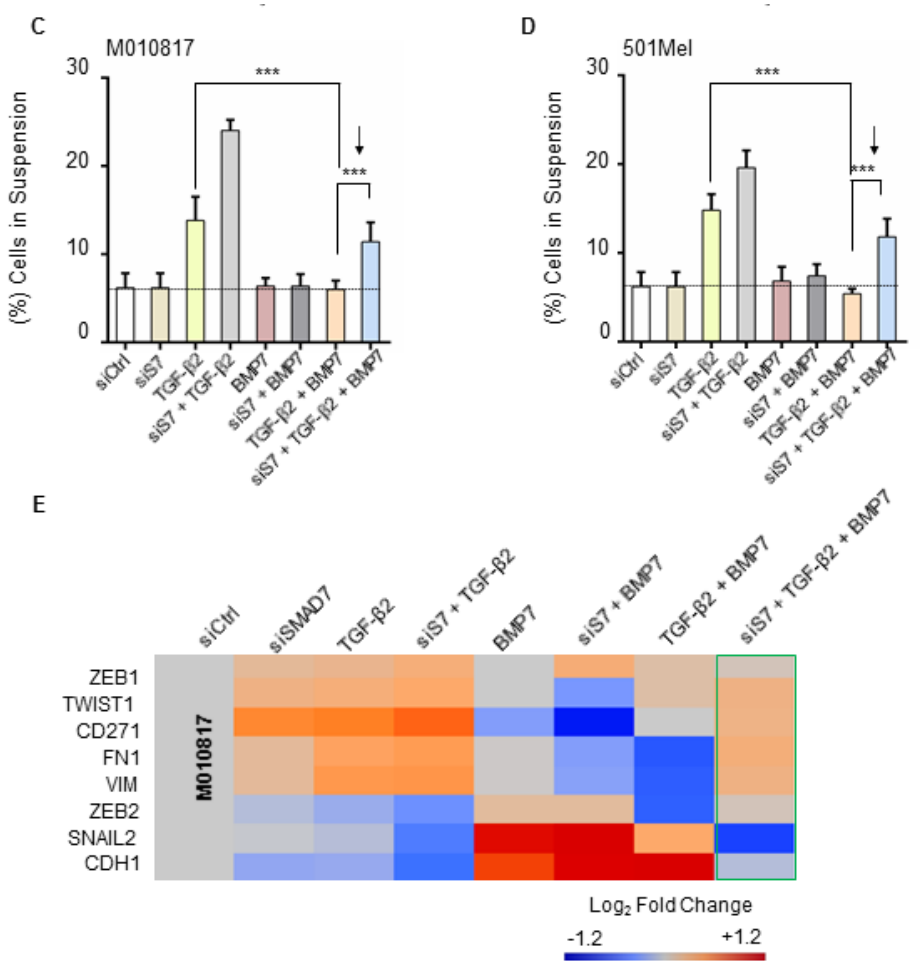

Figure 4. Continues Loss of Smad7 boosts pro-invasive TGF-β/NODAL signaling in the presence of pro-proliferative BMP7. (**c**,**d**) Quantification of cell-substrate adherence capacity of M010817 and 501Mel cells upon treatment with TGF-β2, BMP7 (100ng/µl), or both, with or without siRNA-mediated SMAD7 knockdown. TGF-β2-mediated cell detachment was suppressed by BMP7. The percentage of BMP7/TGF-β2/siSMAD7-treated cells in suspension increased as compared to BMP7/TGF-β2-treated cells (n=3).(**e**) Heat map shows qRT-PCR analysis for selected EMT genes under ligand treatments with two biological and three technical replicates. The expression levels of genes are presented using fold-change values transformed to Log2 format compared to control. Color represents expression after normalization to non-treated control cells. Data represented as a mean of three independent experiments ± SEM. P values calculated with one-way ANOVA followed by comparisons to the control group with Bonferroni correction (adjusted $\alpha = 0.05/5 = 0.01$). P< 0.01**, P < 0.001*** (**a-d**).

Surprisingly, however, downregulation of SMAD7 did not alter the cell cycle-promoting effect of BMP7 in human melanoma cells. Furthermore, addition of BMP7 reversed the cell cycle arrest observed

upon TGF-β2 plus siSMAD7 treatment, making co-treatment with TGF-β2/siSMAD7 compatible with proliferation (Figure 4, A and B). In contrast to the capacity of BMP7 to override the cytostatic effect of TGF-β2, BMP7 only partially counteracted the loss-of-adhesion phenotype mediated by TGF-β2/siSMAD7. Although cell detachment in BMP7/TGF-β2/siSmad7-treated cells was not as prominent as in TGFβ-2/siSMAD7-treated cells, the number of cells in suspension was still significantly increased as compared to BMP7/TGFβ-2-treated cells, in which TGF-β2 signal activity had not been enhanced by siSMAD7 (Figure 4, C and D)

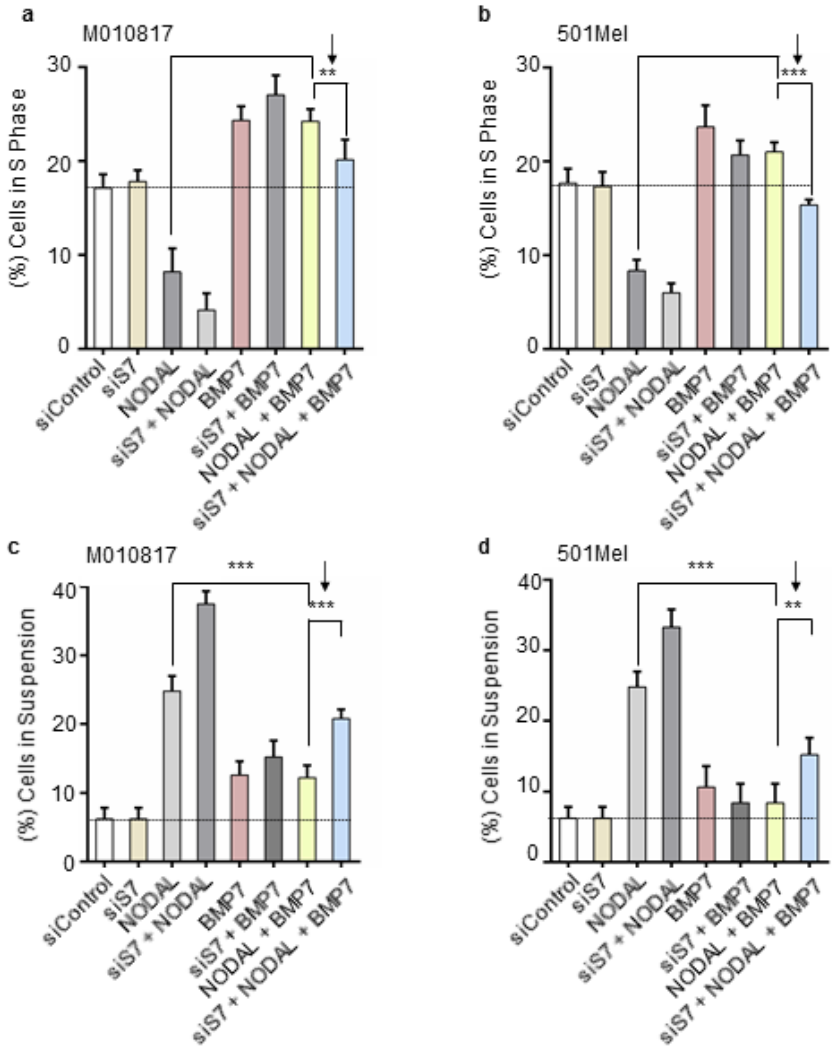

Supplementary Figure S3 Cell cycle analysis upon combinatorial TGF-β superfamily factor treatment of human melanoma cell lines. (a,b) Quantification of cell cycle S phase was measured 3 days post treatment through PI and EdU staining. M010817 and 501Mel cells were treated with either TGF-β2 (10ng/µl), BMP7 (100ng/µl) alone or both, together with siRNA mediated SMAD7 knockdown. Treatment with BMP7 resulted in escape of cells from the NODAL-mediated cell cycle arrest and increase in the proliferation rate. SMAD7 knock

down in BMP7/NODAL-treated cells results in decreased S cell cycle phase as compared to BMP7/NODAL-treated cells. **(c,d)** Quantification of cell-substrate adherence capacity (see Supplementary Figure S1) of M010817 and 501Mel cells treated with the indicated factor combinations. NODAL-mediated cell detachment was suppressed by BMP7. The percentage of BMP7/NODAL/siSmad7-treated cells in suspension increased as compared to BMP7/NODAL-treated cells (n=3).

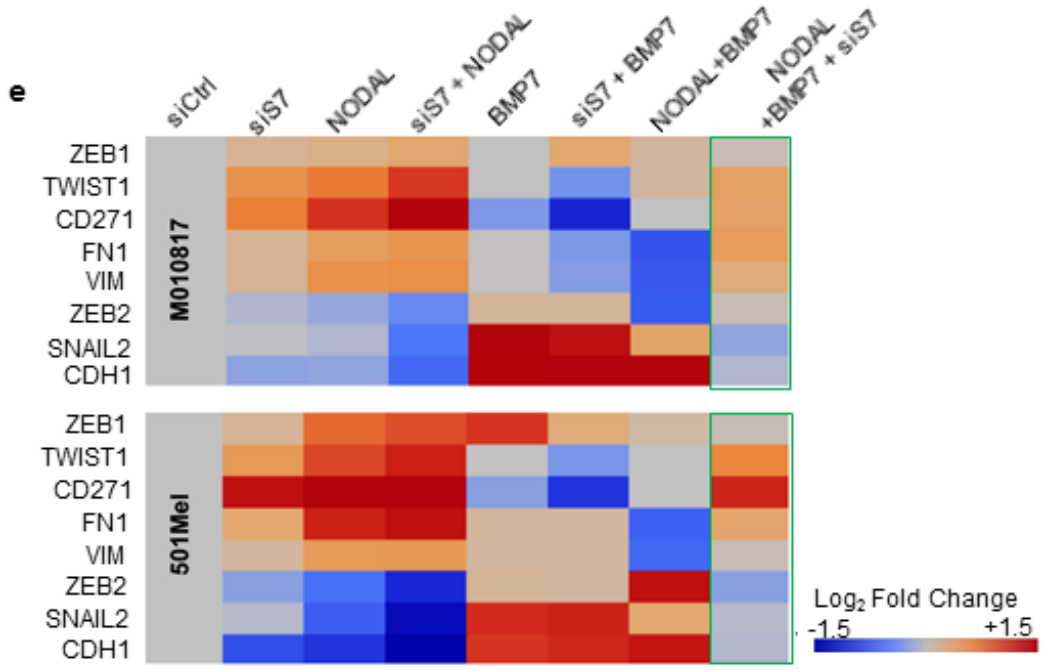

Supplementary Figure S3 Continues **Cell cycle analysis upon combinatorial TGF-β superfamily factor treatment of human melanoma cell lines (e)** Heat maps show the qRT-PCR analysis results of selected EMT genes under combinatorial ligand treatments. **(a-e)** Data represented as a mean of three independent experiments ± SEM. P<0.05*, P<0.01**, P<0.001***. P values calculated with one-way ANOVA followed by comparisons to the control group with Bonferroni correction (adjusted $\alpha = 0.05/5 = 0.01$). ***)

Consistent with these observations, siSMAD7 treatment of cells concomitantly exposed to TGF-β2 and BMP7 restored an EMT gene expression signature characteristic for invasive melanoma cells (Figure 4E). Similarly, the dominant anti-invasive activity of BMP7 over NODAL was reverted upon SMAD7 knock down. While BMP7/NODAL-treated cells had a non-invasive phenotype, BMP7/NODAL/siSMAD7-treated cells displayed reduced cell adhesion and an EMT signature

reminiscent of invasive cells (Supplemental Figure 3, C-E). Nonetheless, BMP7/NODAL/siSMAD7-treated cells exhibited a proliferative capacity comparable to that of control cells (Supplemental Figure 3, A and B). Thus, reducing SMAD7 levels does not alter proliferation *in vitro*, but boosts the pro-invasive activity of TGF-β2/NODAL even in the presence of BMP7.

Contrary to the binary cell states proposed in the phenotype switching hypothesis, our finding suggests that reduced SMAD7 levels in the context of complex TGF-β superfamily signaling increases the invasive potential of melanoma cells while sustaining their proliferative capacity. To clarify whether these cells eventually retain cell proliferation and invasiveness, we pulsed human melanoma cells with the thymidine analogue EdU, which incorporates into replicating DNA during S phase, after 48 hours of silencing SMAD7 in the presence of pro-proliferative BMP7 and pro-invasive TGF-β2 (Figure 5A). Furthermore, we tested whether proliferative cells expressed the EMT-TF ZEB1, which is characteristic of invasive melanoma cells (Caramel et al. 2013). Strikingly, double staining revealed that cultures of BMP7/TGF-β2/siSMAD7-treated cells contained significantly higher numbers of EdU- and ZEB1-double positive cells (23 ± 3%) in comparison to BMP7/TGF-β2 -treated (9 ± 2%) or untreated control cells (4 ± 1%) (Figure 5, B and C).

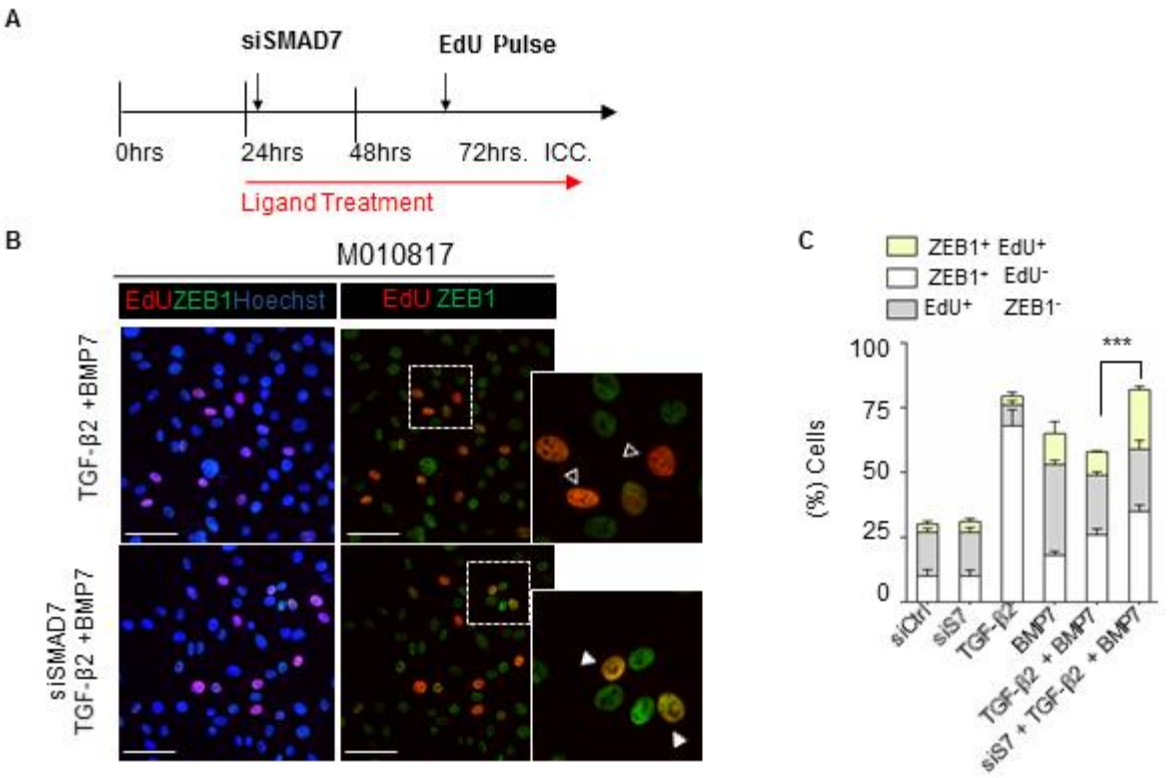

Figure 5. Loss of SMAD7 promotes emergence of proliferative-invasive MITFhigh/AXLhigh melanoma cells *in vitro* (**A**) Experimental design used in this study. Proliferative M010807 cells were exposed to combinatorial ligand treatment over a 3-day period. Cells were pulsed with EdU, followed by flow cytometry. (**B**) Representative immunofluorescent images of ZEB1/EdU-double-positive cells (white arrowheads). Open arrowheads, EdU+/ZEB1- cells. (**C**) Quantification of single and double labeled cells for ZEB1 and EdU (n=3).

De-regulated TGF-β/SMAD signaling can alter MITF expression depending on the melanoma cell line (Smith et al. 2013). Moreover, as mentioned before, the ratio of MITF/AXL expression has been used to distinguish proliferative and invasive melanoma cells (Cheli et al. 2011; Müller et al. 2014). Therefore, we also assessed the number of cells expressing high *vs.* low levels of MITF, together with AXL expression, upon combinatorial TGF-β superfamily treatment. Importantly, in untreated cultures, in cultures exposed to various combinations of TGF-β superfamily factors, and in siSMAD7-treated cultures in the absence of exogenous TGF-β factors, AXL-positive cells were $MITF^{low}$, and only a minor fraction of cells expressed both AXL and high levels of MITF. In contrast, the number of cells that were

double positive for AXL and high MITF was significantly increased to 18 ± 3% of all cells upon concomitant BMP7/TGF-β2/siSMAD7 treatment (Figure 5, D and E). Together, these data indicate that reducing SMAD7 levels endows proliferative melanoma cells with invasive capacity, which possibly contributes to melanoma cell aggressiveness.

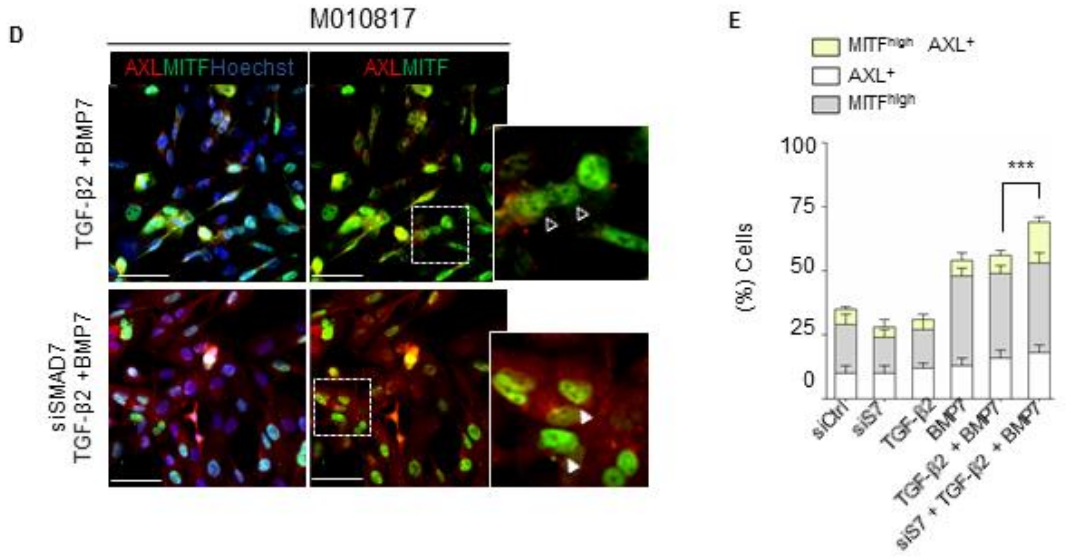

Figure 5. Continues. Loss of SMAD7 promotes emergence of proliferative-invasive MITFhigh/AXLhigh melanoma cells *in vitro* (**D**) Representative immunofluorescent images of MITFhigh/AXLhigh-double-positive cells. (**E**) Quantification of cells expressing AXL, MITFhigh, or both (n=3). Data represented as a mean of three independent experiments ± SEM. $p < 0.001$***. P values calculated with unpaired Student's t-test (**C**,**E**). Scale Bars, 50μm.

6.1.6 Loss of Smad7 in vivo increases the number of cells with both invasive and proliferative features

Our cell culture data revealed the presence of cells that acquired both invasive and proliferative features upon SMAD7 inactivation. To corroborate these *in vitro* findings in a physiologically more relevant setting, we assessed whether Smad7 might also modulate the output of integrated TGF-β/SMAD signaling *in vivo*. As shown above, TGF-β superfamily factors, including TGF-β, NODAL, as well as BMP7 were expressed in melanoma cells derived from *Tyr::Nras^{Q61K} Ink4a$^{-/-}$ Tyr::Cre^{ERT2} R26R::LacZ*

mice (Supplemental Figure 1A). To functionally study the role of Smad7 in melanoma progression, we mated mice carrying a floxed allele of *Smad7*(Kleiter et al. 2010) with the *Tyr::Nras*^{Q61K}*Ink4*$^{-/-}$ melanoma mouse model to obtain *Tyr::Nras*^{Q61K} *Ink4a*$^{-/-}$ *Tyr::Cre*^{ERT2} *Smad7*$^{lox/lox}$ *R26R::LacZ* mice (Figure 6, A and B). TM-mediated *Tyr::Cre*^{ERT2} activation in these mice at 1 month of age resulted in efficient recombination and depletion of Smad7 protein in Dct-expressing melanoma cells (Supplemental Figure 4, A and B). Importantly, loss of Smad7 led to a substantial increase in the percentage of Dct-positive melanocytic cells co-expressing nuclear pSmad2/3 and pSmad1/5/8, demonstrating activation of both canonical SMAD signaling pathways (Supplemental Figure 4, D and E). Despite signal activation, however, conditional depletion of *Smad7* neither had an overt effect on hyperplastic dermal lesions (data not shown) nor on the number of skin melanomas emerging during disease progression (Figure 6C). Consistent with this, EdU incorporation into primary tumors was not significantly altered in *Smad7* cKO as compared to control mice (34 ± 1% *vs.* 37 ±3%) (Figure 6D). Next, we assessed Zeb1 expression in primary tumors of *Tyr::Nras*^{Q61K} *Ink4a*$^{-/-}$ *Tyr::Cre*^{ERT2} *Smad7*$^{lox/lox}$ *R26R::LacZ* mice after EdU application. Intriguingly, the number of Zeb1/EdU double-positive cells was significantly higher (16 ± 4%) in primary tumors of *Smad7* cKO mice when compared to control primary tumors (4 ± 2%) (Figure 6, D and E). To verify that the induction of Zeb1 expression in proliferative cells represented a malignant cell phenotype, we additionally quantified the number of Mitf^{high}/Axl-double-positive cells in skin sections of *Smad7* cKO mice. Notably, hyperplastic lesions displayed significantly higher numbers of double-positive cells (10 ± 2%) compared to control skin sections (2 ± 1%). Similarly, the number of Mitf^{high}/Axl-double-positive cells was dramatically increased in primary tumors of *Smad7* cKO mice (27 ± 3%) when compared to control tumors (6 ± 1%) (Figure 6, F-H).

Together, our findings suggest that inactivation of *Smad7* and a concomitant increase in pSmad2/3 and pSmad1/5/8 does not interfere with tumor growth *in vivo*, despite increased expression of the invasive marker Zeb1 in EdU-positive proliferating cells. Importantly, we also observed an increase in Axl expression in Mitf^{high} proliferative cells upon *Smad7* deletion in primary tumors indicating that

augmented SMAD signaling increases the number of cells associated with both high proliferation and invasion properties.

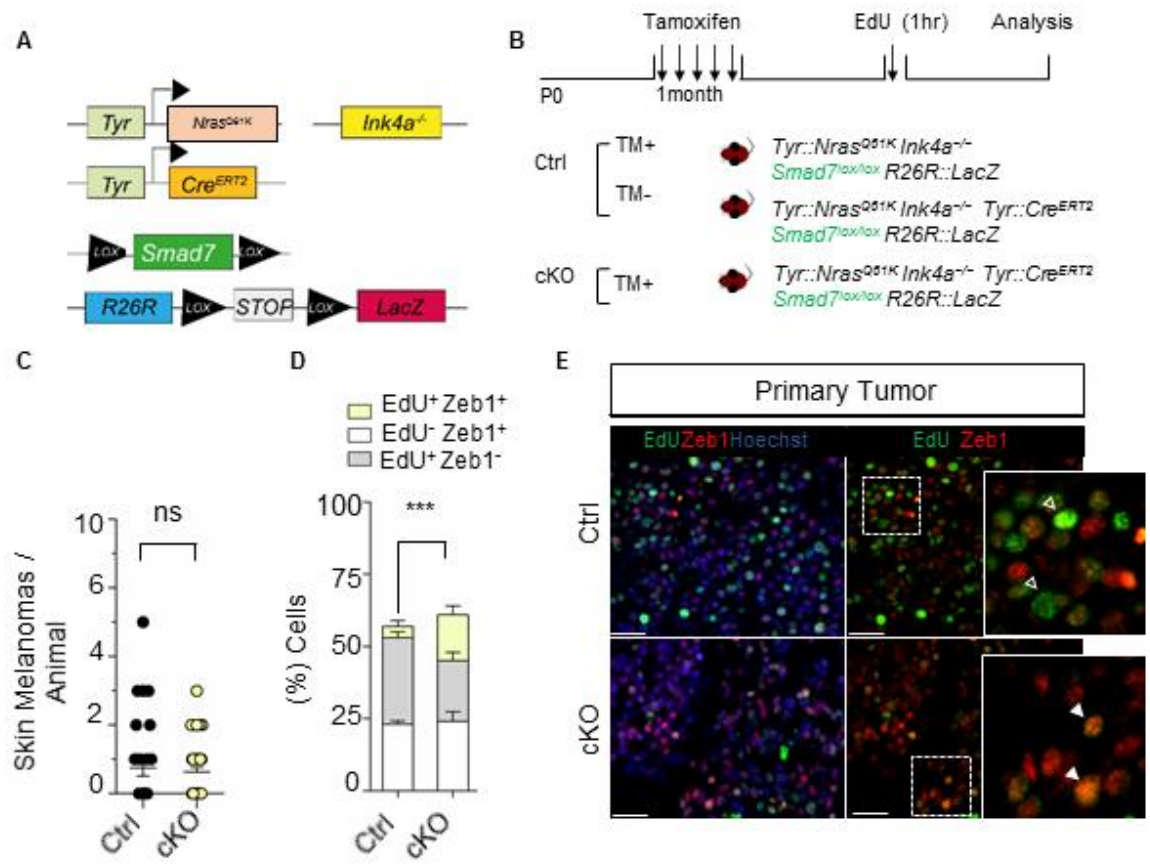

Figure 6. Loss of Smad7 promotes emergence of proliferative-invasive MITFhigh/AXLhigh melanoma cells *in vivo* (**A**) The melanoma mouse model used to analyze the effect of *Smad7* conditional deletion in *Tyr::CreERT2 Tyr::NrasQ61K INK4a*−/− mice. (**B**) Experimental strategy used to analyze the proliferation rate by EdU injection upon *Smad7* loss. (**C**) Quantification of the number of skin melanomas of control and *Smad7* cKO mice (n=12). (**D,E**) Immunostaining and quantification of EdU/Zeb1-double positive cells in *Smad7* cKO and control primary tumors. Grey and white bars indicate single Zeb1+ and EdU+ cells, respectively. Yellow bar represents percentage of EdU+ cells that are Zeb1+. White arrowheads in the images indicate double-positive cells, open arrowheads EdU+/Zeb1- cells

To verify that the induction of Zeb1 expression in proliferative cells represented a malignant cell phenotype, we additionally quantified the number of Mitf^{high}/Axl-double-positive cells in skin sections

of *Smad7* cKO mice. Notably, hyperplastic lesions displayed significantly higher numbers of double-positive cells (10 ± 2%) compared to control skin sections (2 ± 1%). Similarly, the number of Mitf^{high}/Axl-double-positive cells was dramatically increased in primary tumors of *Smad7* cKO mice (27 ± 3%) when compared to control tumors (6 ± 1%) (Figure 6, F-H).

Together, our findings suggest that inactivation of *Smad7* and a concomitant increase in pSmad2/3 and pSmad1/5/8 does not interfere with tumor growth *in vivo*, despite increased expression of the invasive marker Zeb1 in EdU-positive proliferating cells. Importantly, we also observed an increase in Axl expression in Mitf^{high} proliferative cells upon *Smad7* deletion in primary tumors indicating that augmented SMAD signaling increases the number of cells associated with both high proliferation and invasion properties.

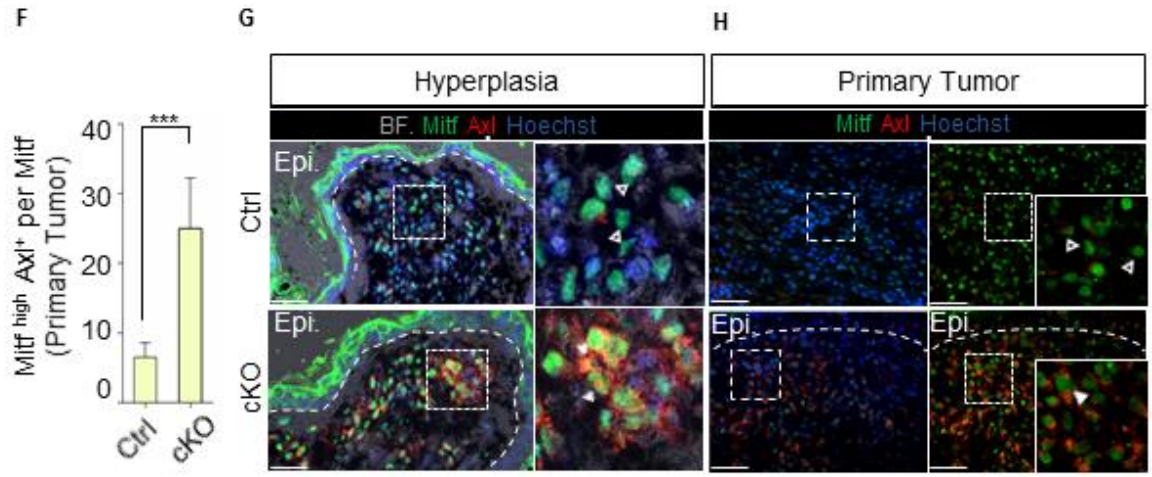

Figure 6. Loss of Smad7 promotes emergence of proliferative-invasive MITFhigh/AXLhigh melanoma cells *in vivo.* (**F-H**) Quantification and immunostaining of Mitfhigh/Axl-double positive cells in cKO and control primary tumors. Percentage of Mitfhigh/Axl-double positive cells calculated over overall number of Mitfhigh and Mitflow cells. Yellow bar represents percentage of Mitfhigh cells that are Axl+. Arrowheads in the images indicate the double-positive cells, open arrowheads Mitf+/Axl- cells. Data represented as the mean ± SEM. $p < 0.001$***. P values calculated with unpaired Student's t-test (**C-F**). Epi, Epidermis; TM, tamoxifen. Scale Bars, 50µm.

6.1.7 Reduced Smad7 expression promotes massive metastatic spread of melanoma *in vivo*

Despite apparently unaltered tumor initiation and primary tumor growth, *Smad7* cKO mice displayed significantly reduced melanoma free survival (Figure 7A). When analyzing these mice, we observed a massive metastatic spread to organs such as the lung, spleen and the liver, which were normally devoid of metastases in control mice (Figure 7B). Pigment-associated Dct-positive cells in these distant metastases did not express Smad7, demonstrating their origin from *Smad7*-depleted recombined melanoma cells (Figure 7C). Quantification of the metastatic burden in lung, spleen, and liver confirmed the high aggressiveness of melanoma caused by *Smad7* inactivation (Figure 7, D-F).

In the above experiment, *Smad7* inactivation was broadly induced in melanocytic cells by systemic TM treatment. To assess whether restricted depletion of *Smad7* is sufficient to promote melanoma metastasis formation, we locally applied 4-OH-TM to the back skin of *Tyr::Nras*^{Q61K} *Ink4a*$^{-/-}$ *Tyr::Cre*^{ERT2} *Smad7*$^{lox/lox}$ *R26R::LacZ* mice (Figure 7G). Although recombination efficiency in the treated areas was lower than in melanocytic skin cells after systemic TM treatment (Supplemental Figure 4B), a reduction in overall survival of mice was observed (Supplemental Figure 4F). Importantly, at the day of sacrifice, the number of lung macro metastases was highly increased upon local *Smad7* depletion, demonstrating the striking metastatic potential of *Smad7* cKO skin melanoma cells (Figure 7H). Thus, loss of Smad7 significantly increases the aggressiveness of melanoma in the context of enhanced pSmad2/3 and pSmad1/5/8 signal activation.

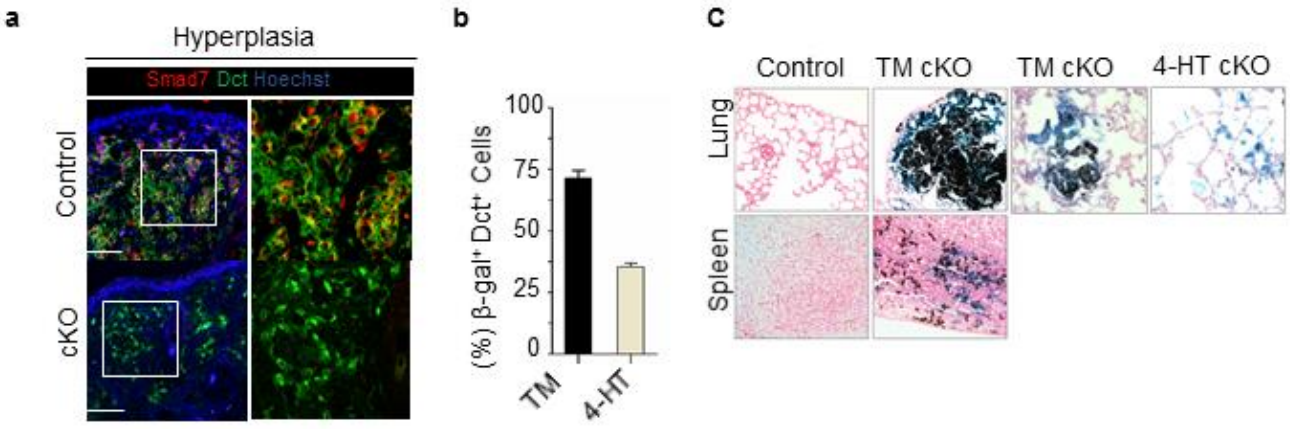

Supplementary Figure S4 Reduced Smad7 expression promotes massive metastatic spread of melanoma *in vivo*. (a) Immunofluorescent staining for Smad7 and Dct on back skin sections at 6 months of age. Melanocytic cells are recombined and show decreased levels of Smad7 (n=6**). (b)** Quantification of the recombination efficiency by analyzing the percentage of Dct/β-Gal+ double-positive cells upon intraperitoneal injection and upon local application of 4-hyroxytamoxifen (4-HT) to the back skin of 3 week old mice (n=6). **(c)** Representative hematoxylin and eosin staining of lung and spleen sections of control and cKO mice at the day of sacrifice. X-Gal staining (blue) illustrates presence of recombined metastatic cells in distant organs.

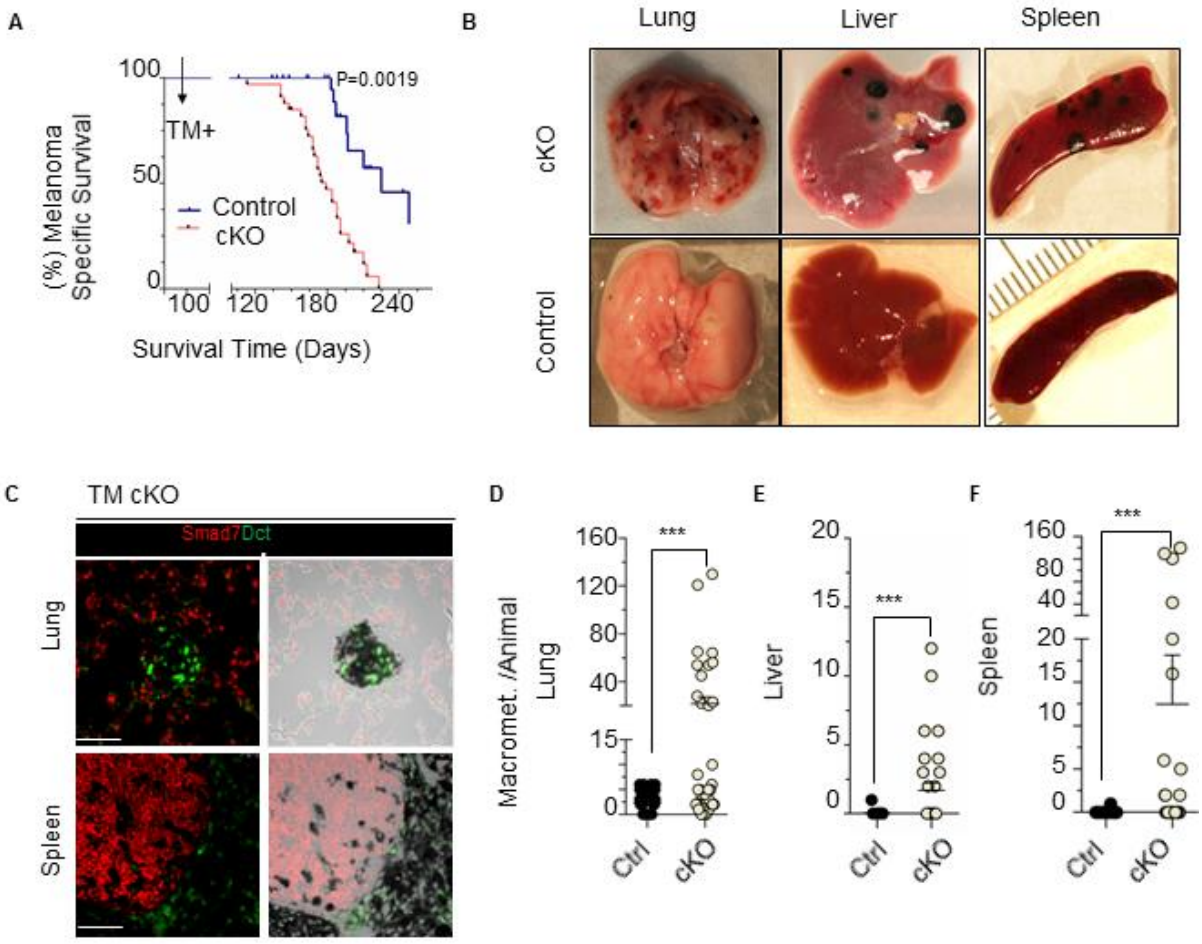

Figure 7. Reduced Smad7 expression promotes metastatic spread of melanoma *in vivo* (**A**) Kaplan–Meier curves comparing melanoma-specific survival of control and *Smad7* cKO animals (n=35 (cKO), n=30 (control)). (**B**) Representative pictures of indicated organ from *Smad7* cKO and control animals. (**C**) Immunofluorescent staining for Smad7 and Dct at the site of distant metastasis in *Smad7* cKO and control animals. Note absence of Smad7 expression in pigmented Dct+ areas. (**D-F**) Quantification of macro-metastasis numbers in lung, spleen and liver in *Smad7* cKO and control littermates

In the above experiment, *Smad7* inactivation was broadly induced in melanocytic cells by systemic TM treatment. To assess whether restricted depletion of *Smad7* is sufficient to promote melanoma metastasis formation, we locally applied 4-OH-TM to the back skin of *Tyr::Nras^{Q61K} Ink4a$^{-/-}$ Tyr::Cre^{ERT2} Smad7$^{lox/lox}$ R26R::LacZ* mice (Figure 7G). Although recombination efficiency in the treated areas was lower than in melanocytic skin cells after systemic TM treatment (Supplemental Figure 4B), a reduction in overall survival of mice was observed (Supplemental Figure 4F). Importantly, at the day of sacrifice, the number of lung macro metastases was highly increased upon local *Smad7* depletion, demonstrating the striking metastatic potential of *Smad7* cKO skin melanoma cells (Figure 7H). Thus, loss of Smad7 significantly increases the aggressiveness of melanoma in the context of enhanced pSmad2/3 and pSmad1/5/8 signal activation.

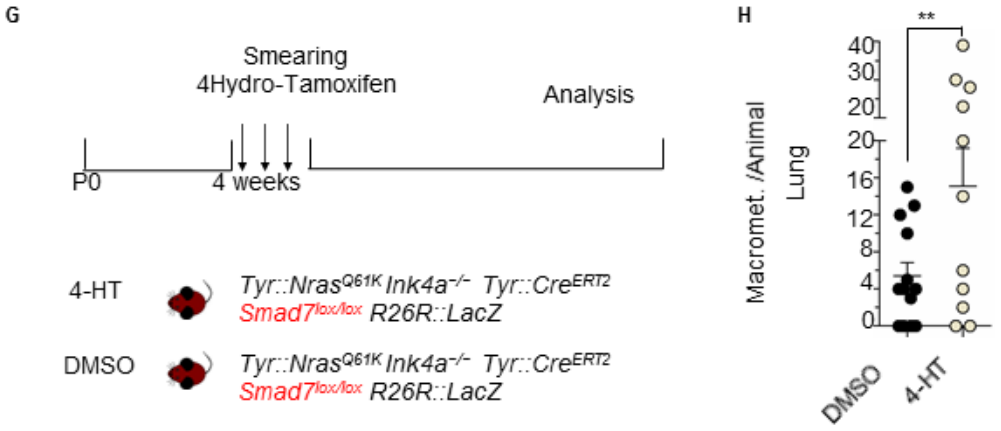

Figure 7. Continues. Reduced Smad7 expression promotes metastatic spread of melanoma *in vivo* (**G**) Experimental strategy used to analyze the effect of local *Smad7* loss in *Tyr::N-RasQ61K Ink4a−/− Tyr::CreERT2 R26R::LacZ* mice by 4-HT administration to the skin. (**H**) Kaplan–Meier curves comparing melanoma-specific survival of control mice and animals, in which *Smad7* has been locally deleted in the skin of 3 week old mice (n= 12 (cKO), n=12 (control)). Data represented as a mean of three independent experiments ± SEM. p<0.01**, p<0.001***. P values calculated with unpaired Student's t-test (**D-F**), or log-rank Mantel–Cox test (**A**), (**H**). TM, tamoxifen, 4-HT, 4-hydoxytamoxifen. Scale Bar, 50µm.

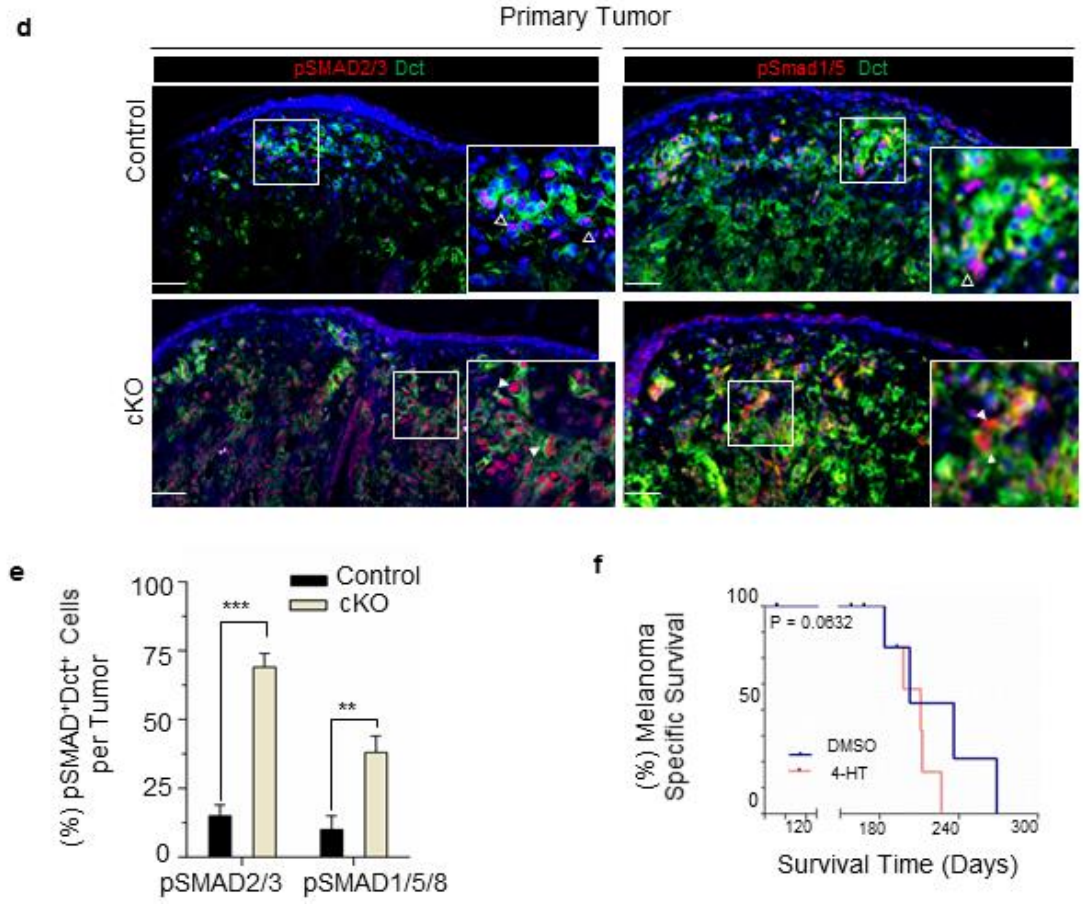

Supplementary Figure S4. ***Continues*** **Reduced Smad7 expression promotes massive metastatic spread of melanoma** ***in vivo*****. (d)** Immunofluorescent staining for pSmad2/3, pSmad1/5/8 and Dct of primary tumors at 6 months (n=6). Control and cKO primary tumors were quantified for active TGF-β signaling by detecting the nuclear localization of pSmad2/3 or pSmad1/5/8 (n=6). **(e)** Quantification of active TGFβ signaling by quantifying number of melanocytic Dct+ cells displaying nuclear localization of pSmad2/3 and pSmad1/5/8, respectively, in primary tumors at 6 months (n=6). **(f)** Kaplan–Meier curves comparing overall survival between 4-HT treated animals and control animals (n=8). Data represented as a mean of three independent experiments ± SEM. P values calculated with unpaired Student's t-test **(b),** Tukey's post-test following one-way ANOVA **(d),** or log-rank (Mantel–Cox) test **(f)**. P< 0.05*, P< 0.01**, P< 0.001***. Scale Bars: 50μm **(a,d)**

7. Methods

All detailed information on experimental procedures and reagents is provided in the Supplementary Tables and Supplemental Experimental Procedures.

7.1 Mice

Animal experiments were done in accordance with a protocol approved by the veterinary authorities of the Canton of Zurich, Switzerland, and were performed in accordance with Swiss law, Welfare, and Treatment of Animals. All implementations were carried out in *Tyr::Nras*^{Q61K} *Ink4a*$^{-/-}$ *Tyr::Cre*^{ERT2} *R26R::LacZ* animals that were having a mixed genetic background. Animals homozygous for the floxed *Smad7* (B6.Cg-*Smad7*$^{tm1.1Ink}$/J) (Kleiter et al. 2010) allele or the floxed *Smad4* allele (*Smad4*$^{tm2.1Cxd}$/J) (Yang et al. 2002) were mated with mice heterozygous for the respective floxed allele(s) and carrying the Cre-recombinase. To conditionally delete genes of interests in the melanocytic linage, *Tyr::CreERT*^{2} line was used (provided by L. Chin, The University of Texas MD Anderson Cancer Center, Houston, Texas, USA). Genotyping was done by PCR on genomic DNA (Qiagen Taq PCR Core Kit 201225), using the primer pairs indicated in (Supplemental Table 4). DNA was prepared and the reactions were carried out as described (Yang et al. 2002; Kleiter et al. 2010) No change in the expected gender and Mendelian inheritance ratio was found. Mice were often examined and sacrificed at an endpoint defined by adverse clinical symptoms, such as multiple skin tumours (Ø > 5mm), weight loss (> 15%), or hunched back.

7.2 Immunofluorescent on cells

Cells were grown on cover slips, ethanol-fixed, and subjected to immunofluorescent labelling using primary antibodies (Supplemental Table 5) in blocking buffer (1% BSA in PBS and 0.05% Tween) overnight at 4°C and secondary antibodies (Supplemental Table 5) for 1h at room temperature. Nuclei were stained with Hoechst 33342 (14533, Sigma-Aldrich), and cells were recorded with a DMI 6000B microscope (Leica).

7.3 Administration of tamoxifen and analysis of mice

Transgenic lines were crossed to the Rosa26 Cre reporter strain (*R26R*), which has an ubiquitously expressed transgene containing a STOP cassette flanked by loxP sites followed by the *LacZ* gene. The resulting mice *Tyr::Nras*^{Q61K} *Ink4a*$^{-/-}$ *Smad4*$^{lox/lox}$ *R26R::LacZ* mice, *Tyr::Nras*^{Q61K} *Ink4a*$^{-/-}$ *Smad4*$^{lox/wt}$ *Tyr::CreERT*^{2} *R26R::LacZ* mice (control groups) and *Tyr::Nras*^{Q61K} *Ink4a*$^{-/-}$ *Smad4*$^{lox/lox}$ *Tyr::CreERT*^{2} *R26R::LacZ* mice (experimental group) were subjected to treatment with tamoxifen (T5648, Sigma Aldrich), which was diluted in ethanol and sunflower oil (1:9 ratio). Conditional ablation of *Smad4* as well as *Smad7* was achieved by intraperitoneal injections of tamoxifen (100 µl, 1 mg d^{-1} for 5 days) into 4-week-old mice and 4-months-old mice. Topical administration of 4- hydroxytamoxifen (4-HT) was performed by preparing a 50mg/ml (130mM) solution of 4-HT (70% Z-isomer, Sigma) in dimethyl sulfoxide; DMSO. 4-week-old mice were treated with Veet cream to remove hair from 2 x 2 cm patch of skin on the dorsal flank. After the area was dried and topical administration of 50mg/ml stock solution in DMSO was diluted into 100% ethanol and freshly applied (1ml, for 3 days). Upon intraperitoneal (IP) Tamoxifen injections or topical 4-HT administration, mice were monitored for tumor numbers and development. In combination with staining for the *R26R::LacZ* Cre-reporter allele, the macroscopic skin phenotype was analysed histologically. Mice were examined regularly and sacrificed at an endpoint defined by adverse clinical symptoms including skin tumor size (Ø > 2mm), weight loss, or hunched back.

7.4 Quantification of skin melanomas and metastases

At day of sacrifice, skin melanoma numbers were counted. Non-recombined tumors were excluded for statistical analysis. Both in conditional *Smad4* and *Smad7* knockout mice (cKO), whole mount X-Gal staining was used to assess the recombined tumors. Quantification of the percentage of mice bearing macro-metastases in each organ including lung, liver and spleen were visually examined under the

binocular at necropsy and calculated by counting pigmented lesions at the organ surface. Affected lymph nodes (accessory axillary, proper axillary, sciatic and subiliac lymph nodes) were further assessed by immunohistostaining. PAX3, DCT and HMB-45 positivity was used to detect melanoma cells on lung, liver, and spleen on histological sections.

7.5 Histologic analysis and immunohistochemistry

Mice were sacrificed by CO_2 inhalation. Samples were fixed in 4% (w/v) paraformaldehyde overnight. To achieve whole mount X-Gal staining, samples were fixed in 4% paraformaldehyde for only 20min and subjected to X-Gal staining. Sections (5μm) were stained with H&E, and serial sections were used for immunohistochemical analysis. Sections were deparaffinized and subjected to an antigen retrieval step using citrate buffer (S2369, Dako) (Rapid Microwave Histoprocessor, Milestone). Primary antibodies (Supplementary Table S5) were applied in blocking buffer (1% BSA in PBS and 0.05% Triton X-100) overnight at 4ºC and visualized using secondary antibodies (Supplementary Table S5) in blocking buffer for 1h at room temperature. Antigen retrieval with heating in citric acid (pH 6.0) was done. Heavily pigmented skin slides were pre-treated with 0.1% $KMnO_4$ for 20 minutes followed by 0.5% oxalic acid for 12 minutes to increase the solution permeabilization. For visualization of β-Galactosidase and phospho-SMADs, biotin anti-chicken and biotin anti-rabbit secondary antibodies was combined with further signal amplification using horse radish peroxidase–streptavidin and the TSA Plus Cy3 Kit (1:50, NEL744001KT, PerkinElmer) according to manufacturers' protocol. Subsequently, nuclei were stained with Hoechst 33342 (14533, Sigma-Aldrich) slides were mounted with Fluorescent Mounting Medium (S3023, Dako). Immunohistochemical / fluorescent sections were analysed using either a Mirax Midi Slide Scanner (Zeiss) or a DMI 6000B microscope. Recombination efficiency of the Rosa26 allele was examined in mice by counting the β-Gal fluorescent cells of each tumor and dividing by the total number of DAPI-positive cells. Analysis of metastases was performed by counting distinct melanoma markers in each lesion (in sections from each level throughout the organ). Lung,

spleen and liver metastases were analysed based on the number of Pax3, Dct fluorescent cells. Groupings included single (1 cell), micro (11–100 cells), and macro (>100 cells).

7.6 Analysis of proliferation and apoptosis

To study tumor proliferation index, we investigated the incorporation of the thymidine analog 5-ethynyl-2'-deoxyuridine (EdU). Prior to sacrifice under isoflurane anaesthesia, mice were injected IP with 50mg EdU / kg body weight. EdU was immunohistochemically detected on formalin-fixed and paraffin-embedded sections according to the manufacturer's guidelines. (Click-iT® EdU Alexa Fluor® 488 Imaging Kit, C310337, Invitrogen). Cell proliferation was also assessed by Ki67 immunostaining. To quantify cells undergoing apoptosis, cleaved caspase-3 staining was used (see Histologic Analysis). Ten high-power fields (40 magnification) from at least 3 independent mice were counted for positive staining. Quantitative analysis was performed by counting cells in 10 independent high-power fields (40×) per age-matched tissue section from six mice per group.

7.7 Correlation Analysis

Melanoma cell cultures were established from surplus material from primary cutaneous melanoma and melanoma metastases removed by surgery as previously described.(Raaijmakers et al. 2015) This was performed at Dermatology Department of University of Zurich. Cell lines were correlated to their high SOX10 and high MITF expression as proliferative and high WNT5A high ZEB1 and SOX9 expression as invasive. Pearson's product moment correlation (r) was calculated for each gene expression values across all patient derived human melanoma cell lines. P-value was determined from the t statistic calculated from R value.

7.8 Cell culture, Cell Cycle Analysis and Ligand Treatments

The 501Mel cell line was obtained from the ATCC collection. The 501Mel cell line carries *BRAF*^{V600E}mutation. M010817 cell line were described previously (Hoek et al. 2006). The M010817 cell line has *NRAS*^{Q61R} mutation (*BRAF* not mutated). Primary cells derived from *Tyr::Nras*^{Q61K} *Ink4a*$^{-/-}$induced tumours were cultured as previously specified (Zingg et al. 2015). Cells were grown in RPMI-1640 medium supplemented with 10% FCS and 4 mM L-glutamine. Ligand treatment experiments were studied in serum-starved medium (0.5% FCS) (24 hours starved before ligand treatment). The effect of ligands on cell phenotype was determined by continuously adding human recombinant ligands that are indicated Supplementary Table S5 for 72 hours to cell monolayers at 70% confluency. For cell cycle analysis, the Click-iT EdU Alexa Fluor 647 Flow Cytometry Assay Kit (Invitrogen) was used. Cells were labelled with PI according to the manufacturer's protocol and the DNA content was measured using a BD FACS Canto II flow cytometer (BD Biosciences) and BD FACS Diva software (BD Biosciences).

7.8 RNA Interference

Silencing RNA (siRNA) transfection of human melanoma cells was carried out using jet PRIME siRNA Transfection Reagent (114-07, Polypus Transfection) solution according to the manufacturer's protocol. To achieve gene specific knockdown of SMAD4 and SMAD7, human melanoma cells were transfected with siRNA (25nM) (Invitrogen) 72 hours before RNA and protein isolation (Supplementary Table S6). As control, scrambled siRNAs with similar guanine cytosine (GC) content were also purchased from Invitrogen and used as negative controls. We confirmed the specificity of these sequences in BLAST. Growth medium was exchanged after 24h and cells were subjected to further assays.

7.9 Quantitative RT-PCR and RNA Sequencing

Total RNA was prepared using RNeasy Mini Kit (74104, Qiagen) and the RNase-Free DNase Set (79254, Qiagen) according to manufacturer's guidelines, reverse transcribed with Maxima First Strand cDNA Synthesis Kit (K1641, Thermo Scientific) followed by an RNase H (EN0202, Thermo Scientific) digestion step. Real-time quantitative PCR (qPCR) was performed on a LightCycler 480 System (Roche) using LightCycler 480 SYBR Green I Master (4707516001, Roche). Control of genomic contamination was measured for each sample by performing the same procedure with or without reverse transcriptase. Primers used mentioned in (Supplementary Table S4). Relative quantitative RNA was normalized using the housekeeping genes β-actin and Gapdh. The entire procedure was repeated in three biologically independent samples. Results were presented as the fold change over controls isolated from the same experiments. Fold induction was calculated using the comparative Ct method (DDCt). Total RNA obtained from 3 control and 3 siRNA mediated knockdown samples. samples Quality checked were done by using Bio-Analyzer and samples were subjected to sequencing on Illumina Hiseq platform at the Functional Genomics Center Zurich (http://www.fgcz.ch/). Differential gene expression analysis was performed using a minimum fold change of 1.5 and a False Discovery Rate inferior to 0.05. Gene ontology network analysis was performed with ClueGO (Version 2.3.2) and Cytoscape (Version 3.4.0). Clusters with less than 10 nodes were omitted.

7.9 Protein Isolation and Western Blotting

Cells were lysed in RIPA buffer (89900, Thermo Scientific) including Halt Phosphatase and Protease Inhibitor Cocktail (78420, 87786, Thermo Scientific. SDS–PAGE was carried out with 20 μg of whole-cell protein lysate using 4–20% Mini-PROTEAN TGX Gels (456–1094, Bio Rad). The gels were blotted onto nitrocellulose membrane and blocked for 1h in Odyssey blocking buffer (927-40000, LI-COR Biosciences). Primary antibodies (Supplementary Table S5) were applied in blocking buffer overnight at 4ºC and visualized using secondary antibodies (Supplementary Table S5) for 45 min at

room temperature. Blots were scanned and quantified with an Odyssey imaging system (LI-COR Biosciences). Quantified band intensities were normalized using either β-Actin or α-Tubulin as housekeeping protein.

7.10 TCGA Analysis

The RNAseq and clinical data sets for skin cutaneous melanoma were downloaded on April 2016 from TCGA (http://cancergenome.nih.gov/). Normalized reads from the level 3 RNA-seq data were used for analysis. Specimens with top and bottom transcript levels for a gene of interest were used for analysis. Patient numbers were gradually increased from a minimum of top and bottom 11% (50 out of 470) to a maximum of top and bottom 11 % (50 out of 470) to optimize potential segregation of Kaplan–Meier curves.

7.11 Attachment Assay Using Fibronectin-Coated Plates

Six well plates were coated with 1.25 Ag/mL of fibronectin (F1141-5MG, Sigma) in PBS overnight at 4C. Wells coated with bovine serum albumin served as negative controls. .10 $X10^4$ cells were seeded in each well at 37ºC. After ligand treatment, suspension cells were collected and were seeded in each fibronectin-coated well at 37ºC. Unattached cells were discarded and the attached cells were gently washed with PBS. Cells were fixed with 1% formaldehyde for 10 min and stained with 0.5% crystal violet for 30 min and solubilized with methanol. The area was calculated using Cell Profiler Program.

7.12 Supplementary Tables

7.12.1 Supplementary Table 1. GO Process

NODE	GOID	GOTerm	P-Value	% Associated Genes	Nr. Genes
1	GO:0092561	DNA-dependent DNA replication	130.0E-6	19.11	30.00
2	GO:0092562	DNA replication	13.0E-9	17.27	57.00
3	GO:0006259	DNA metabolic process	1.3E-3	10.37	107.00
4	GO:0044774	DNA replication initiation	550.0E-6	32.56	14.00
5	GO:0044765	Regulation of transcription involved in G1/S	1.2E-3	39.29	11.00
6	GO:0044774	G1/S transition of mitotic cell cycle	19.0E-6	16.80	42.00
7	GO:0044773	cell cycle G1/S phase transition	25.0E-6	16.41	43.00
8	GO:0098778	cell cycle phase transition	1.1E-3	11.99	68.00
9	GO:9087689	mitotic cell cycle phase transition	890.0E-6	12.24	66.00
10	GO:8976810	mitotic cell cycle process	4.1E-12	13.40	126.00
11	GO:0000278	mitotic cell cycle	2.0E-12	13.06	135.00
12	GO:0051726	regulation of cell cycle	11.0E-12	12.80	135.00
13	GO:0007346	regulation of mitotic cell cycle	32.0E-3	11.43	59.00
15	GO:0045786	negative regulation of cell cycle	14.0E-9	14.44	80.00
16	GO:0000075	cell cycle checkpoint	430.0E-9	18.15	45.00
17	GO:0031570	DNA integrity checkpoint	7.7E-3	16.20	29.00
18	GO:0007049	cell cycle	1.9E-15	11.72	211.00
19	GO:0007067	mitotic nuclear division	60.0E-9	15.07	69.00
20	GO:0022402	cell cycle process	100.0E-12	11.69	160.00
21	GO:0000280	nuclear division	450.0E-9	13.41	81.00
22	GO:0007088	regulation of mitotic nuclear division	290.0E-6	19.31	28.00
23	GO:0051301	cell division	41.0E-6	12.63	75.00
25	GO:0051276	chromosome organization	340.0E-6	11.84	78.00
26	GO:0071103	DNA conformation change	14.0E-3	13.78	39.00
27	GO:0000070	mitotic sister chromatid segregation	27.0E-3	16.78	24.00
28	GO:0007059	chromosome segregation	49.0E-6	14.78	51.00
29	GO:0044427	chromosomal part	15.0E-3	10.40	88.00
30	GO:0051783	regulation of nuclear division	36.0E-6	18.97	33.00
31	GO:0005694	chromosome	4.2E-3	10.33	99.00
32	GO:0051304	chromosome separation	44.0E-3	21.05	16.00
33	GO:0098609	cell-cell adhesion	14.0E-3	9.65	117.00
34	GO:0030155	regulation of cell adhesion	49.0E-3	10.60	73.00
35	GO:0050865	regulation of cell activation	6.3E-3	11.76	64.00
36	GO:0001775	cell activation	6.4E-6	11.42	110.00
37	GO:0045321	leukocyte activation	1.7E-3	11.01	87.00
38	GO:0098602	single organism cell adhesion	18.0E-3	10.40	86.00
39	GO:0016337	single organismal cell-cell adhesion	24.0E-3	10.53	81.00
40	GO:0002682	regulation of immune system process	12.0E-3	9.37	136.00
41	GO:0051240	positive regulation of multicellular process	5.8E-6	10.28	155.00
42	GO:0051094	positive regulation of developmental process	40.0E-6	10.49	129.00
43	GO:0045597	positive regulation of cell differentiation	9.1E-3	10.41	92.00
45	GO:0051241	process	43.0E-3	9.71	104.00
46	GO:0051239	regulation of multicellular organismal process	180.0E-9	9.35	258.00
47	GO:0022008	neurogenesis	40.0E-3	9.12	138.00
48	GO:0032101	regulation of response to external stimulus	5.2E-3	10.88	83.00
49	GO:0050793	regulation of developmental process	3.5E-6	9.41	222.00
50	GO:0030154	cell differentiation	10.0E-9	8.98	339.00
51	GO:0048731	system development	2.3E-12	9.08	405.00
52	GO:0048869	cellular developmental process	780.0E-12	9.03	358.00
53	GO:0048468	cell development	6.8E-3	8.94	177.00
54	GO:0051128	regulation of cellular component organization	17.0E-3	8.57	206.00
55	GO:0050793	regulation of developmental process	3.5E-6	9.41	222.00
57	GO:0051240	positive regulation of multicellular organismal process	5.8E-6	10.28	155.00
57	GO:0048513	animal organ development	43.0E-6	8.68	284.00
58	GO:0009888	tissue development	5.0E-6	9.85	182.00
59	GO:0009653	anatomical structure morphogenesis	100.0E-9	9.57	241.00
59	GO:0007399	nervous system development	700.0E-6	8.98	205.00

NODE	GOID	GOTerm	P-Value	% Associated Genes	Nr. Genes
60	GO:0009790	embryo development	26.0E-3	9.89	100.00
61	GO:0072359	circulatory system development	29.0E-6	11.07	111.00
62	GO:0048646	morphogenesis	500.0E-9	11.55	119.00
63	GO:0072358	cardiovascular system development	320.0E-6	11.89	78.00
64	GO:0048514	blood vessel morphogenesis	13.0E-3	11.55	62.00
65	GO:0001944	vasculature development	160.0E-6	12.06	78.00
66	GO:0001568	blood vessel development	250.0E-6	12.04	75.00
67	GO:0043542	endothelial cell migration	9.1E-3	16.37	28.00
68	GO:0010631	epithelial cell migration	980.0E-6	15.51	38.00
69	GO:0001667	ameboidal-type cell migration	3.4E-3	13.35	47.00
70	GO:0090132	epithelium migration	1.2E-3	15.32	38.00
71	GO:0090130	tissue migration	830.0E-6	15.35	39.00
72	GO:0040017	positive regulation of locomotion	2.5E-3	12.45	58.00
73	GO:0030335	positive regulation of cell migration	1.0E-3	13.10	55.00
74	GO:2000147	positive regulation of cell motility	2.8E-3	12.67	55.00
75	GO:0016477	cell migration	4.5E-12	12.17	157.00
76	GO:0048870	cell motility	280.0E-12	11.49	163.00
77	GO:0040012	regulation of locomotion	1.7E-3	10.83	91.00
78	GO:2000145	regulation of cell motility	1.3E-3	11.11	86.00
79	GO:0051272	positive regulation of cellular component movement	1.3E-3	12.81	57.00
80	GO:0051270	regulation of cellular component movement	270.0E-6	11.14	94.00
81	GO:0030334	regulation of cell migration	220.0E-6	11.63	84.00
82	GO:0006928	movement of cell or subcellular component	96.0E-12	10.79	203.00
83	GO:0050900	leukocyte migration	820.0E-6	13.38	53.00
84	GO:0032879	regulation of localization	52.0E-6	9.02	233.00
85	GO:0006935	chemotaxis	1.2E-3	11.86	70.00
86	GO:0042330	taxis	740.0E-6	12.01	71.00
87	GO:0071621	granulocyte chemotaxis	16.0E-3	18.75	21.00
88	GO:0097530	granulocyte migration	25.0E-3	17.74	22.00
89	GO:0097529	myeloid leukocyte migration	6.1E-3	16.38	29.00
90	GO:0051049	regulation of transport	32.0E-3	8.83	166.00
91	GO:0046903	secretion	2.9E-3	10.00	117.00
92	GO:0032940	secretion by cell	630.0E-6	10.50	108.00
93	GO:0007167	enzyme linked receptor protein signaling pathway	1.7E-3	10.34	106.00
94	GO:0007166	cell surface receptor signaling pathway	2.6E-6	9.11	258.00
95	GO:0010564	regulation of cell cycle process	5.6E-3	11.46	69.00
96	GO:0048518	positive regulation of biological process	70.0E-9	8.31	455.00
97	GO:0048522	positive regulation of cellular process	10.0E-9	8.56	418.00
98	GO:0007165	signal transduction	19.0E-6	7.94	478.00
99	GO:0048584	positive regulation of response to stimulus	1.1E-6	9.67	210.00
100	GO:0048583	regulation of response to stimulus	1.6E-9	9.05	347.00
101	GO:0023056	positive regulation of signaling	290.0E-6	9.62	159.00
102	GO:0009967	positive regulation of signal transduction	500.0E-6	9.75	147.00
103	GO:1902533	positive regulation of intracellular signal transduction	28.0E-3	10.00	96.00
104	GO:0042327	positive regulation of phosphorylation	26.0E-3	9.99	98.00
105	GO:0050730	regulation of peptidyl-tyrosine phosphorylation	41.0E-3	14.10	33.00
106	GO:0050731	positive regulation of tyrosine phosphorylation	8.6E-3	16.11	29.00
107	GO:0043408	regulation of MAPK cascade	18.0E-3	10.71	77.00
108	GO:0001934	phosphorylation	17.0E-3	10.12	95.00
109	GO:0071900	kinase activity	20.0E-3	11.72	58.00
110	GO:0023014	phosphorylation	15.0E-3	10.10	97.00
111	GO:0000165	MAPK cascade	27.0E-3	10.06	93.00
112	GO:0016310	phosphorylation	190.0E-6	9.06	214.00
113	GO:0051338	regulation of transferase activity	41.0E-3	9.84	98.00
114	GO:0006793	phosphorus metabolic process	41.0E-3	8.11	266.00
115	GO:0031401	process	41.0E-3	9.49	114.00
117	GO:0036211	protein modification process	21.0E-3	7.98	315.00

7.12.2 Supplementary Table 2. Cell adhesion and EMT genes

Input IDs	Signal	p-value	Input IDs	Signal	p-value	Input IDs	Signal	p-value
ID2	3.51	1.25E-70	**DVL3**	0.644	1.23E-10	**FZD8**	0.8982	3.68E-05
KRT8	2.706	7.27E-06	**FZD1**	0.6418	3.87E-05	**TGIF1**	0.9364	3.32E-20
KRT18	2.229	0.0003449	**TGFBR2**	0.6328	2.4E-13	**PARD6A**	0.9551	0.02001
ETS1	1.593	6.21E-65	**PIK3R3**	0.6296	1.72E-08	**MET**	0.9565	2.76E-26
SOX9	1.52	9.26E-12	**TSC2**	0.6128	0.000115	**CLDN1**	0.9735	2.39E-14
CDC42	1.484	1.2E-50	**JUND**	0.6121	2.63E-08	**MAP2K3**	1.016	1.12E-15
SNAI2	1.42	2.11E-48	**MKL2**	0.6108	7.87E-09	**OSMR**	1.026	1.38E-27
BMP4	1.383	0.00518	**COL1A1**	0.6088	0.01034	**MUC1**	1.032	5.93E-06
JUN	1.345	6.77E-21	**ACVR1**	0.6003	1.53E-10	**LOXL2**	1.034	7.21E-14
DVL2	1.298	1.21E-15	**GNAI2**	0.581	1.25E-07	**IL6ST**	1.044	6.5E-22
MAP2K6	1.18	1.77E-16	**SKIL**	0.5897	9.36E-06	**LIMK2**	1.06	1.33E-26
GAB1	1.052	1.25E-22	**FRS2**	0.5937	9.46E-07	**SERPINE 1**	1.191	0.000052
RBPJ	0.9931	9.17E-21	**TGFB1**	0.5983	0.002243	**DOCK2**	1.193	2.11E-06
ABL1	0.9532	5.2E-14	**CHUK**	0.6021	1.13E-07	**ITGA2**	1.281	1.35E-37
BCL2	0.8421	9.85E-10	**FARP2**	0.6103	2.46E-09	**PDK1**	1.295	1.78E-35
AKT1	0.8411	5.48E-08	**MAP2K1**	0.6541	4.45E-11	**ITGB1**	1.376	7.98E-51
CALD1	0.7958	1.15E-18	**ME2**	0.6617	3.11E-11	**FOS**	1.395	8.18E-20
ESR1	0.7935	0.02322	**FN1**	0.6625	1.92E-17	**JUNB**	1.448	2.09E-09
PIK3CA	0.7797	8.69E-09	**EGF**	0.6981	2.58E-05	**PTGS2**	1.484	9.97E-06
NFATC1	0.7536	9.77E-06	**FZD5**	0.6987	5.47E-06	**PDGFB**	1.555	2.23E-15
TWIST1	0.7516	0.0000352	**FZD7**	0.722	1.09E-06	**CYP19A1**	1.557	3.76E-06
MAP3K11	0.7473	0.0000293	**HIF1A**	0.7367	2.04E-16	**NOX4**	1.681	1.08E-47
WNT5A	0.7379	0.002297	**CTGF**	-0.7695	7.08E-16	**TGFBR1**	1.708	2.79E-60
TJP1	0.6864	5.92E-13	**CBL**	0.7707	4.26E-14	**S100A4**	1.9	6.37E-10
ILK	0.682	7.99E-13	**MAP3K1**	0.7879	4E-14	**HLA-DQB**	1.982	7.61E-11
ACTG1	0.6554	3.89E-13	**RPS6KA 3**	0.8256	4.84E-20	**COL1A2**	2.436	2.68E-53
SYP	0.6504	0.0002122	**FOSL2**	0.8312	1.08E-09	**ACTG2**	2.639	2.17E-05
AKT2	0.6499	5.11E-06	**RAF1**	0.833	1.06E-19	**FARP2**	2.727	9.19E-11
CFL1	0.6465	8.1E-13	**HEY1**	0.8471	2.42E-09			

7.12.3 Supplementary Table 3 Overlapping genes with MITF and AXL Program

Low vs High SMAD7(TCGA)				siSMAD7 VS siCONTROL			
MITF Program		**AXL Program**		**MITF Program**		**AXL Program**	
MLANA	3.361	**UCN2**	-3.425	**PLK2**	1.739	**UBE2C**	0.876
RAB38	3.208	**SLC16A6**	-3.194	**JUN**	1.300	**GADD45A**	0.783
ABCB5	3.008	**TCN1**	-2.173	**CELF2**	1.160	**FSTL3**	0.582
HMCN1	3.361	**CITED1**	-2.116	**IRF4**	1.120	**UPP1**	1.854
CDK2	3.252	**ENO2**	-2.054	**APOE**	0.937	**FN1**	1.250
SLC7A5	2.821	**UPP1**	-1.794	**ELOVL2**	0.860	**GLRX2**	0.654
VAT1	2.818	**PFKFB4**	-1.671	**CYP27A1**	0.856	**UBE2J1**	0.709
PTPRZ1	2.786	**ANGPTL4**	1.043	**LZTS1**	0.856	**RIN1**	-0.709
MLPH	2.458	**GLRX**	1.103	**TFAP2A**	0.855	**SLC16A3**	0.731
TFAP2A	2.56	**GEM**	1.168	**PLP1**	0.736	**ZYX**	0.774
TYR	2.36	**IL18BP**	1.251	**ERBB3**	0.718	**P4HA2**	0.775
CDH1	2.346	**SPATA13**	1.277	**C1orf85**	0.645	**GBE1**	0.818
TMEM98	1.987	**FAM46A**	1.292	**SIRPA**	0.640	**NGFR**	0.820
GYG2	1.954	**COL6A1**	1.302	**MYO10**	0.620	**C9orf89**	0.821
SLC24A5	1.877	**LOXL2**	1.352	**VAT1**	0.598	**SH3BGRL3**	0.832
MITF	1.65	**ZCCHC6**	1.374	**STAM**	0.589	**SLC25A37**	0.871
PIR	1.876	**FGFRL1**	1.391	**SLC35B4**	-.0.743	**FOSL1**	0.887
SNCA	1.765	**FN1**	1.478	**OSTM1**	-0.903	**TIMP1**	0.892
C1orf85	1.721	**HAPLN3**	1.492	**IGSF8**	-1.184	**HPCAL1**	0.900
IGSF8	1.718	**COL6A2**	1.531	**DNAJA4**	-1.938	**FAM46A**	0.923
GPR143	1.717	**BACH1**	1.555	**FOSB**	-3.104	**DBNDD2**	0.933
DNAJA4	1.678	**CADM1**	1.598			**PHLDA2**	0.953
IGSF11	1.567	**CRIP1**	1.62			**FGFRL1**	1.026
CHL1	1.423	**SLC22A4**	1.665			**LOXL2**	1.034
QPCT	1.346	**NNMT**	1.717			**TNFRSF12**	1.073
TBC1D7	1.325	**S100A4**	1.785			**CD82**	1.107
JUN	1.45	**AIM2**	1.821			**SEC14L2**	1.134
SIRPA	1.235	**PMAIP1**	1.836			**S100A6**	1.141
CYP27A1	1.235	**IGFBP3**	1.876			**CDKN1A**	1.167
TNFRSF1	1.234	**MAP1B**	1.942			**SERPINE1**	1.191
SLC45A2	1.16	**CD52**	2.071			**MT2A**	1.335
EXOSC4	1.168	**SERPINE1**	2.124			**SLC2A1**	1.338
CAPN3	1.982	**CHI3L1**	2.139			**ENO2**	1.358
LZTS1	1.152	**AXL**	2.242			**CD109**	1.368
S100B	1.126	**NGFR**	2.259			**ERO1L**	1.142
SLC19A2	1.123	**CFB**	2.456			**AIM2**	1.358
ROPN1	0.765	**STRA6**	2.982			**AXL**	1.498
FOSB	1.565					**MAP1B**	1.500
DOCK10	1.855					**PLAUR**	1.796
ELOVL2	2.346					**NNMT**	1.830
						IL8	1.358
						IGFBP3	1.358
						GEM	3.632
						UCN2	4.248
						METTL7B	5.479
						ANGPTL	1.358

7.12.4 Supplementary Table 4. Mouse Genotyping Primers

Gene	Forward Sequence (5'-3')	Reverse Sequence (5'-3')
Cre	CTATCCAGCAACATTTGGGCCAGC	CCAGGTTACGGATATAGTTCATGAC
Ink4^{wt}	ATGATGATGGGCAACGTTC	CAAATATCGCACGATGTC
Ink4$^{-/-}$	CTATCAGGACATAGCGTTGG	AGTGAGAGTTTGGGGACAGAG
N-Ras^{Q61K}	GATCCCACCATAGAGGATT	CTGGCGTATTTCTCTTACC
Smad4 ^{wt}	GGCACATTACATTTGCAGTCAG	AGGAAAAACAGGGCTATGTAGAA
Smad4^{lox}	GGCACATTACATTTGCAGTCAG	GACCCAAACGTCACCTTCAC
Smad7^{wt}	TTCAGAGGCAGACCGAACCTCCAA	AGGATTGGGTCAGGGACAGAAGAGCA
Smad7^{lox}	TTCAGAGGCAGACCGAACCTCCAA	TCTCACCTTGCTCCTGCCGAGAAAGTA
LacZ	GGTCGGCTTACGGCGGTGATTT	AGCGGCGTCAGCAGTTGTTTTT

7.12.5 Supplementary Table 5. Antibodies

Primary Antibodies				
Antigen	**Company**	**Source**	**Application / Dilutions**	**Catalog Number**
β-actin	Sigma- Aldrich	Mouse	WB 1:10000	A-5316
α-tubulin	Sigma- Aldrich	Mouse	WB 1:10000	T-6074
β -Gal.	Abcam	Chicken	IF 1:1000	ab9361
Axl	Santa Cruz ca	Goat	WB 1:50 IF 1:100	sc-1096
Caspase3	Cell Signaling Technology	Rabbit	IF 1:200	9661
DCT	Santa Cruz Biotechnology	Goat	IF 1:250	sc-10451
HMB45	Abcam	Mouse	IF 1:200	ab732
pSMAD2/3	Santa Cruz	Goat	IF 1:300	sc-11769
pSMAD2	Cell Signaling Technology	Rabbit	WB 1:50 IF 1:300	3101
pSMAD1/5/8	Cell Signaling Technology	Rabbit	WB 1:50 IF 1:300	9511S
SMAD2	Cell Signaling Technology	Rabbit	WB 1:100	5339
SMAD1	Cell Signaling Technology	Rabbit	WB 1:50	9743
PAX3	Invitrogen	Rabbit	IF 1:300	38081
SMAD7	Santa Cruz	Goat	IF 1:300	sc-9183
SMAD4	Abcam	Rabbit	IF 1:300	ab40759
Ki67	Abcam	Rabbit	IF 1:50	ab15580
MiTF	Santa Cruz	Rabbit	IF: 1:200 WB 1:200	sc-56726

Secondary Antibodies				
Antigen	**Company**	**Source**	**Application / Dilutions**	**Catalog Number**
Alexa 546	Jackson ImmunoResearch	Mouse	IF 1:250	A-1103
Alexa 488	Jackson ImmunoResearch	Rabbit	IF 1:250	711-545-152
Alexa 488	Jackson ImmunoResearch	Goat	IF 1:250	705-545-147
Biotin-SP IgG	Jackson ImmunoResearch	Donkey	IF 1:300	711-065-052
Biotin-SP IgG	Chemicon	Chicken	IF 1:300	AP194B
Streptavidin HRP	Jackson ImmunoResearch	Goat	IF 1:300	016-030-084
IRDye-800CW	Li-COR Biosciences	Donkey	WB 1:10000	926-32214
IRDye-680LT	Li-COR Biosciences	Mouse	WB 1:10000	926-68023

7.12.6 Supplementary Table 6. siRNAs and Primer sequences

Forward and reverse primer sequences used in qPCR and the sequences of the siRNAs aimed against the different SMADs

Human(siRNA)

Gene	Company	Target Exon	siRNA Location	Catalog Number
siSMAD7 #1	Life Technologies	Human 3,4	1028	HSS106264
siSMAD7 #2	Life Technologies	Human 4	1426	HSS180976
siSMAD4 #1	Life Technologies	Human 9,10	1582	HSS106255
siSMAD4 #2	Life Technologies	Human 5	1088	HSS180973
siControl Med.GC	Life Technologies			129353003

Human (RT-PCR Primers)

Genes	Forward Sequence (5'-3')	Reverse Sequence (5'-3')
ACTIN	AGAGCTACGAGCTGCCTGAC	AGCACTGTGTTGGCGTACAG
AXL	GCTGTCAGACGATGGGATG	CCATTCCGCGTAGCACTAA
GAPDH	AATCCCATCACATCTTCC	CATCACGCCACAGTTTCC
ZEB1	TGCACTGAGTGTGGAAAAGC	TGGTGATGCTGAAAGAGACG
TWIST1	ACCATCCTCACACCTCTGCATT	TGCAGGCTTTGATCCCAGTAT
ZEB2	CGCTTGACATCACTGAAGGA	CTTGCCACACTCTGTGCATT
SNAIL2	AGCAAGAAGTCGAGCGAAGA	CAGCTTGAGCGTCTGGATCT
CDH1	CTGCTGCCACCAGATGATGA	CTGTGCAGCTGGCTCAAATC
CDH271	CCT ACGGCTACTACCAGGATG	CACACGGTGTTCTGCTTGT
MITF	CAGGCATGAACACACATTCAC	TCCATCAAGCCCAAGATTTC
VIM	GAGAACTTTGCCGTTGAAGC	GCTTCCTGTAGGTGGCAATC
FN1	AAACCAATTCTTGGAGCAGG	CCATAAAGGGCAACCAAGAG
LOXL2	TGACGACTTCTCCATCCACG	GGAATCCTTTTGTCGCTGCA
SERPINE1	CATGTTCATTGCTGCCCCTT	CGGTCATTCCCAGGTTCTCT
AXL	GCTGTCAGACGATGGGATG	CCATTCCGCGTAGCACTAAT
SIRPa	GCTCTCAGACTTCCAGACC	GTGGAACTCGGATGGTCTCA
CDK2	TTCTGCCATTCTCATCGGGT	AGGAGGATTTCAGGAGCTCG

Mouse (RT-PCR Primers)

Genes	Forward Sequence (5'-3')	Reverse Sequence (5'-3')
Actin	GACGGGGTCACCCACACTGTGCCCATCTA	CTAGAAGCATTTGCGGTGGACGATGGAGG
Gapdh	AATCCCATCACATCTTCC	CATCACGCCACAGTTTCC
Zeb1	TGCACTGAGTGTGGAAAAGC	TGGTGATGCTGAAAGAGACG
Twist1	ACCATCCTCACACCTCTGCATT	TGCAGGCCAGTTTGATCCCAGTAT
Zeb2	CGCTTGACATCACTGAAGGA	CTTGCCACACTCTGTGCATT
Snail2	AGCAAGAAGTCGAGCGAAGA	CAGCTTGAGCGTCTGGATCT
Cdh1	CTGCTGCCACCAGATGATGA	CTGTGCAGCTGGCTCAAATC
Cdh271	TGCTGTTGCTGCTTCTGG	CTCACACACGGTCTGGTTG
Vim	GAGAACTTTGCCGTTGAAGC	GCTTCCTGTAGGTGGCAATC
Bmp7	ATT TCA GCC TGG ACA ACG AG	AGACGGCCTTGTAGGGGTAG
Nodal	ACTTTGCTTTGGGAAGCTGA	AGGAGGGTCAAGTTCCAGGT
Tgfβ2	TGCCAGTGGTGATCAGAA AA	TCCATTTCCATCCAAGATCC
Fn1	AAACCAATTCTTGGAGCAGG	CCATAAAGGGCAACCAAGAG

7.12.7 Supplementary Table 7. Ligand information

Ligand	Company	Source	Application	Catalog Number
TGF-β1	R&D Systems	Human	10 ng/µl	240-B-010
TGF-β2	Peprotech	Human	5-10 ng/µl	100-35B
ACTIVIN	R&D Systems	Human	50 ng/µl	338-AC-010
NODAL	R&D Systems	Human	100 ng/µl	3218-ND-025
BMP2	Peprotech	Human	50 ng/µl	120-02
BMP4	R&D Systems	Human	50 ng/µl	314-BP
BMP7	R&D Systems	Human	100 ng/µl	354-BP

8. Discussion

Phenotype switching, i.e. the reversible switch from a proliferative MITF^{high}/AXL^{low} melanoma cell to an invasive MITF^{low}/AXL^{high} cell, is thought to represent a key mechanism underlying melanoma progression (Keith S. Hoek & Goding 2010; Müller et al. 2014; Chapman et al. 2014). In the present study, however, we demonstrate that phenotype switching is not obligatory for invasion and metastatic spread of melanoma cells and that invasive melanoma cells can overcome restrictions in proliferation by intrinsically modulating their response to combinatorial TGF- β superfamily signaling. Despite the vast literature on TGF- β eliciting an anti-proliferative and pro-invasive effect in melanoma cells (Rodeck et al. 1999; Janji et al. 1999; Miyoshi et al. 1995), we reveal that Smad4-mediated overall canonical TGF- β signaling is required for tumor initiation and primarily promotes, rather than antagonizes, melanoma cell proliferation *in vivo.* Consistent with these data, we identify BMP7 as a factor stimulating melanoma cell proliferation and able to override the anti-proliferative/pro-invasive activity of TGF- β and NODAL. However, invasiveness can be triggered in these cells by lowering levels of the inhibitory SMAD protein SMAD7. Strikingly, activation of integrated TGF- β signaling by SMAD7 inhibition results in the emergence of an invasive program characterized by high AXL and ZEB1 expression in cells maintaining high MITF expression and proliferative capacity. Consequently, the increase in the number of Mitf^{high}/Axl^{high} cells in *Smad7*-depleted melanoma is associated with massive metastasis formation *in vivo*. Our findings demonstrate that proliferation is compatible with increased invasiveness and continued expression of MITF and reveal a novel mechanism underpinning melanoma aggressiveness.

Our data are compatible with earlier studies suggesting that melanoma progression can occur in the absence of phenotype switching. Recently, single cell RNA sequencing revealed the presence of a small subpopulation of MITF^{high}/AXL^{high} cells in every human tumor sample assessed, although MITF and AXL expression were exclusive on the level of the bulk tumor (Tirosh et al. 2016). Likewise, a considerable fraction of circulating tumor cells isolated from invasive melanoma patients was MITF positive (Khoja et al. 2014). Widmer and colleagues showed that in cultures of melanoma cells, hypoxia

could drive invasion without affecting overall proliferation (Widmer et al. 2013). Furthermore, cells in invasive cell clusters did not alter MITF expression during a process referred to as cooperative invasion (Chapman et al. 2014). Finally, time-lapse microscopy *in vitro* and *ex vivo* demonstrated that invading melanoma cells in culture do not necessarily undergo cell cycle arrest and actively proliferate regardless of their MITF expression status (Haass et al. 2014). Our study now reveals how a cellular state of simultaneous proliferation and invasion can be achieved by modulation of combinatorial TGF- β signaling in melanoma cells. Conceivably, changes in overall TGF- β signal activity and thus emergence of invasive-proliferative $MITF^{high}/AXL^{high}$ cells during melanoma progression are dependent on the availability of growth factors, nutrients and/or oxygen in the microenvironment, although this needs to be addressed in future studies.

It is well established that the biological effects of TGF-β superfamily signaling are context-dependent, but how specific responses to TGF- β family factors are controlled is still largely unknown (Massagué 2012). In melanoma, several TGF- β superfamily factors, including TGF- β , ACTIVINA, NODAL, BMP2, BMP4, and BMP7 are known to be expressed and to activate signaling in an autocrine manner (Topczewska et al. 2006; Hsu et al. 2005; Perrot et al. 2013; Lázár-Molnár et al. 2000; Stove et al. 2004). However, BMP7 promoted proliferation, whereas BMP4 induced cell cycle arrest in melanoma cells at concentrations at which both factors activated the pSMAD1/5/8-branch of TGF-β signaling to a comparable extent. In agreement with other studies (Schlegel et al. 2009; Schlegel et al. 2015; Hendrix et al. 2007) cell cycle arrest was also induced upon treatment with either TGF-β or NODAL, which unlike BMP4 act through pSMAD2/3 rather than pSMAD1/5/8. Of note, however, nuclear pSMAD2/3 activity is not only present in TGFβ-treated arrested cells, but also readily detectable in proliferative melanoma cells *in vitro* and *in vivo* (Rodeck et al. 1999; Schlegel et al. 2015; Lo & Witte 2008). Furthermore, loss of SMAD7 enhanced both pSMAD1/5/8 and pSMAD2/3 levels in melanoma cell cultures and in our melanoma mouse model, but predominantly boosted TGF- β /NODAL-induced invasiveness rather than BMP7-induced proliferation. Thus, the phenotype obtained upon reducing

SMAD7 in the context of combinatorial TGF-β superfamily signaling cannot simply be explained by preferential usage of either pSMAD2/3 or pSMAD1/5/8 signaling.

Our finding that BMP7 acts as a pro-proliferative factor in melanoma even in the presence TGF-β/pSMAD2/3 signaling is in line with studies in systems other than melanoma, in which BMP7 was reported to override effects of TGF- β . For instance, TGF-β/NODAL and BMP7 counter-regulate each other during pathophysiological processes in various organs, such as lung, liver, and kidney (Pegorier et al. 2010; Zeisberg et al. 2003; Zeisberg et al. 2007). In breast cancer cells, BMP7 inhibits expression of TGFβ-activated genes associated with epithelial-mesenchymal transition (EMT), resulting in a significant reduction in TGFβ-triggered cell migration and invasiveness in culture (Ying et al. 2015), reminiscent of our findings in melanoma. It remains to be shown whether in these cases the balance between integrated BMP7- and TGF-β-dependent signaling outcome can be tipped by modulation of SMAD7 activity in a manner similar to what we observed in melanoma, where an EMT gene expression signature, loss of cell-substrate adhesion *in vitro*, and metastasis formation *in vivo* were all promoted upon SMAD7 inactivation in spite of the presence of BMP7 and pSmad1/5/8 activity.

Our experiments indicate that overall canonical TGF-β/SMAD signaling is a potent promoter of melanoma progression, already at early stages of the disease. Eliminating the common downstream signaling mediator Smad4 in our murine melanoma model did not interfere with normal melanocyte survival, but counteracted *Nras*^{Q61K}-driven hyperpigmentation and melanoma initiation. Taking advantage of an inducible system allowing gene manipulation at various stages of tumor progression, we also show that Smad4 is required for proliferation in established skin melanoma, revealing the existence of and necessity for pro-proliferative activators of the Smad pathway, such as BMP7, for melanoma propagation. Since pro-proliferative BMP7 appears to be dominant over pro-invasive factors, the question arises of how a metastatic process is induced in melanoma. One possible mechanism might involve spatiotemporal changes in the composition of the TGF-β superfamily factors to which a tumor cell is exposed, where reducing levels of pro-proliferative factors relative to pro-invasive factor

concentrations would promote the development of invasive cells with limited proliferation capacity (Hölzel & Tüting 2016). Whether such phenotype switching indeed occurs *in vivo* remains to be shown. Our study offers an alternative mechanism of metastasis formation, which involves the reduction of SMAD7 levels in the presence of pro-proliferative and pro-invasive TGF-β superfamily factors. Although it is currently unknown how SMAD7 expression is normally regulated in melanoma, targeting SMAD7 level-dependent emergence of proliferative cells with metastatic capacity might represent a powerful treatment strategy, possibly in combination with drugs interfering with tumor cell proliferation. Indeed, high levels of ZEB1 expression, which we show to be induced by SMAD7 inactivation, have been associated with inherent resistance to MAPKi in $BRAF^{V600E}$-mutant melanoma (Richard et al. 2016). Likewise, a shift towards AXL^{high} expression was observed in melanoma samples resistant to RAF and MEK inhibition, whereas high expression of MITF in melanoma cells confers high sensitivity to MAPK pathway inhibition (Tirosh et al. 2016; Müller et al. 2014). Importantly, our study provides a system for investigating how tumor cell intrinsic changes independent of phenotype witching contribute to malignant progression of melanoma.

In our genetic murine model melanoma is initiated and grow spontaneously in a 3D environment together with tumor microenvironment elements. Therefore, an inducible conditional knockout strategy in these mice allowed us studying functional role of SMAD signaling. Few studies have also taken advantage of cKO models of melanoma, although most of the research on gene function in melanoma are based on cell culture and transplantation assays. Importantly, genes shown to be involved in melanoma formation turned out to be also important for normal melanocyte biology. For instance TGF-B signaling has been shown to be required for melanoma stem cell maintenance at the bulge. (Nishimura et al. 2006) as well as crucial for complete differentiation process. During my Phd, I found that TGF-B signaling is required for melanoma growth and metastasis. Deletion of Smad4 completely prevents melanoma initiation without affecting the normal melanocyte homeostasis (Data is not shown). This suggest that in melanoma SMAD signaling plays unique tumor specific role.

8.1 Current Model

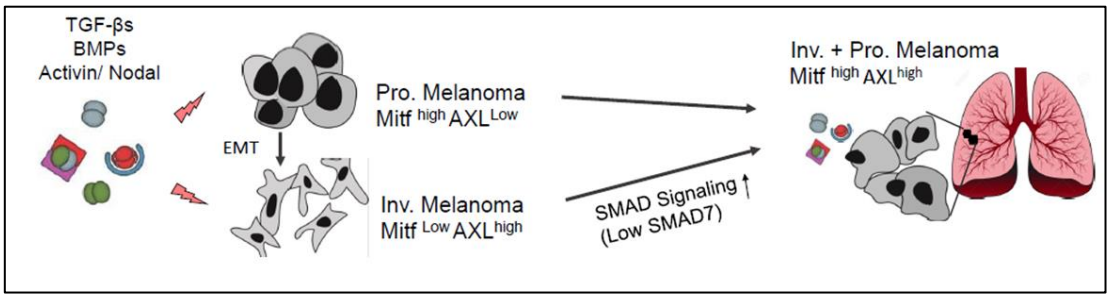

Current Model. Reduced SMAD7 levels in the context of complex TGF-β superfamily signaling increases the invasive potential of melanoma cells while sustaining their proliferative capacity. Loss of Smad7 in the presence of pro-proliferative and pro-invasive ligands leads to an increase in number of Mitf High Axl High cells

9. Curriculum Vitae

Name	Eylül Tuncer
Date of Birth	10.05.1987
Place of Birth	Ankara
Nationality	Turkish
Address	Schwamendingenstrasse 24
City	Zurich
Email	eyluel.tuncer@uzh.ch
Phone	+4178629227

Education

2012 – 2017	PhD. Cancer Biology, University of Zurich, Switzerland
2009 – 2011	M.Sc Medical School, University of Tuebingen, Germany
2007 – 2008	Exchange Program, Dept. of Molecular Genetics, University of Groningen, Netherlands
2004 – 2009	B.Sc. Department of Biology, University of Hacettepe, Ankara, Turkey
2001 – 2004	High School, Middle East Technical University (METU) College, Ankara, Turkey

---

Teaching Experience

2012 – 2017	Supervision of Histology I-III courses offered to medical students, University of Zurich
2017 (Jan-Aug)	Supervision of PhD. student
2014 (Apr-Sep)	Supervision of medical student (lab training)
2013 (Mar-Apr)	Supervision of Bachelor student (lab training)

Research Experience

2012 – 2017 PhD candidate, Institute of Anatomy, University of Zurich, Switzerland

PhD project**:** Role of transforming growth factor-β (TGF-β) signaling in murine melanoma model

2009 – 2011 M.Sc. Degree, Medical School of University Tuebingen, Institute of Hertie Clinical Brain Research / Max Planck International Research School

Project: Retrograde analysis of amygdaloinsular connections

Project: Mutations in SNCA gene (A30P& A53T) affect mitochondrial morphology

Thesis: Characterizing the role of NFAT3 in axonal outgrowth, nerve regeneration and functional recovery

2007 – 2008 BSc. Degree Groningen University, Molecular Genetics and Genomics Dept., Netherlands Project: Implementation of a novel method to knock-out genes in *Lactococcus lactis*

Project: Searching ATP I protein play a role in F_oc oligomerizaton, subunit of ATP synthase

---

Publications

The epigenetic modifier EZH2 controls melanoma growth and metastasis through silencing of distinct tumour suppressors, Daniel Zingg,[1] Julien Debbache,[1] Phil F. Cheng,[2] **Eylul Tuncer**,[1] Yudong Zhang,[1] Raquel Calçada,[1] Jessica Haeusel,[1] Mitchell P. Levesque,[2] Kwok-Kin Wong,[3] Reinhard Dummer,[2] and Lukas Sommer[1.] ***Nat Communication 2015***

EZH2-mediated primary cilium deconstruction drives metastatic melanoma formation Daniel Zingg,[1] Ana T. Antunes,[1] Simon. M. Schaefer,[1] Julien Debbache,[1] Phil F. Cheng,[**2**] **Eylul Tuncer,**[1] Yudong Zhang,[1] Raquel Calçada,[1] Jessica Haeusel,[1] Mitchell P. Levesque,[2] Kwok-Kin Wong,[3] Reinhard Dummer,[2] and Lukas Sommer[1] ***Under Revision Cancer Cell 2017***

SMAD signaling promotes melanoma metastasis independently of phenotype switching Eylül Tuncer[1], Daniel Zingg[1], Sandra Varum[1], Phil Cheng[2], Sandra N. Freiberger[2], Chu-Xia Deng[3], Ingo Kleiter[4], Mitchell P. Levesque[2], Reinhard Dummer[2], and Lukas Sommer[1] ***Under Revision 2017 JCI***

Selected Talks and Poster Presentations

SMAD signaling promotes melanoma metastasis independently of phenotype switching

06/2017 ISSCR 2017 Annual Meeting Boston Convention and Exhibition Center Boston, Massachusetts, USA

05/2017 Joint Oncology Meeting Zurich, Switzerland

05/2016 Seminar of the Institute of Anatomy at University of Zurich, Switzerland

Role of integrated TGF-β superfamily signaling in melanoma progression

07/2016 24th Biennial Congress of the European Association for Cancer Research EACR, Manchester, UK.

01/2016 Brupbacher Meeting, Zurich, Switzerland

04/2015 Cancer Network Zurich Meeting, Emmeten, Switzerland

Loss of the TGF-b inhibitor Smad7 promotes distant metastases in a genetic murine melanoma model

06/2015 International meeting on mouse models of skin cancer, Reykjavik, Iceland

04/2014 International meeting on mouse models of skin cancer, Cancéropôle GSO Montpellier

01/2014 Brupbacher Meeting, Zurich, Switzerland

02/2013 9th Swiss Stem Cells Network (SSCN), Bern, Switzerland

---

Employment History

2010 – 2011 Application Specialist GenMAR, Roche Diagnostic, Ankara Turkey

2008 Biologist, Health Research Hospital - In Vitro Fertilization Unit, Ankara – Turkey: following up andrology and embryology laboratory procedures with advanced theoretical and practical understanding of reproductive biology, embryology, infertility and assisted reproductive technology, in development of co-culture method by using endometrium cells and female serum proteins.

Scholarships & Awards

2010-2011 Max Planck International School Scholarship

2010 İhsan Doğramacı award of achievement 2010

2009-2010 DAAD Scholarship for Master education

2009 1st BSc. student in Biology, 3rd in the Faculty of Science, class of 2009 (3.89/4.00)

2008 Turkish Educational Foundation Scholarship

Travel Grants

2016 From Hartmann foundation University Hospital Zurich to participate international skin cancer meeting in Iceland.

2015 From Hartmann foundation University Hospital Zurich to participate EACR annual meeting in Manchester, UK.

2014 From Cancer Biology PhD Program to participate in the International meeting on mouse models of skin cancer, Montpellier, France

---

Memberships

Member of International Society of Stem Cell Research (ISSCR)

Member of the Swiss Society for Anatomy, Histology and Embryology (SSAHE)

Member of the Swiss Society for Neuroscience (SSN)

Languages

Turkish Mother tongue

English Highly proficient / German proficient

10. Acknowledgments

Since the beginning of my doctoral research in 2012, I have had the chance to meet and work with great people whose presence and collaboration have influenced and boosted my personal and professional life. I would like to take this opportunity to thank these people for their personal, philosophical and scientific support in completing this dissertation. First, I would like to thank Prof. Dr. Lukas Sommer for granting me the opportunity to work with him for my doctoral research in cancer field. He has been my supervisor and mentor on different philosophical and scientific discussions so far. His enthusiasm in looking for new and crazy solutions to big problems during hours long discussions have been the main motivation for my time in his lab and surely will be a driving force for the academic life. Also, I would like to thank my co-examiners Prof. Dr. Burkhard Becher and Prof. Dr. med. Onur Boyman for their contribution to my dissertation for their invaluable feedback.

My parents and my family have been the greatest source of support and inspiration to all my life achievements, and this dissertation is just another one of them. I owe what I have now to their endless support; therefore, these lines will not be sufficient enough to thank them. I would also like to thank Alejandro Núñez Cabello for whom he has been in my life for the last year.

Throughout my studies I have had the privilege to work with the best of colleagues someone can have. I was lucky to work with a large group of people due to my times in University of Zurich. To begin with the lab members, I am thankful to Dr. Daniel Zingg, Dr. Sandra Varum Tavares, Dr. Gaetana Restivo for their prior influence and directions on my research. I would like to thank my fellow cohorts who have been in the same doctoral process; Vadim Parfejevs, Johanna Diener, Ana Antunes, Arriana Bagiollini, Luis Zurkirchen,, Eliza Marzorati, Khan Huynh, as inseparable members of our research group. These people have been there for all the ideas, success, stress and joy we have shared throughout the study years.

I also would like to thank Nicole Bachelin and Monika Jenny for being the best in their administrative support. My research presented in this dissertation has also been shaped by the contribution of the Bachelor and Phd students whom I had the chance to supervise. I want to thank Tim Bartal and Raquel Calcada.

There is no way to express how much it meant to me to have been a member of METU collage. These brilliant friends and colleagues inspired me over the many years. I want to thank you my friends back home from my high school; Duru Aras, Melis Sahin, Cenk Atasaral, Nazli Altin, Petek Barkan, Ahmed Eldazer, Mehmet Melik, and Can Ocal.Lastly, I would like to thank all my friends, especially to Utku Culha , Bircan Bugdayci, Efe Anil Aksoz, Zeynep Bingol my Turkish friends in Zurich, for their personal and intellectual support which made the life during a stressful doctoral process fun and easy. I have been very lucky to meet every single one of them.

11. Bibliography

Abbasi, N.R. et al., 2004. Early diagnosis of cutaneous melanoma: revisiting the ABCD criteria. *JAMA*, 292(22), pp.2771–6.

Ackermann, J. et al., 2005. Metastasizing melanoma formation caused by expression of activated N-RasQ61K on an INK4a-deficient background. *Cancer research*, 65(10), pp.4005–11.

Aguissa-Touré, A.H. & Li, G., 2012. Genetic alterations of PTEN in human melanoma. *Cellular and Molecular Life Sciences*, 69(9), pp.1475–1491.

Alonso, S.R. et al., 2007. A high-throughput study in melanoma identifies epithelial-mesenchymal transition as a major determinant of metastasis. *Cancer Research*, 67(7), pp.3450–3460.

Aoude, L.G. et al., 2015. Genetics of familial melanoma: 20 years after CDKN2A. *Pigment Cell and Melanoma Research*, 28(2), pp.148–160.

Aplin, A.E., 2011. Axl of Evil? *Journal of Investigative Dermatology*, 131(12), pp.2343–2345.

Arozarena, I. et al., 2011. In melanoma, beta-catenin is a suppressor of invasion. *Oncogene*, 30(45), pp.4531–4543.

Arthur, J.S. & Ley, S.C., 2013. Mitogen-activated protein kinases in innate immunity. *Nat Rev Immunol*, 13(9), pp.679–692.

Balch, C.M. et al., 2009. Final version of 2009 AJCC melanoma staging and classification. *Journal of Clinical Oncology*, 27(36), pp.6199–6206.

Ball, N.J. et al., 1994. Ras mutations in human melanoma: a marker of malignant progression. *The Journal of investigative dermatology*, 102(3), pp.285–290.

Bandarchi, B. et al., 2010. From Melanocyte to Metastatic Malignant Melanoma. , 2010.

Barnhill, R.L. & Gupta, K., 2009. Unusual variants of malignant melanoma. *Clinics in Dermatology*, 27(6), pp.564–587.

Bastian, B.C., 2014. The Molecular Pathology of Melanoma: An Integrated Taxonomy of Melanocytic Neoplasia. *Annual Review of Pathology: Mechanisms of Disease*, 9(1), pp.239–271.

Bennett, D.C., 2008. How to make a melanoma: What do we know of the primary clonal events? *Pigment Cell and Melanoma Research*, 21(1), pp.27–38.

Berger, M.F. et al., 2012. Melanoma genome sequencing reveals frequent PREX2 mutations. *Nature*.

Besaratinia, A. & Pfeifer, G.P., 2006. Investigating human cancer etiology by DNA lesion footprinting and mutagenicity analysis. *Carcinogenesis*, 27(8), pp.1526–1537.

Bradford, P.T. et al., 2009. Acral Lentiginous Melanoma: incidence and survival patterns in the United States, 1986-2005. *Archives of Dermatology*, 145(4), pp.427–434.

Brash, D.E., 2015. UV signature mutations. *Photochemistry and Photobiology*, 91(1), pp.15–26.

Breslow, A., 1970. Thickness, cross-sectional areas and depth of invasion in the prognosis of cutaneous melanoma. *Annals of surgery*, 172(5), pp.902–8.

Broekaert, S.M.C. et al., 2010. Genetic and morphologic features for melanoma classification. *Pigment Cell and Melanoma Research*, 23(6), pp.763–770.

Cancer Genome Atlas Network, 2015. Genomic Classification of Cutaneous Melanoma. *Cell*, 161(7), pp.1681–1696.

Cantley, L.C., 2002. The phosphoinositide 3-kinase pathway. *Science (New York, N.Y.)*, 296(5573), pp.1655–7.

Caramel, J. et al., 2013. A Switch in the Expression of Embryonic EMT-Inducers Drives the Development of Malignant Melanoma. *Cancer Cell*, 24(4), pp.466–480.

Carracedo, A. & Pandolfi, P.P., 2008. The PTEN–PI3K pathway: of feedbacks and cross-talks. *Oncogene*, 27(41), pp.5527–5541.

Carreira, S. et al., 2006. Mitf regulation of Dia1 controls melanoma proliferation and invasiveness. *Genes and Development*, 20(24), pp.3426–3439.

Chapellier, M. et al., 2015. Disequilibrium of BMP2 levels in the breast stem cell niche launches epithelial transformation by overamplifying BMPR1B cell response. *Stem Cell Reports*, 4(2), pp.239–254.

Chapman, A. et al., 2014. Heterogeneous tumor subpopulations cooperate to drive invasion. *Cell Reports*, 8(3), pp.688–695.

Cheli, Y. et al., 2011. Mitf is the key molecular switch between mouse or human melanoma initiating cells and their differentiated progeny. *Oncogene*, 30(20), pp.2307–2318.

Chen, X. et al., 2008. Integration of external signaling pathways with the core transcriptional network in embryonic stem cells. *Cell*, 133(6), pp.1106–17.

Chien, A.J. et al., 2009. Activated Wnt/ss-catenin signaling in melanoma is associated with decreased proliferation in patient tumors and a murine melanoma model. *Proceedings of the National Academy of Sciences*, 106(4), pp.1193–1198.

Chin, L., 2003. THE GENETICS OF MALIGNANT MELANOMA : LESSONS FROM MOUSE AND MAN. , 3(August).

Chod, J. et al., 2008. Preoperative transforming growth factor-beta 1 (TGF-beta 1) plasma levels in operable breast cancer patients. *European journal of gynaecological oncology*, 29(6), pp.613–6.

Curtin, J.A. et al., 2005. Distinct Sets of Genetic Alterations in Melanoma. *New England Journal of Medicine*, 353(20), pp.2135–2147.

Damsky, W.E., Rosenbaum, L.E. & Bosenberg, M., 2011. Decoding melanoma metastasis. *Cancers*, 3(1), pp.126–163.

Datto, M.B. et al., 1995. Transforming growth factor beta induces the cyclin-dependent kinase inhibitor p21 through a p53-independent mechanism. *Proceedings of the National Academy of Sciences*, 92(12), pp.5545–5549.

Davies, H. et al., 2002a. Mutations of the BRAF gene in human cancer. *Nature*, 417(6892), pp.949–54.

Davies, H. et al., 2002b. Mutations of the BRAF gene in human cancer. *Nature*, 417(6892), pp.949–954.

Delmas, V. et al., 2007. β-Catenin induces immortalization of melanocytes by suppressing p16INK4a expression and cooperates with N-Ras in melanoma development. *Genes and Development*, 21(22), pp.2923–2935.

Denecker, G. et al., 2014. Identification of a ZEB2-MITF-ZEB1 transcriptional network that controls melanogenesis and melanoma progression. *Cell Death and Differentiation*, 21(8), pp.1250–1261.

Dennler, S., Huet, S. & Gauthier, J.M., 1999. A short amino-acid sequence in MH1 domain is responsible for functional differences between Smad2 and Smad3. *Oncogene*, 18, pp.1643–1648.

Donahue, T.R. & Dawson, D.W., 2011. Nodal/activin signaling: A novel target for pancreatic cancer stem cell therapy. *Cell Stem Cell*, 9(5), pp.383–384.

Dong, J. et al., 2003. BRAF oncogenic mutations correlate with progression rather than initiation of human melanoma. *Cancer Research*, 63(14), pp.3883–3885.

Dooley, S. & ten Dijke, P., 2012. TGF-beta in progression of liver disease. *Cell Tissue Res*, 347(1), pp.245–256.

Dummer, R. et al., 2005. Updated Swiss guidelines for the treatment and follow-up of cutaneous melanoma. *Dermatology*, 210(1), pp.39–44.

Duronio, R.J. & Xiong, Y., 2013. Signaling pathways that control cell proliferation. *Cold Spring Harbor perspectives in biology*, 5(3).

Estey, E. & Döhner, H., 2006. Acute myeloid leukaemia. *The Lancet*, 368(9550), pp.1894–1907.

Fang, R. et al., 2013. Nodal promotes aggressive phenotype via Snail-mediated epithelial-mesenchymal transition in murine melanoma. *Cancer Letters*, 333(1), pp.66–75.

Fimmel, S., Krasagakis, K. & Kru, S., 1999. Desensitization of Melanoma Cells to Autocrine TGF- □ Isoforms. , 187(June 1997), pp.179–187.

Friedman, E. et al., 1995. High levels of transforming growth factor beta 1 correlate with disease progression in human colon cancer. *Cancer Epidemiol Biomarkers Prev*, 4(5), pp.549–554.

Furnari, F.B. et al., 1997. Growth suppression of glioma cells by PTEN requires a functional phosphatase catalytic domain. *Proceedings of the National Academy of Sciences of the United States of America*, 94(23), pp.12479–84.

Furnari, F.B., Su Huang, H.J. & Cavenee, W.K., 1998. The phosphoinositol phosphatase activity of PTEN mediates a serum- sensitive G1 growth arrest in glioma cells. *Cancer Research*, 58(22), pp.5002–5008.

Gaggioli, C. et al., 2007. Tumor-derived fibronectin is involved in melanoma cell invasion and regulated by V600E B-Raf signaling pathway. *The Journal of investigative dermatology*, 127(2), pp.400–10.

Galvin, K.E. et al., 2010. Nodal signaling regulates the bone morphogenic protein pluripotency pathway in mouse embryonic stem cells. *Journal of Biological Chemistry*, 285(26), pp.19747–19756.

Gandini, S. et al., 2005. Meta-analysis of risk factors for cutaneous melanoma: II. Sun exposure. *European Journal of Cancer*, 41(1), pp.45–60.

Garraway, L.A. et al., 2005. Integrative genomic analyses identify MITF as a lineage survival oncogene amplified in malignant melanoma. *Nature*, 436(7047), pp.117–122.

Goding, C.R., 2011. A picture of Mitf in melanoma immortality. *Oncogene*, 30(20), pp.2304–2306.

Goel, V.K. et al., 2006. Examination of Mutations in BRAF, NRAS, and PTEN in Primary Cutaneous Melanoma. *Journal of Investigative Dermatology*, 126(1), pp.154–160.

Goumans, M.J. et al., 2003. Activin receptor-like kinase (ALK) 1 is an antagonistic mediator of lateral TGF [beta]/ALK5 signaling. *Molecular cell*, 12, pp.817–828.

Graham, D.K. et al., 2014. The TAM family: phosphatidylserine-sensing receptor tyrosine kinases gone awry in cancer. *Nature Reviews Cancer*, 14(12), pp.769–785.

Gray-Schopfer, V., Wellbrock, C. & Marais, R., 2007. Melanoma biology and new targeted therapy. *Nature*, 445(7130), pp.851–857.

Gregory, P.A. et al., 2011. An autocrine TGF-beta/ZEB/miR-200 signaling network regulates establishment and maintenance of epithelial-mesenchymal transition. *Molecular biology of the cell*, 22(10), pp.1686–98.

Haass, N.K. et al., 2014. Real-time cell cycle imaging during melanoma growth, invasion, and drug response. *Pigment Cell and Melanoma Research*, 27(5), pp.764–776.

Habas, R. & Dawid, I.B., 2005. Dishevelled and Wnt signaling: is the nucleus the final frontier? *Journal of biology*, 4(1), p.2.

Hannon, G.J. & Beach, D., 1994. p15INK4B is a potential effector of TGF-beta-induced cell cycle arrest. *Nature*, 371(6494), pp.257–61.

Haq, R. et al., 2013. BCL2A1 is a lineage-specific antiapoptotic melanoma oncogene that confers resistance to BRAF inhibition. *Proceedings of the National Academy of Sciences*, 110(11), pp.4321–4326.

Haq, R. et al., 2013. Oncogenic BRAF regulates oxidative metabolism via PGC1α and MITF. *Cancer Cell*, 23(3), pp.302–315.

Hata, A. & Chen, Y.G., 2016. TGF-?? signaling from receptors to smads. *Cold Spring Harbor Perspectives in Biology*, 8(9).

Hayashi, H. et al., 1997. The MAD-related protein Smad7 associates with the TGFbeta receptor and functions as an antagonist of TGFbeta signaling. *Cell*, 89(7), pp.1165–1173.

Hayward, N.K. et al., 2017. Whole-genome landscapes of major melanoma subtypes. *Nature*.

Health, N. et al., 2013. Signatures of mutational processes in human cancer. *Nature*, (July), pp.1–108.

Heldin, C.H., Landstrom, M. & Moustakas, A., 2009. Mechanism of TGF-beta signaling to growth arrest, apoptosis, and epithelial-mesenchymal transition. *Current Opinion in Cell Biology*, 21(2), pp.166–176.

Heldin, C.H., Vanlandewijck, M. & Moustakas, A., 2012. Regulation of EMT by TGFbeta in cancer. *FEBS Lett*, 586(14), pp.1959–1970.

Hendrix, M.J.C. et al., 2007. Reprogramming metastatic tumour cells with embryonic microenvironments. *Nature reviews. Cancer*, 7(4), pp.246–255.

Hermanek, P. et al., 1976. [Malignant melanoma: depth of invasion and histologic typing]. *Beitr Pathol*, 157(3), pp.269–282.

Hodis, E., Watson, I.R., et al., 2012. A landscape of driver mutations in melanoma. *Cell*, 150(2), pp.251–263.

Hodis, E., Watson, I.R., et al., 2012. A Landscape of Driver Mutations in Melanoma. *Cell*, 150(2), pp.251–263.

Hoek, K.S., Eichhoff, O.M., et al., 2008. In vivo switching of human melanoma cells between proliferative and invasive states. *Cancer Research*, 68(3), pp.650–656.

Hoek, K.S. et al., 2006. Metastatic potential of melanomas defined by specific gene expression profiles with no BRAF signature. *Pigment cell research / sponsored by the European Society for Pigment Cell Research and the International Pigment Cell Society*, 19(4), pp.290–302.

Hoek, K.S., Schlegel, N.C., et al., 2008. Novel MITF targets identified using a two-step DNA microarray strategy. *Pigment Cell and Melanoma Research*, 21(6), pp.665–676.

Hoek, K.S. & Goding, C.R., 2010. Cancer stem cells versus phenotype-switching in melanoma. *Pigment Cell and Melanoma Research*, 23(6), pp.746–759.

Hoek, K.S. & Goding, C.R., 2010. Cancer stem cells versus phenotype-switching in melanoma. *Pigment cell & melanoma research*, 23(6), pp.746–59.

Hölzel, M. & Tüting, T., 2016. Inflammation-Induced Plasticity in Melanoma Therapy and Metastasis. *Trends in Immunology*, 37(6), pp.364–374.

Horn, S. et al., 2013. TERT promoter mutations in familial and sporadic melanoma. *Science (New York, N.Y.)*, 339(6122), pp.959–61.

Hsu, M.Y. et al., 2005. Bone morphogenetic proteins in melanoma: Angel or devil? *Cancer and Metastasis Reviews*, 24(2), pp.251–263.

Huang, F.W. et al., 2013. Highly recurrent TERT promoter mutations in human melanoma. *Science (New York, N.Y.)*, 339(6122), pp.957–9.

Huber, A.H. & Weis, W.I., 2001. The Structure of the B-Catenin/E-Cadherin Complex and the Molecular Basis of Diverse Ligand Recognition by B-Catenin. *Cell*, 105, pp.391–402.

Ikehata, H. & Ono, T., 2011. The mechanisms of UV mutagenesis. *Journal of radiation research*, 52(2), pp.115–25.

Imoto, S. et al., 2003. Regulation of Transforming Growth Factor-?? Signaling by Protein Inhibitor of Activated STAT, PIASy through Smad3. *Journal of Biological Chemistry*, 278(36), pp.34253–34258.

Jakowlew, S.B., 2006. Transforming growth factor-beta in cancer and metastasis. *Cancer metastasis reviews*, 25(3), pp.435–57.

Janji, B. et al., 1999. Autocrine TGF-beta-regulated expression of adhesion receptors and integrin-linked kinase in HT-144 melanoma cells correlates with their metastatic phenotype. *Int.J.Cancer*, 83(2), pp.255–262.

Javelaud, D. et al., 2007. Stable overexpression of Smad7 in human melanoma cells impairs bone metastasis. *Cancer research*, 67(5), pp.2317–24.

Javelaud, D., Alexaki, V. & Mauviel, A., 2008. Transforming growth factor-b in cutaneous melanoma. , pp.123–132.

Javelaud, D. & Mauviel, A., 2004. Mammalian transforming growth factor-betas: Smad signaling and physio-pathological roles. *The international journal of biochemistry & cell biology*, 36(7), pp.1161–5.

Jin, Y. et al., 2001. Overexpression of BMP-2/4, -5 and BMPR-IA associated with malignancy of oral epithelium. *Oral Oncology*, 37(3), pp.225–233.

Jonk, L.J.C. et al., 1998. Identification and functional characterization of a smad binding element (SBE) in the JunB promoter that acts as a transforming growth factor-β, activin, and bone morphogenetic protein-inducible enhancer. *Journal of Biological Chemistry*, 273(33), pp.21145–21152.

Kamesaki, H. et al., 1998. TGF-beta 1 induces the cyclin-dependent kinase inhibitor p27Kip1 mRNA and protein in murine B cells. *J Immunol*, 160(2), pp.770–777.

Kennedy, C. et al., 2001. Melanocortin 1 receptor (MC1R) gene variants are associated with an increased risk for cutaneous melanoma which is largely independent of skin type and hair color. *Journal of Investigative Dermatology*, 117(2), pp.294–300.

Kenney, N.J., Adkins, H.B. & Sanicola, M., 2004. Nodal and cripto-1: Embryonic pattern formation genes involved in mammary gland development and tumorigenesis. *Journal of Mammary Gland Biology and Neoplasia*, 9(2), pp.133–144.

Khoja, L. et al., 2014. Prevalence and heterogeneity of circulating tumour cells in metastatic cutaneous melanoma. *Melanoma research*, 24(1), pp.40–6.

Kleiter, I. et al., 2010. Smad7 in T cells drives T helper 1 responses in multiple sclerosis and experimental autoimmune encephalomyelitis. *Brain*, 133(4), pp.1067–1081.

Knight, T. & Irving, J.A.E., 2014. Ras/Raf/MEK/ERK Pathway Activation in Childhood Acute Lymphoblastic Leukemia and Its Therapeutic Targeting. *Frontiers in Oncology*, 4.

Komiya, Y. & Habas, R., 2008. Wnt signal transduction pathways. *Organogenesis*, 4(2), pp.68–75.

Konieczkowski, D.J. et al., 2014. A melanoma cell state distinction influences sensitivity to MAPK pathway inhibitors. *Cancer Discovery*, 4(7), pp.816–827.

Krasagakis, K., Garbe, C. & Orfanos, C.E., 1993. Cytokines in human melanoma cells: synthesis, autocrine stimulation and regulatory functions--an overview. *Melanoma research*, 3(6), pp.425–33.

Krauthammer, M. et al., 2012. Exome sequencing identifies recurrent somatic RAC1 mutations in melanoma. *Nature Genetics*, 44(9), pp.1006–1014.

Kretzschmar, M., Doody, J. & Massagué, J., 1997. Opposing BMP and EGF signalling pathways converge on the TGF-B family mediator Smad1. *Nature*, 389:(6651), p.618—22.

Lamouille, S., Xu, J. & Derynck, R., 2014. Molecular mechanisms of epithelial-mesenchymal transition. *Nature reviews. Molecular cell biology*, 15(3), pp.178–96.

Lawrence, M.G. et al., 2011. Reactivation of embryonic nodal signaling is associated with tumor progression and promotes the growth of prostate cancer cells. *Prostate*, 71(11), pp.1198–1209.

Lawrence, M.S. et al., 2013. Mutational heterogeneity in cancer and the search for new cancer-

associated genes. *Nature*, 499(7457), pp.214–218.

Lázár-Molnár, E. et al., 2000. Autocrine and paracrine regulation by cytokines and growth factors in melanoma. *Cytokine*, 12(6), pp.547–54.

Leevers, S.J., Paterson, H.F. & Marshall, C.J., 1994. Requirement for Ras in Raf activation is overcome by targeting Raf to the plasma membrane. *Nature*, 369(6479), pp.411–414.

Levy, C., Khaled, M. & Fisher, D.E., 2006. MITF: master regulator of melanocyte development and melanoma oncogene. *Trends in Molecular Medicine*, 12(9), pp.406–414.

Li, Y. & Koeneman, K.S., 2009. BMP7, a putative regulator of epithelial homeostasis in the human prostate, is a potent inhibitor of prostate cancer bone metastasis in vivo. *Urologic Oncology: Seminars and Original Investigations*, 27(1), pp.112–113.

Lin, J.Y. & Fisher, D.E., 2007. Melanocyte biology and skin pigmentation. *Nature*, 445(7130), pp.843–50.

Liu, F. et al., 1996. A human Mad protein acting as a BMP-regulated transcriptional activator. *Nature*, 381(6583), pp.620–623.

Liu, F. et al., 2013. A unique gender difference in early onset melanoma implies that in addition to ultraviolet light exposure other causative factors are important. *Pigment Cell and Melanoma Research*, 26(1), pp.128–135.

Lo, R.S. & Witte, O.N., 2008. Transforming growth factor-?? activation promotes genetic context-dependent invasion of immortalized melanocytes. *Cancer Research*, 68(11), pp.4248–4257.

Lu, S. et al., 2006. Loss of transforming growth factor- □ type II receptor promotes metastatic head-and-neck squamous cell carcinoma. , pp.1331–1342.

Maertens, O. et al., 2013. Elucidating distinct roles for NF1 in melanomagenesis. *Cancer discovery*, 3(3), pp.338–349.

Massagué, J., 1998. TGF- β signal transduction. *Annual Review of Biochemistry*, 67, pp.753–791.

Massagué, J., 2008. TGFb in cancer. *Cell*, 134(2), pp.215–230.

Massagué, J., 2012. TGFβ signalling in context. *Nature reviews. Molecular cell biology*, 13(10), pp.616–630.

Massague, J. & Gomis, R.R., 2006. The logic of TGFbeta signaling. *FEBS Letters*, 580(12), pp.2811–2820.

Massagué, J. & Gomis, R.R., 2006. The logic of TGFb signaling. *FEBS Lett*, 580, pp.2811–2820.

Maverakis, E. et al., 2015. Metastatic melanoma – A review of current and future treatment options. *Acta Dermato-Venereologica*, 95(5), pp.516–524.

McAllister, J.C. et al., 2010. The embryonic morphogen, Nodal, is associated with channel-like structures in human malignant melanoma xenografts. *Journal of Cutaneous Pathology*, 37(SUPPL. 1), pp.19–25.

Miyoshi, E. et al., 1995. Transforming growth factor beta up-regulates expression of the N-acetylglucosaminyltransferase V gene in mouse melanoma cells. *Journal of Biological Chemistry*, 270(11), pp.6216–6220.

Mohammad, K.S. et al., 2011. TGF-b-RI Kinase Inhibitor SD-208 Reduces the Development and Progression of Melanoma Bone Metastases.

Mort, R.L. et al., 2015. The melanocyte lineage in development and disease The melanocyte lineage in development and disease. *Development*, 142, pp.620–632.

Müller, J. et al., 2014. Low MITF/AXL ratio predicts early resistance to multiple targeted drugs in melanoma. *Nature communications*, 5, p.5712.

Nazarian, R. et al., 2010. Melanomas acquire resistance to B-RAF(V600E) inhibition by RTK or N-RAS upregulation. *Nature*, 468(7326), pp.973–7.

Nelson, W.J., 2004. Convergence of Wnt, -Catenin, and Cadherin Pathways. *Science*, 303(5663), pp.1483–1487.

Neuzillet, C. et al., 2015. Pharmacology & Therapeutics Targeting the TGF β pathway for cancer therapy. , 147, pp.22–31.

Nishanian, T.G. & Waldman, T., 2004. Interaction of the BMPR-IA tumor suppressor with a developmentally relevant splicing factor. *Biochemical and Biophysical Research Communications*, 323(1), pp.91–97.

Nishimura, E.K. et al., 2006. Article Key Roles for Transforming Growth Factor b in Melanocyte Stem Cell Maintenance.

Nobori, T. et al., 1994. Deletions of the cyclin-dependent kinase-4 inhibitor gene in multiple human cancers. *Nature*, 368(6473), pp.753–6.

Omholt, K. et al., 2003. NRAS and BRAF Mutations Arise Early during Melanoma Pathogenesis and Are Preserved throughout Tumor Progression. *Clinical Cancer Research*, 9(17), pp.6483–6488.

Onken, M.D. et al., 2006. Functional gene expression analysis uncovers phenotypic switch in aggressive uveal melanomas. *Cancer Research*, 66(9), pp.4602–4609.

Opdecamp, K. et al., 1997. Melanocyte development in vivo and in neural crest cell cultures: crucial dependence on the Mitf basic-helix-loop-helix-zipper transcription factor. *Development (Cambridge, England)*, 124(12), pp.2377–2386.

Padua, D. & Massagué, J., 2009. Roles of TGFbeta in metastasis. *Cell research*, 19(1), pp.89–102.

Park, K.S., 2011. TGF-beta family signaling in embryonic stem cells. *International Journal of Stem Cells*, 4(1), pp.18–23.

Pegorier, S. et al., 2010. Bone morphogenetic protein (BMP)-4 and BMP-7 regulate differentially transforming growth factor (TGF)-beta1 in normal human lung fibroblasts (NHLF). *Respiratory research*, 11, p.85.

Pereira, P.N.G. et al., 2012. Antagonism of Nodal signaling by BMP/Smad5 prevents ectopic primitive streak formation in the mouse amnion. *Development*, 139(18), pp.3343–3354.

Perrot, C.Y., Javelaud, D. & Mauviel, A., 2013. Insights into the transforming growth factor-β signaling pathway in cutaneous melanoma. *Annals of Dermatology*, 25(2), pp.135–144.

Pfeifer, G.P., 2010. Environmental exposures and mutational patterns of cancer genomes. *Genome Medicine*, 2(8), p.54.

Pomerantz, J. et al., 1998. The Ink4a tumor suppressor gene product, p19(Arf), interacts with MDM2 and neutralizes MDM2's inhibition of p53. *Cell*, 92(6), pp.713–723.

Postovit, L.-M. et al., 2008. Human embryonic stem cell microenvironment suppresses the tumorigenic phenotype of aggressive cancer cells. *Proceedings of the National Academy of Sciences of the United States of America*, 105(11), pp.4329–34.

Potrony, M. et al., 2015. Update in genetic susceptibility in melanoma. *Annals of translational medicine*, 3(15), p.210.

Raaijmakers, M.I.G. et al., 2015. A new live-cell biobank workflow efficiently recovers heterogeneous melanoma cells from native biopsies. *Experimental Dermatology*, 24(5), pp.377–380.

Rauen, K.A., 2013. The RASopathies. *Annu Rev Genomics Hum Genet*, 14, pp.355–369.

Richard, G. et al., 2016. ZEB1-mediated melanoma cell plasticity enhances resistance to MAPK inhibitors. *EMBO molecular medicine*, pp.1–19.

Roberts, P. & Der, C., 2007. Targeting the Raf-MEK-ERK mitogen-activated protein kinase cascade for the treatment of cancer. *Oncogene*, 26, pp.3291–3310.

Rodeck, U., Nishiyama, T. & Mauviel, A., 1999. Independent regulation of growth and SMAD-mediated transcription by transforming growth factor beta in human melanoma cells. *Cancer Res*, 59(3), pp.547–550.

Roh, M.R. et al., 2015. Genetics of melanocytic nevi. *Pigment Cell and Melanoma Research*, 28(6), pp.661–672.

Rosen, V., 2009. BMP2 signaling in bone development and repair. *Cytokine and Growth Factor Reviews*, 20(5–6), pp.475–480.

Rothhammer, T. et al., 2005. Bone Morphogenic Proteins Are Overexpressed in Malignant Melanoma and Promote Cell Invasion and Migration. *Cancer Res.*, 65(2), pp.448–56.

Rothhammer, T. et al., 2007. Functional implication of BMP4 expression on angiogenesis in malignant melanoma. *Oncogene*, 26(28), pp.4158–70.

Rubinfeld, B., 1997. Stabilization of beta -Catenin by Genetic Defects in Melanoma Cell Lines. *Science*, 275(5307), pp.1790–1792.

Rustin, M.H. a., 1990. *Andrews' Diseases of the Skin - Clinical Dermatology*,

Salmena, L., Carracedo, A. & Pandolfi, P.P., 2008. Tenets of PTEN Tumor Suppression. *Cell*, 133(3), pp.403–414.

Santarpia, L.L., Lippman, S. & El-Naggar, A., 2012. Targeting the Mitogen-Activated Protein Kinase RAS-RAF Signaling Pathway in Cancer Therapy. *Expert Opin Ther Targets*, 16(1), pp.103–119.

Scandura, J.M. et al., 2004. Transforming growth factor beta-induced cell cycle arrest of human hematopoietic cells requires p57KIP2 up-regulation. *Proc Natl Acad Sci U S A*, 101(42), pp.15231–15236.

Schadendorf, D. et al., 2015. Melanoma. *Nature Reviews Disease Primers*, p.15003.

Schiller, M., Javelaud, D. & Mauviel, A., 2004. TGF-beta-induced SMAD signaling and gene regulation: consequences for extracellular matrix remodeling and wound healing. *Journal of*

dermatological science, 35(2), pp.83–92.

Schlegel, N.C. et al., 2009. Id2 suppression of p15 counters TGF-β-mediated growth inhibition of melanoma cells. *Pigment Cell and Melanoma Research*, 22(4), pp.445–453.

Schlegel, N.C. et al., 2015. PI3K signalling is required for a TGFβ-induced epithelial-mesenchymal-like transition (EMT-like) in human melanoma cells. *Experimental Dermatology*, 24(1), pp.22–28.

Schmierer, B. & Hill, C.S., 2007. TGFbeta-SMAD signal transduction: molecular specificity and functional flexibility. *Nature reviews. Molecular cell biology*, 8(12), pp.970–982.

Schuster, N. & Krieglstein, K., 2002. Mechanisms of TGF-beta-mediated apoptosis. *Cell and Tissue Research*, 307(1), pp.1–14.

Scott, M.C. et al., 2002. Human melanocortin 1 receptor variants, receptor function and melanocyte response to UV radiation. *Journal of cell science*, 115(Pt 11), pp.2349–2355.

Sensi, M. et al., 2011. Human Cutaneous Melanomas Lacking MITF and Melanocyte Differentiation Antigens Express a Functional Axl Receptor Kinase. *Journal of Investigative Dermatology*, 131(12), pp.2448–2457.

Serrano, M. et al., 1996. Role of the INK4a locus in tumor suppression and cell mortality. *Cell*, 85(1), pp.27–37.

Shain, A.H. & Bastian, B.C., 2016. From melanocytes to melanomas. *Nature Reviews Cancer*, 16(6), pp.345–358.

Shanmugasundaram, K. et al., 2013. PI3K regulation of the SKP-2/p27 axis through mTORC2. *Oncogene*, 32(16), pp.2027–2036.

Sharma, R. et al., 2013. Hyperactive Ras/MAPK signaling is critical for tibial nonunion fracture in neurobromin-decient mice. *Human Molecular Genetics*, 22(23), pp.4818–4828.

Shi, M. et al., 2011. Latent TGF-β structure and activation. *Nature*, 474(7351), pp.343–349.

Shi, Y. & Massagué, J., 2003. Mechanisms of TGF-beta signaling from cell membrane to the nucleus. *Cell*, 113(6), pp.685–700.

Siegel, P.M. & Massagué, J., 2003. Cytostatic and apoptotic actions of TGF-beta in homeostasis and cancer. *Nature reviews. Cancer*, 3(11), pp.807–21.

Siegel, R.L., Miller, K.D. & Jemal, A., 2016. Cancer statistics. , 66(1), pp.7–30.

Siegel, R.L., Miller, K.D. & Jemal, A., 2016. Cancer statistics, 2016. *CA: A Cancer Journal for Clinicians*, 66(1), pp.7–30.

Silvestri, C. et al., 2010. TGFβ signal transduction. In *Handbook of Cell Signaling, 2/e*. pp. 521–532.

Slominski, a et al., 2001. Malignant melanoma. *Archives of pathology & laboratory medicine*, 125(10), pp.1295–1306.

Smith, M.P. et al., 2013. Effect of SMURF2 targeting on susceptibility to MEK inhibitors in melanoma. *Journal of the National Cancer Institute*, 105(1), pp.33–46.

Smith, M.P. et al., 2016. Inhibiting Drivers of Non-mutational Drug Tolerance Is a Salvage Strategy for

Targeted Melanoma Therapy. *Cancer Cell*, 29(3), pp.270–284.

De Snoo, F.A. & Hayward, N.K., 2005. Cutaneous melanoma susceptibility and progression genes. *Cancer Letters*, 230(2), pp.153–186.

Stark, M.S. et al., 2011. Frequent somatic mutations in MAP3K5 and MAP3K9 in metastatic melanoma identified by exome sequencing. *Nature Genetics*, 44(2), pp.165–169.

Stone, S. et al., 1995. Complex Structure and Regulation of the P16 (MTS1) Locus. *Cancer Research*, 55(14), pp.2988–2994.

Stott, F.J. et al., 1998. The alternative product from the human CDKN2A locus, p14(ARF), participates in a regulatory feedback loop with p53 and MDM2. *EMBO Journal*, 17(17), pp.5001–5014.

Stove, C. et al., 2004. Melanoma cells secrete follistatin, an antagonist of activin-mediated growth inhibition. *Oncogene*, 23(31), pp.5330–5339.

Strizzi, L. et al., 2012. Nodal expression and detection in cancer: Experience and challenges. *Cancer Research*, 72(8), pp.1915–1920.

Strub, T. et al., 2011. Essential role of microphthalmia transcription factor for DNA replication, mitosis and genomic stability in melanoma. *Oncogene*, 30(20), pp.2319–2332.

Takata, M., Murata, H. & Saida, T., 2010. Molecular pathogenesis of malignant melanoma: A different perspective from the studies of melanocytic nevus and acral melanoma. *Pigment Cell and Melanoma Research*, 23(1), pp.64–71.

Tamura, M. et al., 1999. PTEN interactions with focal adhesion kinase and suppression of the extracellular matrix-dependent phosphatidylinositol 3-kinase/Akt cell survival pathway. *Journal of Biological Chemistry*, 274(29), pp.20693–20703.

Theohari, I. et al., 2012. Differential effect of the expression of TGF-?? pathway inhibitors, Smad-7 and Ski, on invasive breast carcinomas: Relation to biologic behavior. *APMIS*, 120(2), pp.92–100.

Thiery, J.P. et al., 2009. Epithelial-Mesenchymal Transitions in Development and Disease. *Cell*, 139(5), pp.871–890.

Thomson, S. et al., 2008. Kinase switching in mesenchymal-like non-small cell lung cancer lines contributes to EGFR inhibitor resistance through pathway redundancy. *Clinical and Experimental Metastasis*, 25(8), pp.843–854.

Tirosh, I. et al., 2016. Dissecting the multicellular ecosystem of metastatic melanoma by single-cell RNA-seq. *Science (New York, N.Y.)*, 352(6282), pp.189–96.

Topczewska, J.M. et al., 2006. Embryonic and tumorigenic pathways converge via Nodal signaling: role in melanoma aggressiveness. *Nature Medicine*, 12(8), pp.925–932.

Tsao, H., Chin, L., Garraway, L.A., et al., 2012. Melanoma: From mutations to medicine. *Genes and Development*, 26(11), pp.1131–1155.

Tsao, H., Chin, L., Garraway, L. a, et al., 2012. Melanoma: from mutations to medicine. *Genes & development*, 26(11), pp.1131–55.

Valastyan, S. & Weinberg, R.A., 2011. Tumor metastasis: Molecular insights and evolving paradigms. *Cell*, 147(2), pp.275–292.

Vandamme, N. & Berx, G., 2014a. Melanoma Cells Revive an Embryonic Transcriptional Network to Dictate Phenotypic Heterogeneity. *Frontiers in Oncology*, 4.

Vandamme, N. & Berx, G., 2014b. Melanoma cells revive an embryonic transcriptional network to dictate phenotypic heterogeneity. *Frontiers in oncology*, 4(December), p.352.

Verfaillie, A. et al., 2015. Decoding the regulatory landscape of melanoma reveals TEADS as regulators of the invasive cell state. *Nature communications*, 6, p.6683.

Viros, A. et al., 2008. Improving melanoma classification by integrating genetic and morphologic features. *PLoS Medicine*, 5(6), pp.0941–0952.

Wang, C. et al., 2009. Crystal Structure of the MH2 domain of Drosophila Mad. *Science in China, Series C: Life Sciences*, 52(6), pp.539–544.

Wang, S. & Hirschberg, R., 2003. BMP7 antagonizes TGF-beta -dependent fibrogenesis in mesangial cells. *American journal of physiology. Renal physiology*, 284(5), pp.F1006-13.

Wang, Y., Zhao, Y. & Ma, S., 2016. Racial differences in six major subtypes of melanoma: descriptive epidemiology. *BMC Cancer*, 16(1), p.691.

Webster, M.R., Kugel, C.H. & Weeraratna, A.T., 2015. The Wnts of change: How Wnts regulate phenotype switching in melanoma. *Biochimica et Biophysica Acta - Reviews on Cancer*, 1856(2), pp.244–251.

Wellbrock, C. & Marais, R., 2005. Elevated expression of MITF counteracts B-RAF-stimulated melanocyte and melanoma cell proliferation. *Journal of Cell Biology*, 170(5), pp.703–708.

Widmer, D.S. et al., 2013. Hypoxia contributes to melanoma heterogeneity by triggering HIF1α-dependent phenotype switching. *The Journal of investigative dermatology*, 133(10), pp.2436–43.

Wong, T.H. & Rees, J.L., 2005. The relation between melanocortin 1 receptor (MC1R) variation and the generation of phenotypic diversity in the cutaneous response to ultraviolet radiation. *Peptides*, 26(10), pp.1965–1971.

Worby, C.A. & Dixon, J.E., 2014. PTEN. *Annual Review of Biochemistry*, 83(1), pp.641–669.

Wrana, J.L. et al., 1992. TGFβ signals through a heteromeric protein kinase receptor complex. *Cell*, 71(6), pp.1003–1014.

Wu, C.H. & Nusse, R., 2002. Ligand receptor interactions in the Wnt signaling pathway in Drosophila. *J Biol Chem*, 277(44), p.41762–9.

Wu, H., Goel, V. & Haluska, F.G., 2003. PTEN signaling pathways in melanoma. *Oncogene*, 22(20), pp.3113–3122.

Wu, X. et al., 2014. AXL kinase as a novel target for cancer therapy. *Oncotarget*, 5(20), pp.9546–63.

Yan, X., Liu, Z. & Chen, Y., 2009a. Regulation of TGF-b signaling by Smad7 Overview of TGF-b Signaling Pathways. , pp.263–272.

Yan, X., Liu, Z. & Chen, Y., 2009b. Regulation of TGF-beta signaling by Smad7. *Acta biochimica et biophysica Sinica*, 41(4), pp.263–272.

Yang, J. et al., 2004. Twist , a Master Regulator of Morphogenesis , Plays an Essential Role in Tumor Metastasis Ben Gurion University of the Negev. *Cell*, 117, pp.927–939.

Yang, X. et al., 2002. Generation of Smad4/Dpc4 conditional knockout mice. *Genesis*, 32(2), pp.80–81.

Yao, Z. et al., 2010. TGF-beta IL-6 axis mediates selective and adaptive mechanisms of resistance to molecular targeted therapy in lung cancer. *Proceedings of the National Academy of Sciences of the United States of America*, 107(35), pp.15535–40.

Yin, M. et al., 2012. TGF-β Signaling, Activated Stromal Fibroblasts, and Cysteine Cathepsins B and L Drive the Invasive Growth of Human Melanoma Cells. *The American journal of pathology*, 181(6), pp.2202–16.

Ying, X., Sun, Y. & He, P., 2015. Cellular Physiology and Biochemistry Cellular Physiology and Biochemistry Bone Morphogenetic Protein-7 Inhibits EMT-Associated Genes in Breast Cancer. *Cell Physiol Biochem*, 37, pp.1271–1278.

Yu, J. et al., 2016. MicroRNA-182 targets SMAD7 to potentiate TGFβ-induced epithelial-mesenchymal transition and metastasis of cancer cells. *Nature Communications*, 7, p.13884.

Zeisberg, M. et al., 2003. BMP-7 counteracts TGF-beta1-induced epithelial-to-mesenchymal transition and reverses chronic renal injury. *Nature medicine*, 9(7), pp.964–968.

Zeisberg, M. et al., 2007. Fibroblasts derive from hepatocytes in liver fibrosis via epithelial to mesenchymal transition. *Journal of Biological Chemistry*, 282(32), pp.23337–23347.

Zhou, X.P. et al., 2001. Germline mutations in BMPR1A/ALK3 cause a subset of cases of juvenile polyposis syndrome and of Cowden and Bannayan-Riley-Ruvalcaba syndromes. *American journal of human genetics*, 69(4), pp.704–11.

Zingg, D. et al., 2015. The epigenetic modifier EZH2 controls melanoma growth and metastasis through silencing of distinct tumour suppressors. *Nature communications*, 6(May 2014), p.6051.

Zuo, L. et al., 1996. Germline mutations in the p16INK4a binding domain of CDK4 in familial melanoma. *Nature Genetics*, 12(1), pp.97–99.